MODELING MOISTURE DIFFUSION BEHAVIORS IN POLYMERS AND POLYMER COMPOSITES

A Dissertation

by

YIMING FAN

Submitted to the Office of Graduate and Professional Studies of
Texas A&M University
in partial fulfillment of the requirements for the degree of

DOCTOR OF PHILOSOPHY

Chair of Committee,	Anastasia Muliana
Committee Members,	Alan Freed
	Sevan Goenezen
	Maryam Sakhaeifar
Head of Department,	Andreas A. Polycarpou

August 2018

Major Subject: Mechanical Engineering

ABSTRACT

This study presents a transient analysis of fluid diffusion behavior in polymers, fiber reinforced polymer (FRP) composites, and polymeric sandwich composites. The studied polymers and polymer composites consist of pure resins and polymeric foams, which are considered to have isotropic diffusion behavior; FRP composites, which typically have anisotropic diffusion behavior because of the presence of the fibers; and sandwich composites, which have different constitutes with different diffusion behaviors at various geometries. Diffusivity coefficients are first determined by assuming the diffusion to follow the classical Fickian diffusion. Different constitutive models are considered in order to understand the diffusion behavior of fluid through polymers and polymer composites. In some cases, fluid sorption led to quite significant changes of volume, and the diffusion process cannot be well described by the Fickian diffusion. In such situations, the coupled deformation-diffusion model for linear elastic isotropic materials is adopted, as a first approximation. This coupled deformation-diffusion model reduces to a Fickian diffusion model when the coupling parameters are absent and the volume changes in the solid polymers during diffusion are negligible. A finite difference method is used in order to solve for the coupled deformation-diffusion model. The coupled deformation-diffusion model is used to predict the one-dimensional moisture diffusion in thin polymer plates and the multi-axial three-dimensional moisture diffusion in dogbone specimens and polymeric foams. FRP composites typically have anisotropic diffusion behavior, where diffusivity in the fiber direction is faster than in the transverse direction. A micromechanical model that includes fiber volume contents and diffusivities of the constituents (fiber and matrix) is considered in order to gain fundamental insight into the effects of microstructural morphologies and constituents' diffusivities on the diffusion

process in the FRP specimens. The matrix and the fibers are modeled separately. And the micromechanical model is implemented in a continuum three-dimensional FE. The micromechanical model uses anisotropic diffusion constant from calibration and the simulation results are compared with the experimental results of thin laminates with different fiber arrangements. Finally, a multi-scale analysis of fluid diffusion in sandwich composites is performed. The simulation results are compared with the experimental data.

ACKNOWLEDGEMENTS

I would like to thank my committee chair, Dr. Muliana, my committee members, Dr. Freed, Dr. Goenezen, and Dr. Sakhaeifar for their guidance and support throughout my graduate study and research. I would also like to thank Dr. Park for his advice and support of my research.

In addition, I thank my friends and colleagues and the department faculty and staff for making my time at Texas A&M University a great experience.

Finally, I would like to express my gratitude to my parents for their love and support.

CONTRIBUTORS AND FUNDING SOURCES

This work was supervised by a dissertation committee consisting of Professor Muliana, Professor Freed and Professor Goenezen of the Department of Mechanical Engineering and Professor Sakhaeifar of the Department of Civil Engineering.

Part of the experimental data analyzed for Section 4 was provided by Professor La Saponara of the Department of Mechanical and Aerospace Engineering, UC Davis. Part of the experimental data analyzed for Section 3 and Section 4 was provided by Professor Andreas Echtermeyer of the Department of Mechanical and Industrial Engineering, NTNU. All other work for the dissertation was completed by the student. This research is sponsored by the National Science Foundation and Office of Naval Research.

NOMENCLATURE

b	Coefficient of moisture expansion
$\underline{B^{(\alpha)}}$	Subcell concentration matrix
C	Fluid concentration
C_t	Total normalized concentration
D	Diffusivity
D_{matrix}	Diffusivity of matrix
D_f	Diffusivity of fiber
E	Young's modulus
$\underline{E}$	Linearized strain
$\underline{D^{(f)}}$	Fiber diffusivity
$\underline{D^{(m)}}$	Matrix diffusivity
$\underline{D^{(\alpha)}}$	Subcell diffusivity
$\underline{f}$	Flux of fluid
$\underline{f^{(\alpha)}}$	Flux through the subcell
$\underline{f^{(\alpha)}_i}$	Flux in direction i through the subcell α
$\underline{f_i}$	Homogenized flux through the composite in direction i
H	Thickness
G	Shear modulus
$\underline{I_3}$	Identity matrix
$M\%$	Percent mass change
M_m	Maximum moisture content

M_t	Current mass at time t
M_{solid}	Mass of solid
M_{fluid}	Mass of fluid
S	Stress
t	Time
$\underline{U}$	Displacement field
V	Unit-cell total volume
$V^{(\alpha)}$	Subcell volume
v_f	Fiber volume fraction
$V\%$	Percent volume change
V_t	Current volume at time t
V_{solid}	Volume of solid
w	Width
z_t	Current thickness at time t
z	Thickness
α	Coupling parameter
β	Coupling parameter
ε	axial strain
θ	Volumetric strain
λ	Lame constant
σ	axial stress
φ	Effective composite concentration gradient
$\varphi^{(\alpha)}$	Subcell concentration gradient

$\varphi^{(\alpha)}_{i}$	Concentration gradient in direction i through the subcell

TABLE OF CONTENTS

Page

LIST OF FIGURES

Page

LIST OF TABLES

Page

1. INTRODUCTION

Polymers and polymer composites are appealing for lightweight structures that require strength, stiffness, corrosion resistance and thermal insulation. They have been widely used in many engineering applications such as aircraft, marine vessels, oil and gas pipelines and large wind turbine blades. For example, vinyl ester is a resin that commonly used in marine vessels due to its corrosion resistance to the sea water. Fiber-reinforced vinyl ester structures have further improved strength and can also provide controlled anisotropy for structural designs. Polymeric sandwich composites which consists of two thin and strong FRP sheets and a low-density polymeric foam core can significantly reduce weight of the structure while providing high load carrying capacity under bending and impact conditions. Polymeric sandwich composites are currently used for hulls for advanced marine vessels. Another example is the applications of polymer composites in offshore applications. Composites pipelines and tethers are already in operation and composites risers have been considered for future applications [34]. Polymer composites are strong, stiff and light-weighted, and they are ideal for risers which are usually more than 1,000 ft. in length. Another application is in wind turbine blades, where using sandwich composites can significantly reduce weight while maintaining high stiffness of the blades, see for example: Thomsen [91] and Fernandes et al. [31].

During service, polymer and polymer composites structures are often subjected to various environmental conditions in addition to complex mechanical loadings. One concern is that when a polymer is exposed to wet condition, fluid diffuses through the polymer that can cause weight and volume changes, and eventually changes in the properties (mechanical, physical, and/or chemical) of the polymer. Several studies have reported weight increase and reductions in the

mechanical properties (e.g. tensile modulus, tensile strength, shear strength and fracture toughness) after exposure to ambient humidity and temperature [6, 23, 47, 50, 69, 76, 95]. Usually it takes very long time for the fluid to diffuse into the polymer and polymer composite structures. For thick walled structures, such as hulls of ships or some high-pressure pipelines, the water may never penetrate the entire thickness of the laminate, causing a gradient of water concentration in the composite. It is also noted that a gradient of water in the laminate can cause internal stresses altering the strength of the material, when compared to the ones measured in totally dry or wet conditions [49]. In order to obtain better predictions of the long-term properties, a more accurate knowledge of the concentration profiles of the water in the laminate needs to be known.

Hence, in order to support engineering applications of polymers and polymer composites where they are exposed to significant moisture changes, understanding the diffusion of fluid through polymers and its effect of the response of polymers and structures is necessary. This has been done through experimental observation and development of constitutive models of fluid diffusion.

This section presents a literature review. The literature review focuses on the experimental observation on fluid diffusion in polymers and polymer composites, environmental conditions that affects fluid diffusion, diffusion-induced deformation and its effects on diffusion process, testing and calibration of diffusion properties, constitutive models proposed for fluid diffusion and the analytical and numerical tools for analyzing fluid diffusion.

1.1 Literature Review

The mechanism of moisture/fluid absorption in neat resins has been widely studied. Neat resins are usually assumed as isotropic media, which means that the materials have the same diffusion properties in different directions. Typical experimental observations on the diffusion of fluid in glassy polymer resins are based on one-dimensional gravimetric studies, where the weight is recorded with time. The water uptake in polymer resins can be calculated if the diffusivity is known. Measurement methods for diffusivity of isotropic polymers, following the Fickian diffusion, are well established. The typical method is given by ASTM D5229 [1]. When a very thin specimen is considered for the immersion test, following the ASTM D5229–92(04) without sealing the edges, the diffusion process can be approximated by 1-D diffusion through the thickness. Then the diffusivity and mass uptake can be achieved by solving the 1-D Fickian diffusion equation. The data is then fitted with different diffusion models. Fickian diffusion is commonly used in describing the diffusion of fluid through solid polymers, where the rate of the diffusion process is much faster than that of polymer relaxation, and there is limited swelling, e.g. Crank [29], Shen and Springer [77], Göpferich [36]. It is noted that in the Fickian diffusion, the solid body is assumed to be rigid (undeformed), which can give a reasonable approximation when the moisture-induced deformation in the body is significantly small.

Compared to neat resins, the presence of fibers could greatly affect the moisture diffusion in fiber-reinforced composites. The fibers themselves are often seen as non-permeable to water, assuming to have zero diffusivity. Zhang et al. [100] showed that for short-glass fiber-reinforced polyamide 6,6, the diffusion coefficient became gradually smaller as the fiber content increased. Alvarez et al. [6] reported that the equilibrium moisture content of the fiber-reinforced

composites slightly increased with an increase of fiber contents. It is shown that at full saturation, FRP panels absorbed more liquid compared to neat resin panels and the equilibrium moisture contents decreased with increasing FRP panel sizes [32]. Fichera and Carlsson [32] used scanning electron microscope (SEM) and found imperfect fiber/matrix bonding and randomly distributed voids, which were used to explain the difference between moisture contents. Several investigations of moisture absorption in fiber-reinforced polymer composites have suggested significant differences between the diffusion along the fiber direction and the diffusion perpendicular to the fiber direction [18, 19]. Specifically, the diffusivity along the fiber direction can be 2-4 times larger than the transverse diffusivity for glass fiber laminates [18, 73] and about 14 times higher for carbon fiber rods [35]. Humeau et al. [44], performed computed tomography scans of GF/epoxy samples and observed that voids are elongated in the fiber direction. However, they reported that the anisotropy in diffusivity of samples without voids was as great as for the samples with voids, and concluded that voids elongation could not explain the anisotropic diffusion behavior.

Sandwich composites are special form of laminated composites and consist of two thin and strong skins separated by a thick and light core [39]. The fiber-reinforced polymer skins carry the in-plane stresses and bending deformations while the polymer foam carries the shear loads and provides more bending stiffness. Such design makes sandwich composite a lightweight structure with good load carrying capacity, see Chen and Lakes [27], Valbo [93]. One essential concern for sandwich composites during service is the presence of fluid absorption and weight change in the sandwich structures. It is reported that the mechanical properties and load carrying capacities of sandwich composites are subjected to change under moisture diffusion, see examples: Granville [38], Scudamore and Cantwell [75], Siriruk et al. [87] There's an interface

between the face sheets and the polymeric foam and the different properties of these two materials could lead to debonding when the sandwich composites are exposed to fluid ingression. Morganti et al. [63] studied the effects of moisture on sandwich composites and reported that moisture diffusion degrades the matrix elastic properties and induces microcracks between fibers and matrix. Weitsman et al. [96] found reduction in delamination toughness at the core/facing interface and also damages induced by sea water on polymeric foams. Siriruk et al. [85] showed that the interfacial fracture toughness of the sandwich structure decreased by 30% due to the combined sea water ingression and low temperature. Ishiaku et al. [47] conducted experiments on glass fiber/carbon fiber/Nylon 6 sandwich hybrid composites consisting of skin-core morphologies. Experimental results showed a decrease in tensile modulus, tensile strength, and fracture toughness after exposure to ambient temperature and humidity. Similar response is also found by Kolat et al. [53], Siriruk et al. [86] and Scudamore and Cantwell [48] in sandwich structures. The loss of interfacial toughness could lead to debonding of the core/facing interface and cause irreversible failures in sandwich composite structures. Several other studies also showed that the polymeric foam core degrades after a long-time exposure to fluid, see for examples: Aviles and Montero [9] and Manujesh et al. [61] In order to predict the lifetime performance of sandwich composites, it is necessary to understand the moisture diffusion process in sandwich composites. However, there's only limited studies on moisture diffusion in sandwich composites.

Katzman et al. [52] studied moisture diffusion in sandwich composites with graphite–epoxy face sheets and a core of Rohacell® polymethacrylimide 200WF foam. Sandwich specimens which edges sealed with aluminum foil tape were exposed to different relative humidity under different temperature. The graphite-epoxy face sheets were cut from the

Rohacell cores and the moisture content were measured separately. Experimental data shows that the diffusion constants for the Rohacell foam are about 60-100 times greater than the face sheets depends on the temperature. It is also showed that the equilibrium moisture content of foam is in a range of 4% to 12% depending on the relative humidity and is much higher compared to that of face sheets (1%). It is noted that the face sheets of sandwich composites retard the moisture diffusion into the foam core. Aviles and Montero [11] investigated moisture diffusion in sandwich composites with E-glass/polyester face sheets and PVC foam core exposed to 95% relative humidity and immersed in water. It is shown that the water uptake occurs more rapidly through the thickness direction compared to in-plane direction. And the authors reported prevention of water ingression into the sandwich structure by the face sheets.

As discussed above, typical approach to predict moisture diffusion in polymers includes characterization of diffusion properties and applying diffusion models. Characterization of diffusion properties of polymers includes measuring the weight changes and record them with immersion time. ASTM D5229 provides a good approach to calibrate the diffusion properties of isotropic materials. The data is then fitted with diffusion models, in most cases, a one-dimensional Fickian diffusion model. This approach is based the assumption that the polymer is isotropic, and both the polymer specimens and structures have a high width-thickness ratio to ensure that the diffusion through thickness direction is dominant. However, FRP, polymeric foams and sandwich composites usually do not meet one or more of these assumptions. Thus, different characterization method and diffusion models should be considered. The diffusivity of an fiber-reinforced composite ply is anisotropic [80]. The diffusivity along the fibers is different from the diffusivity across the fibers. The standard method for obtaining diffusivity for a composite ply is the same as for polymers (ASTM D5229). A thin-plate sample is made, the

edges are sealed, the sample is fully immersed in fluid and the diffusivity from the Fickian model is calculated. The approach works well for obtaining the through thickness diffusivity, because regular thin plies or laminates can be tested. It is usually assumed that the through thickness diffusivity and in-plane diffusivity across the fibers are the same. This is a good assumption for transversely isotropic materials. The diffusivity in fiber direction is more difficult to obtain. Using a standard thin laminate is not well suited for measuring diffusivity in the fiber direction. The large surface area would have to be sealed and it would take a long time for water to get into the specimen. Making very thick specimens and cutting them in a way that the fiber ends are forming the large surface has solved the problem [7, 13, 14, 16, 28]. In order to improve the predictions, the edge correction factor introduced by Shen and Springer [77], has been applied. The edge correction factor includes moisture diffusion contribution from all surfaces of the polymer and is more reasonable for specimens with relatively high thickness to width ratio. However, the edge correction factor is still based on one-dimensional Fickian diffusion and assuming that there is no interaction between diffusion from all sides, see example: Huo et al. [45], Aviles and Montero [11]. For a better calibration, the three-dimensional Fickian model is used for the calibration method instead of the one-dimensional model. Whitney [97] considered three-dimensional Fickian model and gave a better calibration method for the diffusion coefficient. The three-dimensional calibration method was shown to be the most rigorous by Arnold et al. [7].

One-dimensional Fickian model has been widely applied in predicting moisture diffusion in solid polymers. However, many approaches neglect the fact that the polymeric structure they studied are not thin enough to ensure that diffusion through the thickness direction contributes most to the moisture absorption. Although some researchers reported good correlation between

the experimental and simulation results based on one-dimensional Fickian model, many investigations reported some discrepancies between the experimental results and one-dimensional Fickian diffusion model. This depends strongly on the material systems used in the composites. For example, Katzman et al. [52] showed that moisture content behaviors for the graphite–epoxy face sheets can be well described by one-dimensional Fickian diffusion; however the prediction was not so good for the Rohacell®cores. Simulation results showed that the one-dimensional Fickian diffusion model over-predict the moisture absorption behavior in sandwich composites which usually have a low width-thickness ratio [10, 46, 52]. In some studies, a general three-dimensional Fickian model is used to describe the moisture diffusion in thick composite laminates, for example, Blikstad [17] and Yu et al. [99]. Blikstad et al. [18] compared both one-dimensional and three-dimensional Fickian model and reported that a three-dimensional solution has a better agreement with experiments. It is noted that the one-dimensional Fickian diffusion only describes diffusion in one direction, for thick laminates, a three-dimensional Fickian solution is more accurate.

In the Fickian diffusion, the solid body is assumed to be rigid (undeformed), which can give a reasonable approximation when the moisture-induced deformation in the body is significantly small. However, a non-fickian diffusion has been reported in many studies. For glassy polymers, the diffusion of moisture leads to extensive swelling of the polymers and it is noted that the moisture diffusion process is stress-dependent. Morgan et al. [62] showed that moisture sorption in epoxies is affected by applied stress, due to external mechanical stimulus, and exposure to thermal spike. It is also showed that moisture diffusion in epoxy matrix composites led to plasticization of the resin, along with swelling and reduction in mechanical properties and glass transition temperature [23, 30, 78, 79] Swelling of the composites due to

moisture absorption has been noted for a long time [21], however, only few investigations have been performed to measure and evaluate the volumetric change. Cairns [25] recorded the moisture expansion of glass/epoxy composites and reported a slightly non-linear expansion curve. Bouadi and Sun [22] measured the transverse swelling strains of the glass/epoxy composites and found higher strains compared to those of epoxy resins. Patel et al. [68] showed that moisture increases the rates of stress relaxation on condensation-cured S5370 foamed siloxanes while dry environments generally causes reduced stress relaxation rates. Swelling of the sandwich composites caused by moisture absorption has also been observed. Weitsman et al. reported sea water induced expansional strain (up to 2.8%) in H100 and H200 PVC foams and noted the difference with the comparable value for composite facing of sandwich composites (0.15%-0.2%).

Furthermore, the diffusion process in polymers and polymeric composites also changes with the temperature, i.e., it may exhibit prominent coupling between heat conduction and diffusion of fluid (Sih et al. [82, 83]; Popineau et al. [71]; La Saponara [55]). Sih et al. [81, 84] showed that the coupling behaviors between the diffusion of fluid and heat conduction depends strongly on the ratio of their diffusivities and a coupling constant, both of which are material specific. Experimental studies have been conducted at different ambient temperatures, assessing a higher moisture diffusivity coefficient in water as the temperature increases (e.g., Popineau et al. [71]; La Saponara [55]). Several studies on polymer diffusion have also shown that the diffusion process in FRP composites changes with the temperatures. It is reported that the rate of moisture diffusion in FRP increased with increasing temperatures [55, 59]. Bonniau and Bunsell [20] performed experiments with different thickness of glass/epoxy composites and showed that the moisture diffusion is temperature-dependent, and the moisture distributed uniformly along the

cross sections at saturation. Blikstad [17] showed that the temperature dependence of moisture diffusion is anisotropic for fiber-reinforced composites. However, it has been noted that the equilibrium moisture content seems to be insensitive to temperatures, e.g. Zhang et al. [100], Loos and Springer [59]. The coupling between heat transfer and moisture diffusion for composites immersed in several service fluids is reported by La Saponara [55].

It is noted that in the Fickian diffusion, the solid body is assumed to be rigid (undeformed), which can give a reasonable approximation when the moisture-induced deformation in the body is significantly small. However, it has also been shown in the literature that, for many polymers, the diffusion process deviates from the assumptions of the Fickian model: it is governed by the interaction of diffusion and relaxation, resulting in large swelling, irreversible deformation, see for example, Alfrey et al. [5], Carter and Kibler [26], Joshi and Astarita [51], Cai and Weitsman [24], Bao et al. [15], etc. This interaction of processes is categorized as "anomalous diffusion behavior". In order to include the effect of volumetric expansion on the diffusion of fluid, there have been constitutive models derived for coupled deformation-diffusion behaviors in elastic solids, where swelling of polymers due to fluid sorption can influence the diffusion process, e.g., Treloar [92], Baek and Srinivasa [12], Hong et al. [43]. Weitsman [94] formulated the governing equations for stress-assisted diffusion in elastic and viscoelastic bodies. The coupled deformation-diffusion equations for the linearized elastic isotropic bodies are similar to the one presented by Gurtin [40]; however, Weitsman [94] considered stresses as the independent variables for the deformation instead of strains, as formulated by Gurtin [40].

Another example of stress-assisted diffusion model is the Langmuir model, which can be reduced to Fickian diffusion and Darcy equations for special cases, for example, Carter and

Kibler [26]; Lee and Peppas [57]; Perreux and Suri [70]; Popineau et al. [71]; Helbling and Karbhari [41]; LaPlante et al. [56]; La Saponara [55]; Grace and Altan [37]. In the Langmuir model, the macroscopic sorption is modeled by two stages, consisting of a Fickian diffusion-dominated stage and a relaxation-dominated stage, where fluid molecules interact with the macromolecular structure of the polymer. Whitney and Browning [98] also discussed stress-dependent diffusion and a two-stage diffusion model has been proposed. Aifantis [4] considered the diffusion as the flow of a fluid in a porous rigid solid body, assisted by pore pressure. The model reduces to Fickian diffusion and Darcy equation as special cases.

One-dimensional Fickian model has been widely used to predict moisture diffusion in fiber-reinforced polymer (FRP) composites and some good prediction have been reported, see for example, Browning et al. [23], Blikstad [18] and Katzman et al. [52]. It is reported that one-dimensional Fick's law tends to over predict the diffusion process [97]. And the thick FRP laminates which have a high width-thickness ratio do not meet the assumption that the fluid diffusion is dominant by through-thickness diffusion. Whitney and Browning [98] developed three-dimensional solution for orthotropic materials and presented method for calculating three-dimensional diffusion coefficient. Good correlation between the three-dimensional Fick's law and the moisture diffusion in fiber-reinforced composites has been reported. See also example, Blikstad [18]. Taking into consideration the anisotropy of the fiber-reinforced composites, Shen and Springer [80] formulated a relationship between the diffusivity of matrix, diffusivity of fibers, fiber volume fraction and fiber orientation. They proposed an expression of transverse and parallel diffusivity in order to describe the diffusivity of composites. See also Loos and Springer [59]. The idea is based on an analogy between moisture diffusion and thermal conduction [88]. The model has been widely applied in capturing the moisture diffusion in FRP composites [58,

97]. Several theories were developed to predict anisotropic diffusivity based on the diffusivity of the matrix and the geometrical arrangement of the fibers [73, 80]. A comparison of micromechanical analytical models has been reported by Bao and Yee [13].

It is noted that several experimental studies have shown that typical diffusivity of the FRP composites in the transverse direction is around 1.5-3 times lower than the diffusivity of the corresponding resin, e.g. Bond [19]. Experimental investigations mentioned above have shown that diffusivity along the fiber direction can be 2-14 times higher than the one in the transverse direction. In this situation, it is clear that the diffusivity in FRP composite cannot be adequately captured by considering only matrix and fiber constituents, with zero diffusivity for the fiber. Rocha et al. [73] proposed a FE model with high diffusivity interphase, in order to explain anisotropic diffusivity in composites. They concluded that the fiber barrier effect is partly responsible for the anisotropic diffusion in composites, but this alone does not explain the effect observed. Cairns and Adams [25] applied micromechanics analysis on glass/epoxy matrix composites, however, details of the model were not discussed. A micromechanical model that considered the heterogeneity in composites was developed by Muliana and Kim [65] for thermal conductivity in a unidirectional fiber-reinforced lamina and was adopted to simulate moisture diffusion in glass/epoxy composites, and good correlation was reported by Gagani et al [33].

There have been only limited investigations on modeling diffusion in polymeric sandwich composites. The thick-layered nature of sandwich composites leads to heterogeneities at various scales: skin, core, fiber-matrix constituents, which causes multiple diffusion mechanisms, making it hard to predict the fluid sorption in the material.

Fickian diffusion was frequently used to describe moisture diffusion in sandwich composites. Many researchers considered one-dimensional Fickian diffusion, in which only moisture

diffusion through thickness is considered. Katzman [52] applied one-dimensional diffusion model and showed that the multi-layer diffusion model and the Fick's law agreed very well with the test data of graphite-epoxy face sheets while not so good for the Rohacell cores. Aviles and Montero [10] applied one-dimensional diffusion model for the PVC foam core and the sandwich composites (E-glass/polyester face sheets and PVC foam core) and reported good agreement between measure and predicted moisture absorption curves. Huo et al. [45] studied moisture diffusion behavior in sandwich composites with E-glass fiber-reinforced thermoset polyurethane matrix face sheet, closed cell rigid polyurethane foam. A multi-step diffusion model is used in calibrating diffusivity and finite element method is used to solve for the Fickian model. The simulation results showed a good correlation with experimental findings.

1.2 Motivation and Research Objectives

Experiment studies show that the fluid sorption in polymer and polymer composites leads to weight and volumetric changes. Diffusion properties are different based on the material and it can be affected by the diffusion-induced volumetric expansion and variation of temperature. Fickian diffusion model has been widely applied in predicting moisture diffusion in polymers and polymer composites. Even though some good agreements with experiment results are reported. It has been noted the Fickian model has limitations and is not able to describe fluid sorption in many kinds of materials.

Fickian model assumes the material is a rigid body and neglects the volumetric changes in the diffusion process. When volume changes are not negligible, Fickian diffusion tends to over predicts the diffusion process in the materials. The penetration of moisture tends to cause extensive

swelling in glassy polymers and it is showed that the deformation can affect the diffusion process. The current study applies a coupled deformation-diffusion model and is able to capture the volumetric expansion and the moisture diffusion process. Fiber-reinforced composites are typically anisotropic materials and the diffusion properties depends on the directions. It is found that the diffusion properties are different along the fiber direction and transverse to the fiber direction. The coupled deformation-diffusion model is considered for FRP with significant volumetric change during diffusion process. And a micromechanical model is used to describe the anisotropic diffusion in FRP laminates. Furthermore, the thick-layered nature of sandwich composites leads to heterogeneities at various scales: skin, core, fiber-matrix constituents, making it hard to predict the moisture diffusion process in the structure. This work includes a multi-scale analysis of the fluid sorption in the structural materials of the sandwich composites and finally provides a precise prediction of the diffusion process in the sandwich composites. This research can support the design of polymers and polymer composites structures which may serve under various environmental conditions in addition to complex mechanical loadings.

The objectives of the current study are:

1) *Determination of fluid diffusion in structural materials of sandwich composites (matrix materials of FRP and polymeric foams)*

This section examines the fluid sorption behaviors of matrix materials of FRP, i.e. epoxy and vinylester, and thick foam core materials, i.e. polyurethane foam and PVC foam. It is noted that the Fickian diffusion model, which is commonly used to describe moisture sorption in polymers, does not include the influence of volume change and over-predicts the diffusion process when the measured volume changes during the diffusion process are not negligible.

Hence, this part of the study is to understand the effect of deformations due to volume changes on the diffusion process of solid polymers. When the volume changes due to diffusion of fluid are not negligible, a coupled deformation-diffusion model is considered to describe such a diffusion process. An attempt is made by considering a coupled deformation-diffusion model for isotropic homogeneous elastic materials undergoing small deformation proposed by Gurtin [40]. A finite difference method is used to obtain solutions to coupled deformation-diffusion governing equations in elastic solids. Parametric studies are conducted first in order to understand the coupling effect in the diffusion process. The coupled deformation-diffusion model is then used to describe the diffusion behaviors of polymers.

2) *Determination of anisotropic fluid diffusion in fiber-reinforced polymer composites*

This part is to examine the fluid sorption behaviors of fiber-reinforced composites. Fluid diffusion in FRP is typically anisotropic. Diffusivity along the fiber direction and diffusivity transverse to the fiber direction need to be characterized. Fickian model assumes that the material is isotropic and thus cannot describe the diffusion process in FRP. This study presents a micromechanical model. The diffusion properties of matrix and fiber bundles are modeled separately. And the micromechanical model is applied in modeling the anisotropic diffusion behavior in FRP.

3) *Determination of fluid diffusion in sandwich composites (A multi-scale analysis)*

The next objective is to understand the behavior of polymeric sandwich composites under moisture diffusion. The goal of this part is to examine the diffusion properties at various scales of the sandwich composites: matrix material of FRP, FRP skin, polymeric foam core. And a multi-scale analysis is used to provide a prediction for the moisture diffusion in sandwich composites.

2. COUPLED DEFORMATION DIFFUSION CONSTITUTIVE MODEL*

When the volume changes in the polymers during diffusion process are not negligible, the Fickian model overpredicts the diffusion response in the polymers. This study considers an alternative model, in which the effect of deformation is incorporated in the diffusion process. There have been several constitutive models describing coupled deformation-diffusion behaviors, mainly for materials undergoing large deformations such as rubbers and hydrogels, in which swelling is apparent during the moisture sorption (typical volume changes of 200% or larger). Some of these models are discussed above in Section 1. In this study, the recorded volume changes and deformation changes are relatively small (<10%) compared to those of rubber or hydrogel. However, this magnitude of volume changes shows a noticeable effect on the diffusion behaviors. This study adopts the governing equations of coupled diffusion and deformation in homogeneous isotropic elastic solids, discussed by Gurtin [40], in order to improve the prediction of the diffusion process when volume changes are not negligible. This is a first approximation of the coupled deformation-diffusion process, as the model considers small deformation gradient and constant material parameters. Alternatively, one can consider nonlinear deformation-diffusion models, e.g. Parthasarathy et al. [67], in which large deformations and variations of the material parameters with external stimuli are taken into account. However, such models lead to extensive numerical solutions. Considering the less than 10% volume changes in this study, models with large deformations might only give a slight improvement.

2.1 Coupled Deformation-diffusion Model

The model of Gurtin [40] assumes small deformation gradients and a linear deformation-diffusion relation, analogous to linear thermo-elasticity, for solids. It is also assumed that the solid bodies are initially under dry conditions, and they are also stress- and strain-free. A numerical implementation of the model using a finite difference method is presented, which is correlated to experimental results.

For quasi-static deformation and in absence of body forces, the equation of equilibrium from the balance of linear momentum is:

$$div\underline{S} = 0 \tag{1}$$

where $\underline{S}$ is the stress in the body. In the absence of body moments, the balance of angular momentum leads to a symmetric stress tensor. The conservation of mass of the fluid in the solid body leads to:

$$\frac{dC}{dt} = - div(\underline{f}) \tag{2}$$

where $\underline{f}$ is the flux of fluid through the polymer, and C is the fluid concentration at the current time. Since it is assumed that the deformation gradient in the body is small ($\|\underline{\nabla U}\| \ll 1$, at all time, where $\underline{U}$ is the displacement field), a linearized strain measure $\underline{E}$ is considered:

$$\underline{E} = \frac{1}{2}(\nabla\underline{U} + \nabla\underline{U}^T) \tag{3}$$

A linear constitutive relation among stress, strain and concentration is considered. For a homogeneous, isotropic and elastic body, the constitutive relation takes the form:

$$\underline{S} = l\,(tr\underline{E})\,\underline{1} + 2G\underline{E} - b\underline{C}\,\underline{1} \tag{4}$$

where λ and G are the elastic material constants, and β governs the coupling between the fluid concentration and stress. It is noted that the elastic constants should satisfy the following inequalities: $G > 0$ and $2G+3\lambda > 0$. If it is expected that the concentration of fluid in a solid body would impose pressure (compressive volumetric stress), then it is necessary that $\beta > 0$, i.e. the concentration of fluid leads to volumetric expansion. A linear relation is also imposed between the flux $\underline{f}$, the concentration gradient and the gradient of the volumetric strain ∇q (with $q = tr\underline{E}$), which is

$$\underline{f} = -D\nabla C + \alpha\nabla\theta \tag{5}$$

Here, D is the diffusivity constant, and α is the coupling constant that measures fluid flow per unit changes of volumetric strain at zero concentration gradient. The diffusivity D should satisfy the condition that $D > 0$, which means the fluid flows in the direction of decreasing concentration at zero gradient of volumetric strain.

Substituting the constitutive equations for the stress and flux into the equations of the balance of linear momentum and conservation of mass of the fluid, the governing equations of the coupled deformation-diffusion are obtained:

$$G\Delta\underline{U} + (\lambda + G)\nabla\theta - \beta\nabla C = 0 \tag{6}$$

$$\frac{\partial C}{\partial t} = D\Delta C - \alpha\Delta\theta \tag{7}$$

Typical specimens used for laboratory-scale moisture sorption tests are thin plate structures (for example, with width/thickness ratios designed by testing standards such as ASTM D5229-92(04)), so that the diffusion process can be assumed to be predominantly in the thickness direction. Thus, the above three-dimensional model is reduced to one-dimensional coupled

diffusion-deformation, where the axial stress, axial strain, and elastic constant reduce to $S_{11}=\sigma$, $E_{11}=\varepsilon$, and Young's modulus E, respectively. In that case, the constitutive equations are:

$$f = -D\frac{\partial C}{\partial x} + \alpha\frac{\partial^2 U}{\partial x^2} \tag{8}$$

$$\sigma = E\varepsilon - \beta C = E\frac{\partial U}{\partial x} - \beta C \tag{9}$$

Imposing the balance of linear momentum and the conservation of mass of the fluid, the following one-dimensional coupled governing differential equations are obtained:

$$\frac{\partial C}{\partial t} = D\frac{\partial^2 C}{\partial x^2} - \alpha\frac{\partial^3 U}{\partial x^3} \tag{10}$$

$$E\frac{\partial^2 U}{\partial x^2} - \beta\frac{\partial C}{\partial x} = 0 \tag{11}$$

In the above equations, both concentration and displacements are time- and space-dependent, that is $C(x,t)$, $U(x,t)$ for one-dimensional case. For the case where the coupling parameter α is neglected, the diffusion equation reduces to Fickian diffusion. The finite difference method is used to solve the above governing equations, as summarized in Section 2.2.

2.2 Finite Difference Approach and Parametric Studies

This section presents a finite difference method used to solve the coupled deformation-diffusion governing equations. Parametric studies are also conducted in order to understand the coupling effects in the diffusion process. For this purpose, consider a thin plate immersed in a fluid

with through-the-thickness diffusion, while the diffusion of fluid from the thin edges through the solid body is neglected. Since the plate is completely immersed, it is assumed that the fluid diffuses into the two wide in-plane surfaces with the same rate and, further, that the diffusion process is symmetric with respect to the central axis of the thickness of the plate. Let half of the thickness of the epoxy plate be *H*, which is discretized with an increment of length Δx, and the total number of segments is *np*, thus $np = \frac{H}{\Delta x}$. The node numbers vary from $n = 0$ to $n = np$.

The finite difference method is used to solve the governing equations (10)-(11), i.e., the one-dimensional diffusion-deformation equations. The time derivatives of the concentration and displacement are defined using the forward difference and mid-point difference, respectively, as the following:

$$\frac{\partial C}{\partial t} \approx \frac{C_n^{m+1} - C_n^m}{\Delta t} \tag{12}$$

$$\frac{\partial C}{\partial x} \approx \frac{C_{n+1}^m - C_{n-1}^m}{2\Delta x} \tag{13}$$

$$\frac{\partial^2 C}{\partial x^2} \approx \frac{C_{n+1}^m - 2C_n^m + C_{n-1}^m}{\Delta x^2} \tag{14}$$

$$\frac{\partial^2 U}{\partial x^2} \approx \frac{U_{n+1}^m - 2U_n^m + U_{n-1}^m}{\Delta x^2} \tag{15}$$

$$\frac{\partial^3 U}{\partial x^3} \approx \frac{U_{n+2}^m - 2U_{n+1}^m + 2U_{n-1}^m - U_{n-2}^m}{2\Delta x^3} \tag{16}$$

where the superscript *m* indicates current time t^m , and the subscript *n* denotes concentration and displacement at node *n*, which is located at $x = n\Delta x$. The differential equations are now transformed into difference equations, which are:

$$C_n^{m+1} = \frac{D\Delta t}{\Delta x^2}(C_{n+1}^m - 2C_n^m + C_{n-1}^m) + \frac{\alpha\Delta t}{2\Delta x^3}(U_{n+2}^m - 2U_{n+1}^m + 2U_{n-1}^m - U_{n-2}^m) + C_n^m \quad (17)$$

$$\frac{E}{\Delta x^2}\left(U_{n+1}^m - 2U_n^m + U_{n-1}^m\right) - \frac{\beta}{2\Delta x}\left(C_{n+1}^m - C_{n-1}^m\right) = 0 \quad (18)$$

Initially, the polymer plate is under dry conditions, and is also stress- and strain-free. Upon immersion, the surfaces of the plate are in contact with a fully saturated fluid, corresponding to a normalized concentration C = 1. The normalized concentration is defined as $C = \frac{M_t - M_{solid}}{M_{fluid}}$, where M_t is the total mass at current time t, M_{solid} is the mass of dry solid, and M_{fluid} is the total mass of fluid at fully saturated conditions. The initial conditions are taken as normalized concentrations $C_n^0 = 0,$ for $n = 0,1,\ldots,np-1$, and $U_n^0 = 0,$ for $n = 0,1,\ldots,np.$ At the boundaries, the following conditions are satisfied at all times (m = 0, 1, ...) : the concentration at the outer surface (right end) remains fully saturated, which is described as $C_{np}^m = 1$. At any time, the right end of the plate is stress-free, i.e. $S_{np}^m = 0$. Due to the symmetric condition imposed on the plate, the displacement at the left boundary is fixed, i.e. $U_0^m = 0$. On the left boundary, a zero flux condition is considered: $f_0^m = 0$. In order to impose the conditions on the left boundary, a forward difference method is used for nodes on or near the left and right boundaries. Thus, the derivatives of the displacement and concentration near the boundaries are:

$$\frac{\partial^3 U}{\partial x^3} \approx \frac{-U_0^m + 3U_1^m - 3U_2^m + U_3^m}{\Delta x^3} \quad \text{and} \quad \frac{\partial^2 C}{\partial x^2} \approx \frac{C_0^m - 2C_1^m + C_2^m}{\Delta x^2}, \quad n = 0$$

$$\frac{\partial^3 U}{\partial x^3} \approx \frac{-3U_0^m + 9U_1^m - 9U_2^m + 3U_3^m}{2\Delta x^3}, \quad n = 1 \quad (19)$$

$$\frac{\partial^3 U}{\partial x^3} \approx \frac{-U^m_{np-3} + 3U^m_{np-2} - 3U^m_{np-1} + U^m_{np}}{\Delta x^3}, \quad n = np - 1$$

As mentioned above, experimental data was obtained by measuring the overall weight and dimension changes in the specimens. The total mass of fluid in the polymeric solids was measured, consistently with the majority of gravimetric studies and ASTM D5229-92(04). In this study, in order to correlate simulation results to the experimental data, it is necessary to quantify the total fluid concentration in the solid body. Concentration was not measured directly during the tests. The total normalized concentration in the polymeric plates form the finite difference approach is defined as:

$$C_t = C^m = \sum_{n=0}^{np-1} \left(\frac{C^m_n + C^m_{n+1}}{2} \right) \Delta x \tag{20}$$

C_t is the total normalized concentration at time t. The relative concentration change in the plate is:

$$C = \frac{C_t}{1' H} \tag{21}$$

where C is the normalized concentration at the current time *t*, which represents the ratio of fluid absorbed by the polymer to the maximum fluid that can be absorbed (concentration of fluid at fully saturated conditions, C = 1).

In order to understand responses from the coupled deformation-diffusion model, parametric studies are presented. Consider a plate with 1 mm thickness, so H is 0.5 mm. Material parameters (elastic modulus E, diffusivity D, and coupling effects β and α) are used in the parametric study (see Table 1). They were chosen based on a range of properties of polymers, i.e., elastic modulus around 2 GPa, diffusivity around 3 x10^{-8}mm^2/s, moisture free expansion around 0.1. For the coupling coefficient α, we consider it to be of the same order as the diffusivity.

Table 1 Summary of the parameters

Coupling term α	$0.0001\frac{mm^2}{hr}$
Coupling term β	$5 \times 10^{12}\,\frac{kg}{mm \cdot hr^2}$
Diffusivity D	$0.0001\frac{mm^2}{hr}$
Young's modulus E	0.77 GPa = $1 \times 10^{13}\,\frac{kg}{mm \cdot hr^2}$
Half height H	0.5 mm

In order to examine the effect of each parameter mentioned above, each specific parameter is varied while fixing the other three material parameters (since the coupling among parameters is assumed negligible in this linear model). This is done to understand the influence of each material parameter on the moisture sorption responses. Figure 1 illustrates the evolution of normalized fluid concentration in the middle of the plate ($x = 0$), at different material parameters. From Figure 1 (top left), it is seen that, as the value of diffusivity increases, the diffusion process becomes faster, as it should be physically expected. Similarly, increasing the material's elastic modulus E accelerates the diffusion process, as shown in Figure 1 (bottom right). However, increasing the values of the coupling parameters slows down the diffusion process, as depicted in Figure 1 (top right and bottom left).

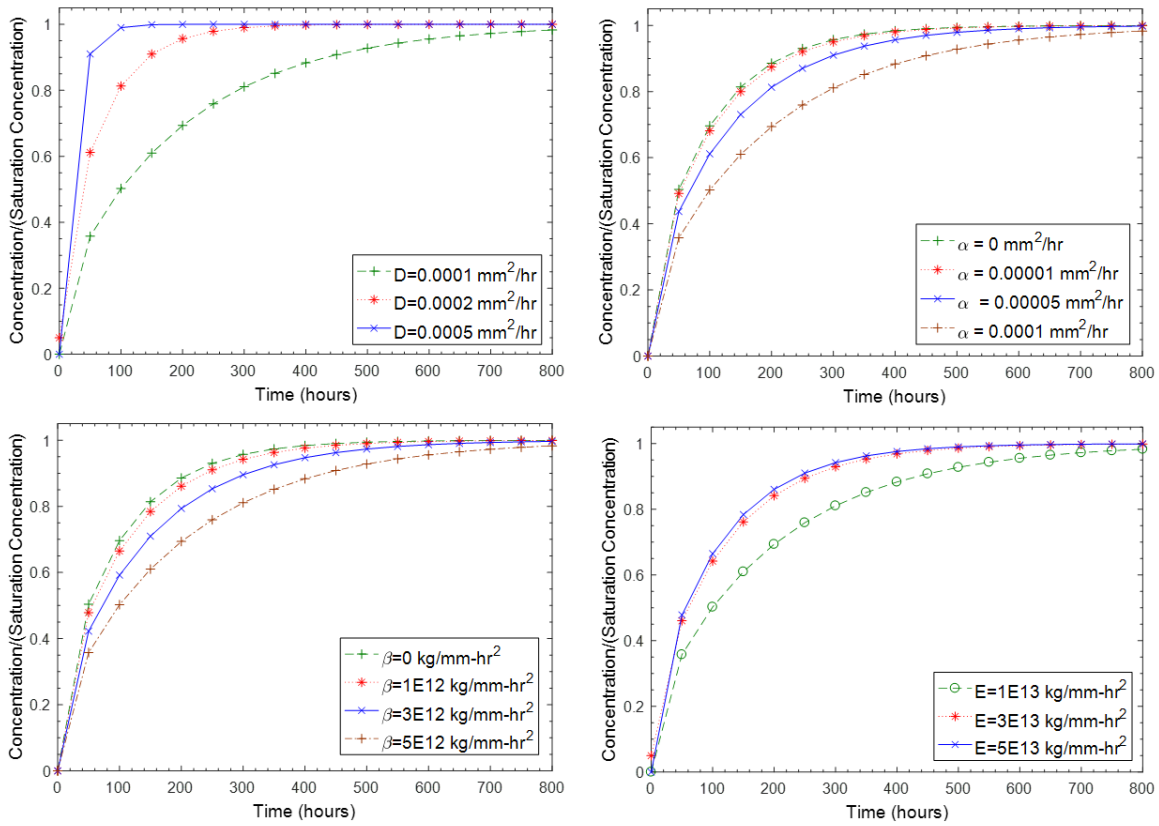

Figure 1. Evolution of the normalized concentration with respect to the concentration at saturation, at the left boundary (x = 0) with varying material parameters: (top left) constant α, β, elastic modulus E; (top right) constant β, diffusivity D, elastic modulus E; (bottom left) constant α, diffusivity D, elastic modulus *E*; (bottom right) constant α, β, diffusivity D.

One-dimensional coupled deformation-diffusion model can describe the volumetric change and moisture diffusion as long as through-thickness diffusion is dominant and the through thickness strain can represent the volume change. The finite difference method is used to solve the governing equations (10) and (11). The time derivatives of the concentration and displacement are defined using the forward difference and mid-point difference, respectively, as the following:

$$\frac{\partial C}{\partial t} \approx \frac{C_{nkl}^{m+1} - C_{nkl}^{m}}{\Delta t} \tag{22.1}$$

$$\frac{\partial C}{\partial x} \approx \frac{C^m_{n+1,kl} - C^m_{n-1,kl}}{2\Delta x} \tag{22.2}$$

$$\frac{\partial C}{\partial y} \approx \frac{C^m_{n,k+1,l} - C^m_{n,k-1,l}}{2\Delta y} \tag{22.3}$$

$$\frac{\partial C}{\partial z} \approx \frac{C^m_{nk,l+1} - C^m_{nk,l-1}}{2\Delta z} \tag{22.4}$$

$$\frac{\partial^2 C}{\partial x^2} \approx \frac{C^m_{n+1,kl} - 2C^m_{nkl} + C^m_{n-1,kl}}{\Delta x^2} \tag{22.5}$$

$$\frac{\partial^2 C}{\partial y^2} \approx \frac{C^m_{n,k+1,l} - 2C^m_{nkl} + C^m_{n,k-1,l}}{\Delta y^2} \tag{22.6}$$

$$\frac{\partial^2 C}{\partial z^2} \approx \frac{C^m_{nk,l+1} - 2C^m_{nkl} + C^m_{nk,l-1}}{\Delta z^2} \tag{22.7}$$

$$\frac{\partial U}{\partial x} \approx \frac{U^m_{n+1,kl} - U^m_{n-1,kl}}{2\Delta x} \tag{22.8}$$

$$\frac{\partial V}{\partial y} \approx \frac{V^m_{n,k+1,l} - V^m_{n,k-1,l}}{2\Delta y} \tag{22.9}$$

$$\frac{\partial W}{\partial z} \approx \frac{W^m_{nk,l+1} - W^m_{nk,l-1}}{2\Delta z} \tag{22.10}$$

$$\frac{\partial^2 U}{\partial x^2} \approx \frac{U^m_{n+1,kl} - 2U^m_{nkl} + U^m_{n-1,kl}}{\Delta x^2} \tag{22.11}$$

$$\frac{\partial^2 V}{\partial y^2} \approx \frac{V^m_{n,k+1,l} - 2V^m_{nkl} + V^m_{n,k-1,l}}{\Delta y^2} \tag{22.12}$$

$$\frac{\partial^2 W}{\partial z^2} \approx \frac{W^m_{nk,l+1} - 2W^m_{nkl} + W^m_{nk,l-1}}{\Delta z^2} \tag{22.13}$$

$$\frac{\partial^3 U}{\partial x^3} \approx \frac{U^m_{n+2,kl} - 2U^m_{n+1,kl} + 2U^m_{n-1,kl} - U^m_{n-2,kl}}{2\Delta x^3} \tag{22.14}$$

$$\frac{\partial^3 V}{\partial y^3} \approx \frac{V^m_{n,k+2,l} - 2V^m_{n,k+1,l} + 2V^m_{n,k-1,l} - V^m_{n,k-2,l}}{2\Delta y^3} \tag{22.15}$$

$$\frac{\partial^3 W}{\partial z^3} \approx \frac{W^m_{nk,l+2} - 2W^m_{nk,l+1} + 2W^m_{nk,l-1} - W^m_{nk,l-2}}{2\Delta z^3} \tag{22.16}$$

$$\frac{\partial^2 U}{\partial x \partial y} \approx \frac{U^m_{n+1,k+1,l} - U^m_{n,k+1,l} - U^m_{n+1,k,l} + U^m_{nkl}}{\Delta x \Delta y} \tag{22.17}$$

$$\frac{\partial^2 U}{\partial x \partial z} \approx \frac{U^m_{n+1,k,l+1} - U^m_{n,k,l+1} - U^m_{n+1,k,l} + U^m_{nkl}}{\Delta x \Delta z} \tag{22.18}$$

$$\frac{\partial^2 W}{\partial x \partial z} \approx \frac{W^m_{n+1,k,l+1} - W^m_{n,k,l+1} - W^m_{n+1,k,l} + W^m_{nkl}}{\Delta x \Delta z} \tag{22.19}$$

$$\frac{\partial^2 V}{\partial x \partial y} \approx \frac{V^m_{n+1,k+1,l} - V^m_{n,k+1,l} - V^m_{n+1,k,l} + V^m_{nkl}}{\Delta x \Delta y} \tag{22.20}$$

$$\frac{\partial^2 W}{\partial y \partial z} \approx \frac{W^m_{n,k+1,l+1} - W^m_{n,k,l+1} - W^m_{n,k+1,l} + W^m_{nkl}}{\Delta y \Delta z} \tag{22.21}$$

$$\frac{\partial^2 V}{\partial y \partial z} \approx \frac{V^m_{n,k+1,l+1} - V^m_{n,k,l+1} - V^m_{n,k+1,l} + V^m_{nkl}}{\Delta y \Delta z} \tag{22.22}$$

$$\frac{\partial^3 V}{\partial x^2 \partial y} \approx \frac{(V^m_{n+1,k+1,l} - 2V^m_{n,k+1,l} + V^m_{n-1,k+1,l}) - (V^m_{n+1,kl} - 2V^m_{n,kl} + V^m_{n-1,kl})}{\Delta x^2 \Delta y} \tag{22.23}$$

$$\frac{\partial^3 U}{\partial x \partial y^2} \approx \frac{(U^m_{n+1,k+1,l} - 2U^m_{n+1,kl} + U^m_{n+1,k-1,l}) - (U^m_{n,k+1,l} - 2U^m_{nkl} + U^m_{n,k-1,l})}{\Delta x \Delta y^2} \tag{22.24}$$

$$\frac{\partial^3 W}{\partial x^2 \partial z} \approx \frac{(W^m_{n+1,k,l+1} - 2W^m_{nk,l+1} + W^m_{n-1,k,l+1}) - (W^m_{n+1,kl} - 2W^m_{nkl} + W^m_{n-1,kl})}{\Delta x^2 \Delta z} \tag{22.25}$$

$$\frac{\partial^3 W}{\partial y^2 \partial z} \approx \frac{(W^m_{n,k+1,l+1} - 2W^m_{nk,l+1} + W^m_{n,k-1,l} + 1) - (W^m_{n,k+1,l} - 2W^m_{nkl} + W^m_{n,k-1,l})}{\Delta y^2 \Delta z} \tag{22.26}$$

$$\frac{\partial^3 U}{\partial x \partial z^2} \approx \frac{(\mathrm{U}^m_{n+1,k,l+1} - 2U^m_{n+1,kl} + U^m_{n+1,k,l-1}) - (\mathrm{U}^m_{nk,l+1} - 2U^m_{nkl} + U^m_{nk,l-1})}{\Delta x \Delta z^2} \tag{22.27}$$

$$\frac{\partial^3 V}{\partial y \partial z^2} \approx \frac{(V^m_{n,k+1,l+1} - 2V^m_{n,k+1,l} + V^m_{n,k+1,l-1}) - (V^m_{nk,l+1} - 2V^m_{n,kl} + V^m_{nk,l-1})}{\Delta y \Delta z^2} \tag{22.28}$$

where the superscript *m* indicates current time t^m, and the subscript *n,k,l* denotes concentration and displacement at node *nkl*, which is located at $x = n\Delta x$, $y = k\Delta y$ *and* $z = l\Delta z$. The differential equations can now be transformed into difference equations.

Initially, the polymer is at dry condition and upon immersion, the outer surfaces of the specimens are in contact with a fully saturated fluid, corresponding to a normalized concentration $C = 1$. The total fluid concentration in the solid body from the three-dimensional finite difference approach results is quantified as follows. Figure 2 shows a schematic of a set of eight finite difference nodes on the vertices of a rectangular parallelepiped. The concentration in the volume of rectangular parallelepiped between the eight nodes C^m_{rp} is represented by:

$$C^m_{rp} = \frac{1}{8}(C^m_{nkl} + C^m_{n,k+1,l} + C^m_{n,k,l+1} + C^m_{n,k+1,l+1} + C^m_{n+1,kl} + C^m_{n+1,k+1,l} + C^m_{n+1,k,l+1} + C^m_{n+1,k+1,l+1}) \tag{23}$$

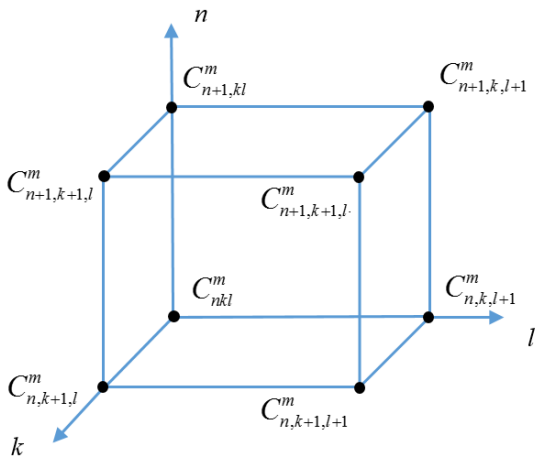

Figure 2. A schematic of three-dimensional finite difference approach.

The total normalized concentration in the polymeric specimen from the finite difference approach is defined as:

$$C_t = C^m = \sum_{r=1}^{r} \left(C^m_{rp}\right) \Delta V \tag{24}$$

where r is the number of rectangular parallelepiped and C_t is the total normalized concentration at time t. The relative concentration change in the polymeric specimen is:

$$C = \frac{C_t}{1 \times V} \tag{25}$$

where V is the volume of the specimen and C is the normalized concentration at the current time t, which represents the ratio of fluid absorbed by the polymer to the maximum fluid that can be absorbed (concentration of fluid at fully saturated conditions, $C = 1$).

3. CONSTITUTIVE MODEL FOR ANISOTROPIC DIFFUSION*

When dealing with isotropic materials, it is possible to predict the fluid diffusion by applying the Fickian model or the coupled deformation-diffusion model depending on how much the volume changes during moisture diffusion. The diffusivity of an fiber-reinforced composite is anisotropic [80] and the diffusivity along the fibers is different from the diffusivity across the fibers. The glass fibers themselves are often seen as non-permeable to water, assuming to have zero diffusivity. The existing theories could not predict the anisotropic behavior found experimentally and a new approach had to be developed for describing the diffusion along and across fiber directions.

In order to describe the anisotropic diffusion behavior, the effects of fibers should be included in the diffusion model. Shen and Springer formulated an anisotropic diffusion model by considering the diffusivity of fiber and the fiber volume content. The model is established on the similarities between heat conduction and moisture diffusion through the material. Springer model attempted to include the effects of fibers and the anisotropy of the material by adopting the model of thermal conduction in unidirectional materials. The anisotropic thermal conductivities were introduced by Springer and Tsai [90]:

*Reprinted with permission from "Micromechanical modeling of anisotropic water diffusion in glass fiber epoxy reinforced composites" by A. Gagani, Y. Fan, A. Muliana, A. Echtermeyer, 2017. Journal of Composite Materials, doi: 10.1177/0021998317744649, Copyright 2017 by SAGE Publications

$$K_{11} = (1-\nu_f)K_r + \nu_f K_f \tag{26}$$

$$K_{22} = (1-2\sqrt{\frac{\nu_f}{\pi}})K_r + \frac{K_r}{B_K}\left[\pi - \frac{4}{\sqrt{1-\frac{B_K^2\nu_f}{\pi}}}\tan^{-1}\frac{\sqrt{1-\frac{B_K^2\nu_f}{\pi}}}{1+\frac{B_K^2\nu_f}{\pi}}\right] \tag{27}$$

$$B_K = 2(\frac{K_r}{K_f}-1) \tag{28}$$

Shen and Springer [77] developed the expression of the diffusivities in the directions parallel and normal to the fibers (D_{11} and D_{22}) (longitudinal and transverse directions). The Springer model takes into account the different diffusivities of the fiber and matrix, and also the volume fraction of the fiber in the FRP composites. For FRP, the Springer model is given by:

$$D_{11} = (1-\nu_f)D_r + \nu_f D_f \tag{29}$$

$$D_{22} = (1-2\sqrt{\frac{\nu_f}{\pi}})D_r + \frac{D_r}{B_D}\left[\pi - \frac{4}{\sqrt{1-\frac{B_D^2\nu_f}{\pi}}}\tan^{-1}\frac{\sqrt{1-\frac{B_D^2\nu_f}{\pi}}}{1+\frac{B_D^2\nu_f}{\pi}}\right] \tag{30}$$

$$B_D = 2(\frac{D_r}{D_f}-1) \tag{31}$$

where v_f is the volume fraction of the fiber, D_f is the diffusivity of the fiber and D_r is the diffusivity of the matrix. It should be noted that the Springer model considers an isotropic diffusion property for fibers. As a result, there is only one diffusivity term for fiber, namely D_f. The Springer model is valid for a fiber volume fraction (v_f) less than 0.785. The Springer model

reduces to the Fickian diffusion when the fiber volume fraction is zero, which means the material is pure resin. It is noted that Eqs. (30) and (31) also impose a constraint to the ratio of the matrix and fiber diffusivity, $\frac{D_r}{D_f} < 1 + 0.5\sqrt{\frac{\pi}{v_f}}$.

When the diffusivity of the fiber (D_f) is assumed to be small compared to the diffusivity of the matrix (D_r), and D_{11} and D_{22} for the Springer model are expressed as:

$$D_{11} = (1 - v_f) D_r \tag{32}$$

$$D_{22} = (1 - 2\sqrt{\frac{v_f}{\pi}}) D_r \tag{33}$$

In this study, the Springer model under-predicts the moisture absorption in FRP composites, as will be shown later in this manuscript. The reason could be that the Springer model did not consider the fiber and matrix arrangements, and it is mainly for 1D diffusion in two different fiber axes. In order to improve the results, a micromechanical model for thermal conduction in unidirectional FRP developed by Muliana and Kim [65] is adopted. This model has been recently used for predicting the anisotropic diffusion in GFRP composites (Gagani et al. [33]). The micromechanics model incorporates the anisotropic diffusivity of the fiber $\mathbf{D}^{(f)}$ =diag($D_{11}^{(f)}$, $D_{22}^{(f)}$, $D_{33}^{(f)}$) while assuming isotropic diffusivity of the matrix $\mathbf{D}^{(m)} = D^{(m)} \mathbf{I}_3$, where $\mathbf{I}_3$ is the identity matrix.

The micromechanics model based on mainly the diffusivities of the resin and fiber bundles in the composite. The model is formulated to determine the overall (homogenized) anisotropic diffusivity of FRP composites, comprising of unidirectional fibers embedded in matrix. The micromechanics model is based on a simple unit-cell with four fiber and matrix subcells, as depicted in Figure 3.

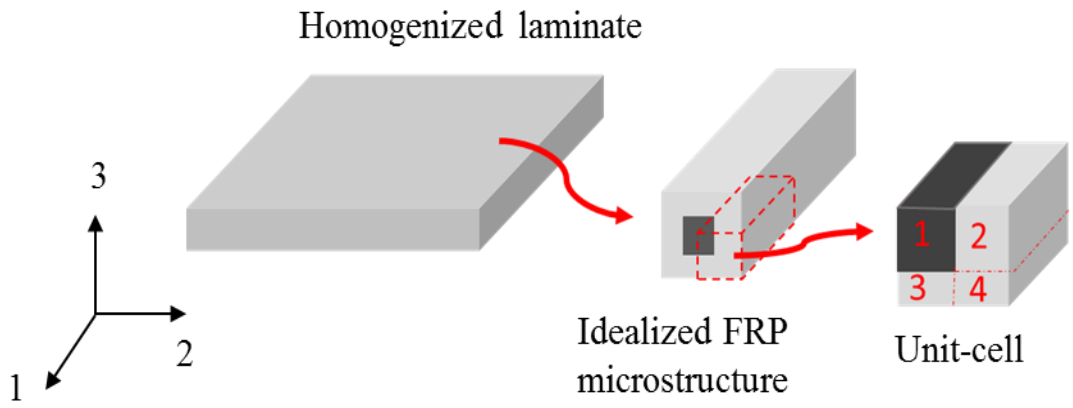

Figure 3. A simplified microstructure of FRP composite.

This unit-cell model has been successfully used to determine the mechanical and non-mechanical response of FRP composites, such as thermo-viscoelastic, piezoelectric, and heat conduction behaviors [3, 64, 65]. The first subcell is the fiber constituent and the remaining subcells are matrix. It is noted here that the fiber constituent in case of typical FRP composite is actually a fiber bundle that consists of fiber filaments. Thus, fluid can penetrate within the filaments inside the fiber bundle, which might explain the relatively high diffusivity along the fiber direction in FRP composites. Perfect bonding at the interphases between the fiber bundle and matrix is assumed, and a periodic boundary condition is imposed on the unit-cell.

In determining the diffusivity of the composite, it is also assumed that volumetric expansion (swelling) is negligible, thus both fiber and matrix diffusion behaviors follow the Fickian diffusion. The flux of the fluid that passed through the homogenized composite faces, $\bar{\mathbf{f}}$, is formulated based on the volume average of the flux in the four subcells:

$$\bar{\mathbf{f}} = \frac{1}{V}\sum_{\alpha=1}^{4}\mathbf{f}^{(\alpha)}\left(\mathbf{X}^{(\alpha)}\right)dV^{(\alpha)} \approx \frac{1}{V}\sum_{\alpha=1}^{4}V^{(\alpha)}\mathbf{f}^{(\alpha)} \tag{34}$$

where $\mathbf{f}^{(\alpha)}$ and $V^{(\alpha)}$ are the flux and volume of subcell (α), respectively, and and $\mathbf{X}^{(\alpha)}$ is the spatial location of each point within the unit-cell. It is also assumed that field variables within one subcell are uniformly distributed. A total volume of the unit-cell is $V = \sum_{\alpha=1}^{4} V^{(\alpha)}$. When the fiber volume fraction is considered, then $V = \sum_{\alpha=1}^{4} V^{(\alpha)}$=1. The flux in the composite is formed due to the gradient of fluid concentration and a linear relation is considered between the flux and concentration gradient in the homogenized composite:

$$\bar{\mathbf{f}} = -\bar{\mathbf{D}}\,\bar{\boldsymbol{\varphi}}; \quad \bar{\boldsymbol{\varphi}} = grad(C) \tag{35}$$

Here $\bar{\mathbf{D}}$ and $\bar{\boldsymbol{\varphi}}$ are the effective diffusivity and concentration gradient of the homogenized composite, respectively, and C is the water concentration in the homogenized composite which is time and spatial dependent. The concentration gradient of the homogenized composite is related to the concentration gradient of each subcell by formulating a concentration matrix for each subcell $\mathbf{B}^{(\alpha)}$. The idea of formulating the concentration matrix to relate the field variables of the constituents to the field variable of the composite was originally proposed by Hill[42] for a linear elastic response of composites. The concentration gradient in each subcell is given by:

$$\boldsymbol{\varphi}^{(\alpha)} = \mathbf{B}^{(\alpha)}\bar{\boldsymbol{\varphi}} \tag{36}$$

A linear relation like in Eq. (35) is adopted for the constitutive relation in each subcell:

$$\mathbf{f}^{(\alpha)} = -\mathbf{D}^{(\alpha)}\boldsymbol{\varphi}^{(\alpha)} \tag{37}$$

where $\mathbf{D}^{(\alpha)}$ is the subcell diffusivity. Substituting Eq. (36) into Eq. (37) gives:

$$\mathbf{f}^{(\alpha)} = -\mathbf{D}^{(\alpha)}\mathbf{B}^{(\alpha)}\bar{\boldsymbol{\varphi}} \tag{38}$$

Substituting Eq. (38) into Eq. (34) gives the effective flux in terms of diffusivity properties of the constituents and volume content:

$$\bar{\mathbf{f}} \approx -\frac{1}{V}\sum_{\alpha=1}^{4} V^{(\alpha)}\mathbf{D}^{(\alpha)}\mathbf{B}^{(\alpha)}\bar{\boldsymbol{\varphi}} \tag{39}$$

Finally, the effective diffusivity of the composite is determined by comparing Eq. (35) and Eq. (39):

$$\bar{\mathbf{D}} = \frac{1}{V}\sum_{\alpha=1}^{4} V^{(\alpha)}\mathbf{D}^{(\alpha)}\mathbf{B}^{(\alpha)} \tag{40}$$

The conservation of mass of the fluid in the composite body leads to:

$$\frac{dC}{dt} = -Div(\bar{\mathbf{f}}) \tag{41}$$

where *t* denotes the time variable.

In order to determine the diffusion behavior and diffusivity of the homogenized composite, micromechanical relations between the subcells need to be obtained. Consider a unit-cell model in Figure 3 placed in the Cartesian coordinate, with fibers are aligned in 1 direction, and 2 and 3 are the directions lateral and transverse to the fiber composite. The flux and water concentration along the fiber direction are expressed as:

$$V^{(1)}f_1^{(1)} + V^{(2)}f_1^{(2)} + V^{(3)}f_1^{(3)} + V^{(4)}f_1^{(4)} = \bar{f}_1 \tag{42}$$

$$\varphi_1^{(1)} = \varphi_1^{(2)} = \varphi_1^{(3)} = \varphi_1^{(4)} = \bar{\varphi}_1 \tag{43}$$

The flux and water concentration across the fiber direction are expressed as:

$$f_2^{(1)} = f_2^{(2)} \tag{44}$$

$$f_2^{(3)} = f_2^{(4)} \tag{45}$$

$$\frac{V^{(1)}}{V^{(1)}+V^{(2)}}\varphi_2^{(1)} + \frac{V^{(2)}}{V^{(1)}+V^{(2)}}\varphi_2^{(2)} = \bar{\varphi}_2 \tag{46}$$

$$\frac{V^{(3)}}{V^{(3)}+V^{(4)}}\varphi_2^{(3)}+\frac{V^{(4)}}{V^{(3)}+V^{(4)}}\varphi_2^{(4)}=\bar{\varphi}_2 \tag{47}$$

$$f_3^{(1)}=f_3^{(3)} \tag{48}$$

$$f_3^{(2)}=f_3^{(4)} \tag{49}$$

$$\frac{V^{(1)}}{V^{(1)}+V^{(3)}}\varphi_3^{(1)}+\frac{V^{(3)}}{V^{(1)}+V^{(3)}}\varphi_3^{(2)}=\bar{\varphi}_3 \tag{50}$$

$$\frac{V^{(2)}}{V^{(2)}+V^{(4)}}\varphi_3^{(3)}+\frac{V^{(4)}}{V^{(2)}+V^{(4)}}\varphi_3^{(4)}=\bar{\varphi}_3 \tag{51}$$

The volume fractions of the four subcells are expressed in terms of the volume fraction of the fiber V_f, which are:

$$\begin{aligned} &V^{(1)}=V_f; \qquad 0\le V_f\le 1\\ &V^{(2)}=V^{(3)}=\sqrt{V_f}-V_f\\ &V^{(4)}=1-2\sqrt{V_f}+V_f \end{aligned} \tag{52}$$

Using the micromechanical relations, Eqs. (42)-(51) and constitutive relations for the constituents in Eq. (37), the concentration matrix for each subcell can be obtained. Finally, the effective diffusivity is determined from Eq. (40). In this study, the fiber bundle is assumed transversely isotropic and the polymeric matrix is considered isotropic with regards to their diffusion behaviors. The fiber diffusivity is $\mathbf{D}^{(f)}$ =diag($D_{11}^{(f)}$, $D_{22}^{(f)}$, $D_{22}^{(f)}$), while the diffusivity of matrix is $\mathbf{D}^{(m)} = D^{(m)}\,\mathbf{I}_3$, where $\mathbf{I}_3$ is the identity matrix. The diffusivity of the composite is given as:

$$\bar{\boldsymbol{D}}=diag(\bar{D}_{11},\bar{D}_{22},\bar{D}_{33});\ \ \bar{D}_{33}=\bar{D}_{22} \tag{53}$$

$$\bar{D}_{11}=\frac{1}{V}\left(V^{(1)}D_{11}^{(f)}+V^{(2)}D^{(m)}+V^{(3)}D^{(m)}+V^{(4)}D^{(m)}\right) \tag{54}$$

$$\bar{D}_{22}=\frac{1}{V}\left(V^{(1)}\frac{D^{(m)}D_{22}^{(f)}\left(V^{(1)}+V^{(2)}\right)}{V^{(1)}D^{(m)}+V^{(2)}D_{22}^{(f)}}+V^{(2)}\frac{D^{(m)}D_{22}^{(f)}\left(V^{(1)}+V^{(2)}\right)}{V^{(1)}D^{(m)}+V^{(2)}D_{22}^{(f)}}+V^{(3)}D^{(m)}+V^{(3)}D^{(m)}\right) \tag{55}$$

In order to solve for the governing equation in Eq. (41), the finite element (FE) method is used and the constitutive relation in Eq. (39) is implemented at each Gaussian point within continuum 3-D elements. Each continuum element has eight nodes. The concentration of the fluid is evaluated at the nodes. The total amount of fluid concentration in the composite during the diffusion process is determined as follows;

$$C(t) = \frac{1}{V}\sum_{m=1}^{Ne} C^{(m)}\Delta V^{(m)}\,; \quad C^{(m)} = \frac{1}{8}\sum_{i=1}^{8} C_i^{(m)} \tag{56}$$

where *Ne* is total number of finite elements used in solving the diffusion equation in the composite body. The amount of fluid concentration at each instant of time in Eq. (56) is correlated to the fluid concentration obtained from experiment. The total fluid concentration is related to the fluid uptake as follow:

$$C(t) = \frac{M(t)}{M_\infty} \tag{57}$$

The micromechanics model is implemented in a continuum three-dimensional finite element. At each Gaussian integration point within the element, the constitutive model for the diffusion behavior is determined from the micromechanics model. In this study the user material subroutine within ABAQUS commercial FE, written in Fortran, is used to integrate the micromechanics model to FE analyses. For the post-processing, the total amount of fluid in the composites is determined by integrating the field variables at the nodes obtained from the FE analyses. For this purpose a Matlab code was generated for reading the nodal field variables and numerically integrating them to obtain the overall fluid concentration.

In order to simulate the fluid sorption mimicking the FRP and resin specimens, finite element meshes with 8 node hexahedral elements were generated for the plate with dimension

50x50x1.5mm. A convergence study was first conducted in order to determine sufficient numbers of elements by comparing the overall fluid concentration to the analytical solution of isotropic diffusion in resin. In this study, a total of 4000 elements was sufficient in capturing the fluid sorption response. Figure 4 shows the FE meshes.

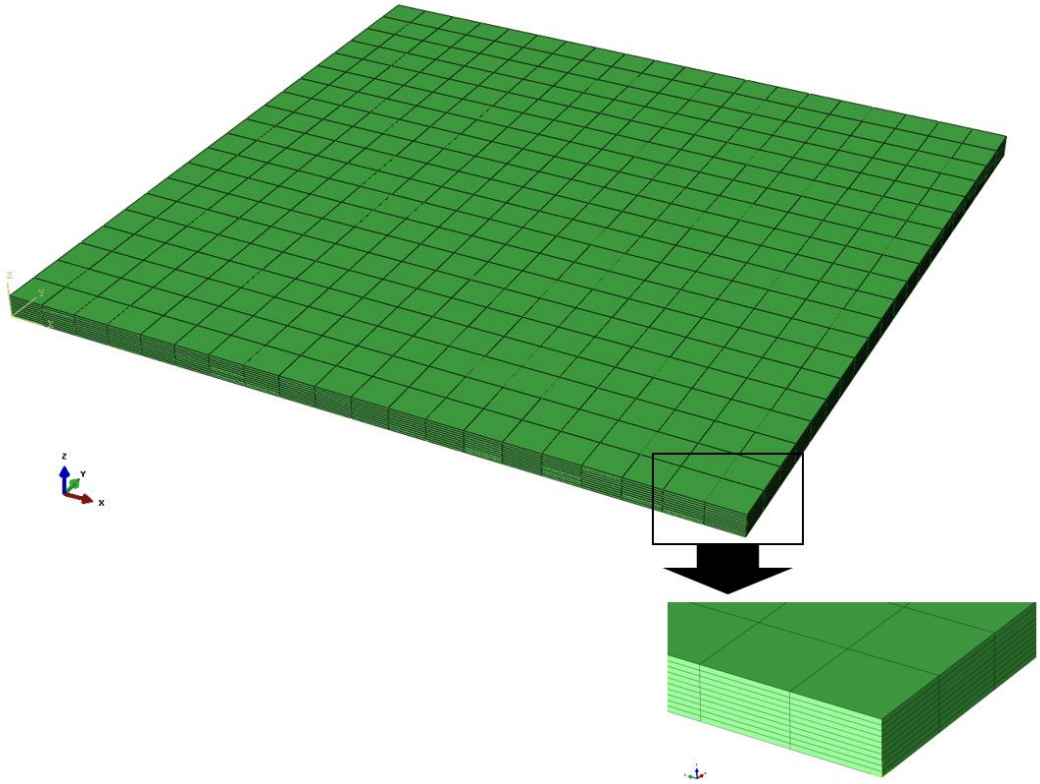

Figure 4. Mesh used for the FE analysis.

Parametric studies are performed to analyze the effects of anisotropic diffusion properties of fibers. The micromechanics model is used. As for the collaboration with Professor Andreas Echtermeyer's lab, two sets of parametric studies are performed. Namely the parallel set and the transverse set. Brief discussion on the two sets of testing will be included in Section 4. The

purpose of this parametric study is to guide the material parameter characterization, i.e., $D_{11}^{(f)}$, $D_{22}^{(f)}$ of the fiber bundles. The matrix is assumed to be isotropic and its diffusivity is calibrated from experiment. The fiber is assumed to be transversely isotropic and the diffusivities along and transverse to the fiber direction, namely D_{11} and D_{22} are examined. In order to understand the effects of diffusion parameters, each diffusivity is varied while fixing the other diffusivity. The micromechanics model is used in the parametric study. Figure 5 illustrates the water uptake response in FRP parallel to the fiber axis. It is seen that the transverse diffusivity of the fiber bundle ($D_{22}^{(f)}$) has insignificant influence on the diffusion response in the parallel fiber direction. The diffusion in the parallel direction is governed by the axial diffusivity of the fiber, diffusion of the matrix, and fiber volume content. Figure 6 shows the diffusion response along the transverse fiber direction. In this case, the transverse fiber diffusivity ($D_{22}^{(f)}$) has a significant effect while the axial fiber diffusivity ($D_{11}^{(f)}$) has insignificant effect, which is expected. This information can guide the determination of the anisotropic fiber diffusivity from the experimental data.

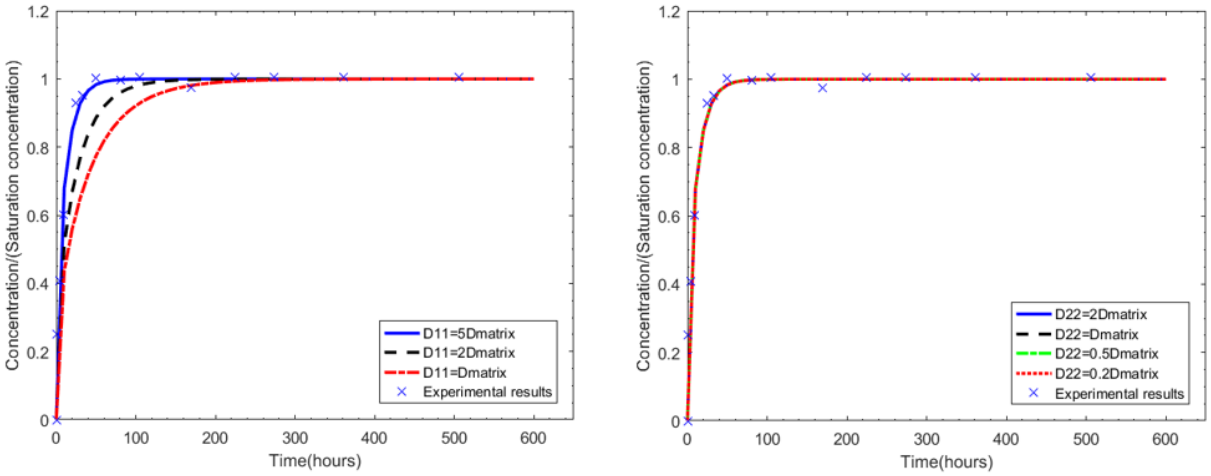

Figure 5. Diffusion response of FRP in the parallel fiber direction: the effect of fiber anisotropy.

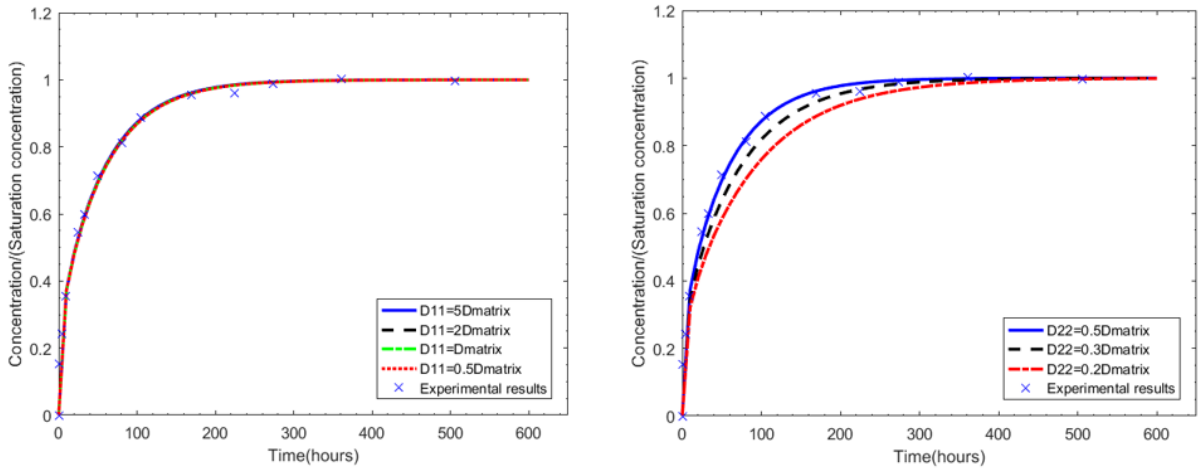

Figure 6. Diffusion response of FRP in the transverse fiber direction: the effect of fiber anisotropy.

Parametric study is also performed based on the testing date from Professor La Saponara's lab. And the results show the same trends compared to the results of Professor Andreas Echtermeyer's data. Figure 7 show the diffusion response in the transverse fiber direction. It can be seen that the diffusion in the transverse direction is governed by the

diffusivity transverse to the fiber direction (D_{22}), while the effects of diffusivity along the fiber direction (D_{11}) is insignificant. The results of this parametric study can help determining the diffusion parameters from experimental data.

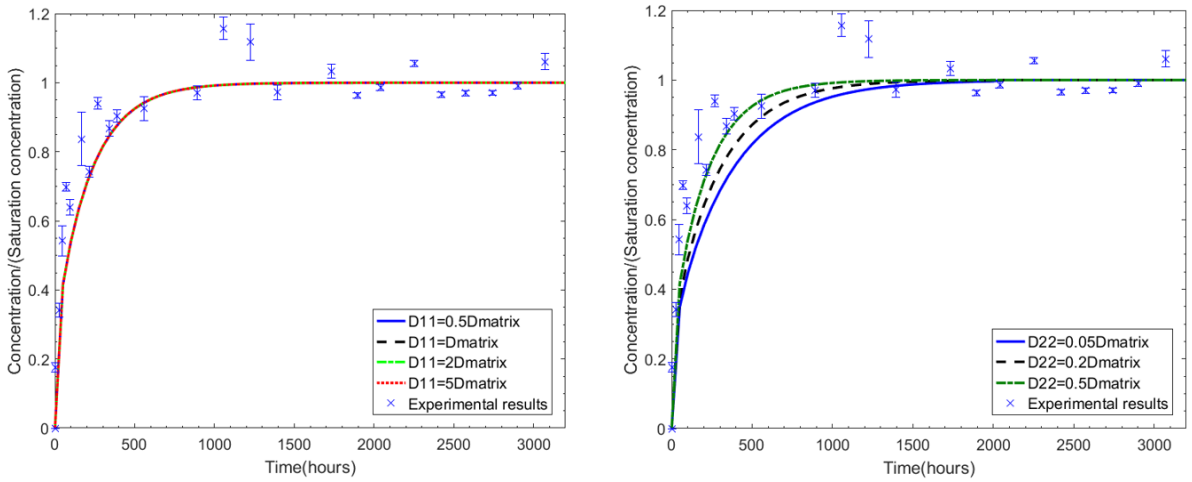

Figure 7. Diffusion response with varying diffusivities along the fiber direction (left) and transverse to the fiber direction (right).

4. EXPERIMENTAL VALIDATION

The goal of this research is to model the fluid diffusion in polymers and polymer composites. This research is also a multi-scale experiment and modeling approach in order to understand the heterogeneities diffusion behavior in sandwich composites at various scales: skin, core, fiber-matrix constituents. The research was collaborated with Professor Valeria La Saponara's research group from University of California Davis. Manufacturing of polymer sandwich composites and immersion tests were performed by Professor Valeria La Saponara and her students. The first part of the experimental work was to quantify the effect of the sorption of fluid (deionized water, saline solution mimicking sea water) on the weight, dimension and mechanical properties of samples from the five structural polymers of the sandwich composites, epoxy, vinylester, polyurethane foam, PVC foam, GFRP coupons. This was used to support the development of the constitutive and multi-scale models of fluid sorption. Then tests on sandwich composites specimens was conducted in order to understand the fluid sorption behavior in sandwich composites and validate the constitutive models. This dissertation only includes some key information of the samples and testing procedures. Detailed material preparation and testing procedures are recorded in Fan et al [30].

This research is also collaborated with Professor Andreas Echtermeyer's research group from Norwegian University of Science and Technology. The goal of the collaboration is to understand the anisotropic diffusion behavior in fiber reinforced composites. Diffusivity in the fiber direction is faster than in the transverse direction and current models cannot capture this behavior. Professor Andreas Echtermeyer and his students manufactured GFRP specimens and performed experimental tests to record the mass change of the specimens that fully immersed in

fluids. Section 5 includes brief discussion on the experiments and the details can be found in the published journal paper[33].

4.1 Definition of Parameters

The materials tested in the experiments include the structural polymers of sandwich composites and sandwich composites itself. Different geometry of the specimens was designed based on manufacturability and the widely accepted testing standard ASTM D5229-92(04).

According to the requirements from ASTM D5229-92(04), epoxy, vinyl ester and GFRP specimens are manufactured in the way to maximize the width-to-thickness ratio. And the dimensions of the specimens will be discussed in this chapter. All specimens had open edges. Sealing the edges with aluminum foil or stainless steel was not included in the experiments. The sealant is often glued to the small surface of the samples' edges. The glue may absorb fluids during the test and the seal may fall off from the samples after a long exposure period. Polyurethane foam specimens, PVC foam specimens and sandwich composites specimens were not manufactured based on the ASTM testing standard. The geometries and material calibration method will be discussed in Section 5.

The samples were fully immersed inside custom-made tanks. Different combinations of solid, temperature and fluid are chosen to examine whether the model considered in this study is general enough for different polymers immersed in different fluids under different temperature. In order to record the mass and geometry change of the specimens, the samples were removed from the fluid and weighed following the procedure of ASTM D5229-92(04). In the collaboration with UC Davis, the dimensions of the specimens were also recorded with a caliper

with repeated measurements across the width, the thickness and the length. The parameters used in this dissertation to describe the mass and geometry changes are discussed below.

The percent mass change of each specimen is defined as:

$$M\% = \frac{M_t - M_{solid}}{M_{solid}} \times 100\% \tag{58}$$

where $M\%$ is the percent mass change of the polymeric samples, M_t is the current mass of the combined fluid and solid at time *t*, and M_{solid} is the mass of solid measured before its immersion, at ambient hygrothermal conditions. Alternatively, one can present the percent mass changes during diffusion, by using the amount of concentration of fluid in the solid body. In order to express the percent mass changes in terms of concentration of fluid in the solid polymers, the concentration of the fluid is determined as follows:

$$C = \frac{M_t - M_{solid,o}}{M_{fluid}} \tag{59}$$

where M_t is the mass of the polymer + sorbed fluid at time *t*, and $M_{solid,o}$ is the mass of polymer before immersion. M_{fluid} is the mass of fluid when the polymer is fully saturated. Thus, the concentration has values between 0 (in absence of fluid) and 1 (fully saturated). The percent volume change in the specimen is determined as:

$$V\% = \frac{V_t - V_{solid}}{V_{solid}} \times 100\% \tag{60}$$

where $V\%$ is defined as percent volume change and V_t is the volume of the polymer + sorbed fluid at time *t*. V_{solid} is the volume of the polymer measured before its immersion, at ambient hygrothermal conditions.

In this study, a one-dimensional diffusion process is considered for some thin specimens, thus it is necessary to relate the volume changes to the through-the-thickness deformation of the specimens in the thickness direction. For this purpose, the through-the-thickness strain of the plate is determined as:

$$e = \frac{z_t - z_o}{z_o} \tag{61}$$

z_t is the thickness of the polymer + sorbed fluid at time *t*, and z_o is the thickness of the polymer before immersion.

4.2 Fluid Diffusion in Polymer Resins

This section concerns with the diffusion of liquid through solid polymers at two different temperatures, and examines the effect of moisture-induced deformations on the polymer diffusion process. Two polymers namely epoxy and vinylester, which are commonly used as matrix in fiber-reinforced composites and two polymeric foams namely polyurethane foam and PVC foam are studied. Experimental data are obtained from UC Davis and the following tests have been conducted in order to examine the overall performance of these polymers under moisture diffusion at different temperatures. The specimens were immersed in fluid (deionized and saline water) at room temperature and at 50^{o}C. During the sorption process, the weight and volume (dimension) changes in the specimens were monitored periodically. It shows that elevated temperature accelerates the diffusion process in the polymer. Some of the polymers show more significant volume changes in addition to weight changes during the diffusion process, while for some other polymers volume changes are quite negligible. This issue will be

discussed later in this proposal. It is noted that the measured volume changes in these tested polymers are relatively small (around 10% or less), as compared to those of some other polymers (e.g. polydimethylsiloxane, PDMS, and polysuccinimide) and hydrogels, where volumetric swelling due to fluid sorption can be larger than 200%.

Square samples were made with nominal dimensions of 1.5 mm thickness and 150 mm width, according to the requirements for one-dimensional diffusion from ASTM D5229-92(04). The specimens are made into nominally square plates with dimension that satisfy the relation:

$$\frac{w}{h} \geq 100 \tag{62}$$

where w is the nominal length of one side and h is the nominal thickness.[8] The materials and the average dimensions from three samples of the polymeric specimens can be found in Table 2.

Epoxy samples were fully immersed inside two custom-made tanks, one containing deionized water, the other containing a solution of deionized water and 3.5 % wt. content of NaCl, which simulates sea water. Vinylester samples were immersed only in the saline solution. Experimental data is obtained by measuring the overall weight and dimension changes in the specimens. These three combinations of solid and fluid are chosen to examine whether the model considered in this study is general enough for different polymers immersed in different fluids.

Tests were conducted at room temperature and at 50 °C (in the latter case, immersion heaters were used). The 50 °C was selected to be representative of a service temperature for a fiber-reinforced polymeric structure, and it is below the published glass transition temperature of the epoxy (between 67 °C and 90 °C for the selected cure cycle, depending on the type of test). Information of the type of fluid used for immersion and the temperature are also given in Table 2.

In addition to the square samples mentioned above, dogbone samples of epoxy and vinylester were manufactured and immersed respectively in deionized water and in saline water at room temperature and at 50°C, for the purpose of testing of residual tensile properties.

Table 2 Average dimensions of square plate specimens

Materials	Temperature	Thickness(mm)	Length(mm)	Width(mm)
Epoxy/deionized water	Room	1.29	149.74	150.91
	50°C	1.30	150.74	149.44
Epoxy/saline water	Room	1.48	151.23	150.92
	50°C	1.53	150.93	150.01
Vinylester/saline water	Room	1.30	151.48	152.37
	50°C	1.28	149.93	149.81

The Fickian diffusion is first considered in order to determine the diffusivity of these polymers immersed in different fluids. The Fickian diffusion models the diffusion of fluid through a rigid solid body, and is often used to describe moisture diffusion in glassy polymers. The calibration of diffusivity is performed following ASTM D5229-92(04). The diffusivity D is obtained by measuring the slope of the linear section of the percent mass change versus square root of time plot. Figure 8 is an example of percent mass change versus square root of time graph (linear section) and it shows that initially the percent mass change is proportional to the square root of time. For one-dimensional diffusion, the diffusivity D is obtained using the following equation:

$$D = \pi \left(\frac{h}{4M_m} \right)^2 \left(\frac{M_2 - M_1}{\sqrt{t_2} - \sqrt{t_1}} \right)^2 \tag{63}$$

where $h = 2H$ is the thickness of the polymer plate, M_m is the maximum moisture content (maximum percent mass change). Table 3 presents diffusivities for the tested polymers in different fluids at two temperatures. It is seen that, for both epoxy and vinylester, the diffusivity increases significantly with increasing temperature, which leads to faster fluid sorption. With respect to results in the literature, the authors are not aware of similar studies on exactly these materials in these particular conditions. Scott and Lees [74] state that water absorption may differ significantly among different resin types, and is affected also by curing formulations. The scatter present in the diffusivities of the current study is comparable to that observed by Kumosa et al. [54] for their tests on three polymeric samples per condition. While the gravimetric curves in Abot et al. [2] show scatter, the authors reported only average diffusivities, not allowing comparisons of variability with another study based on three samples per condition.

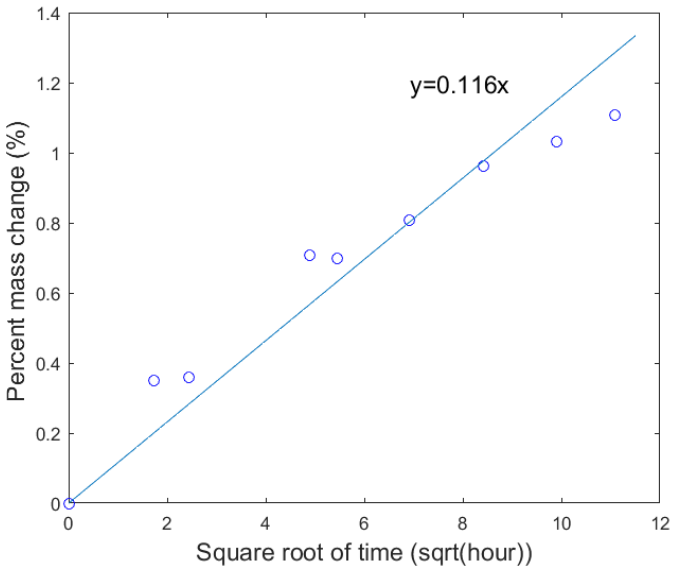

Figure 8. Percent mass change versus square root of time of one epoxy sample immersed in deionized water at room temperature.

Table 3 Moisture diffusivities calibrated from Fickian diffusion model

Materials	Temperature	D (mm^2/s)
Epoxy/deionized water	Room	$1.41x10^{-7} \pm 1.56x10^{-8}$
	50 °C	$4.57x10^{-7} \pm 2.58x10^{-8}$
Epoxy/saline water	Room	$8.28x10^{-8} \pm 9.80x10^{-9}$
	50 °C	$7.42x10^{-7} \pm 1.33x10^{-7}$
Vinylester/saline water	Room	$2.27x10^{-7} \pm 7.40\ x10^{-8}$
	50 °C	$1.39x10^{-6} \pm 1.02\ x10^{-7}$

Fickian diffusion can predict the diffusion process very well when the volume changes (or moisture-induced deformation) are quite small. For example, Fickian diffusion can be used to model the moisture uptake of epoxy samples immersed in deionized and saline water (Figure 9). At 50°C, the Fickian model can predict the evolution of the concentration quite well, while it overpredicts the transient behavior at room temperature. For epoxy samples immersed in saline water, relatively small volume changes are observed, and the Fickian model predicts the diffusion process well at both temperatures. In the responses of epoxy immersed in deionized water at room temperature, the Fickian diffusion seems to overpredict the diffusion process. In order to improve the prediction, the coupled deformation-diffusion model of Gurtin[40] is considered, which is discussed in Section 3. For the vinylester specimens tested here, the diffusion process is much faster than that in the epoxy, and relatively small volume changes are observed, which follow the Fickian diffusion. Figure 10 shows an example of diffusion of saline water in vinylester specimens

at 50 ºC. It is seen that saturated condition is reached in a short period, making it quite difficult to determine saturation points and the diffusivity parameters.

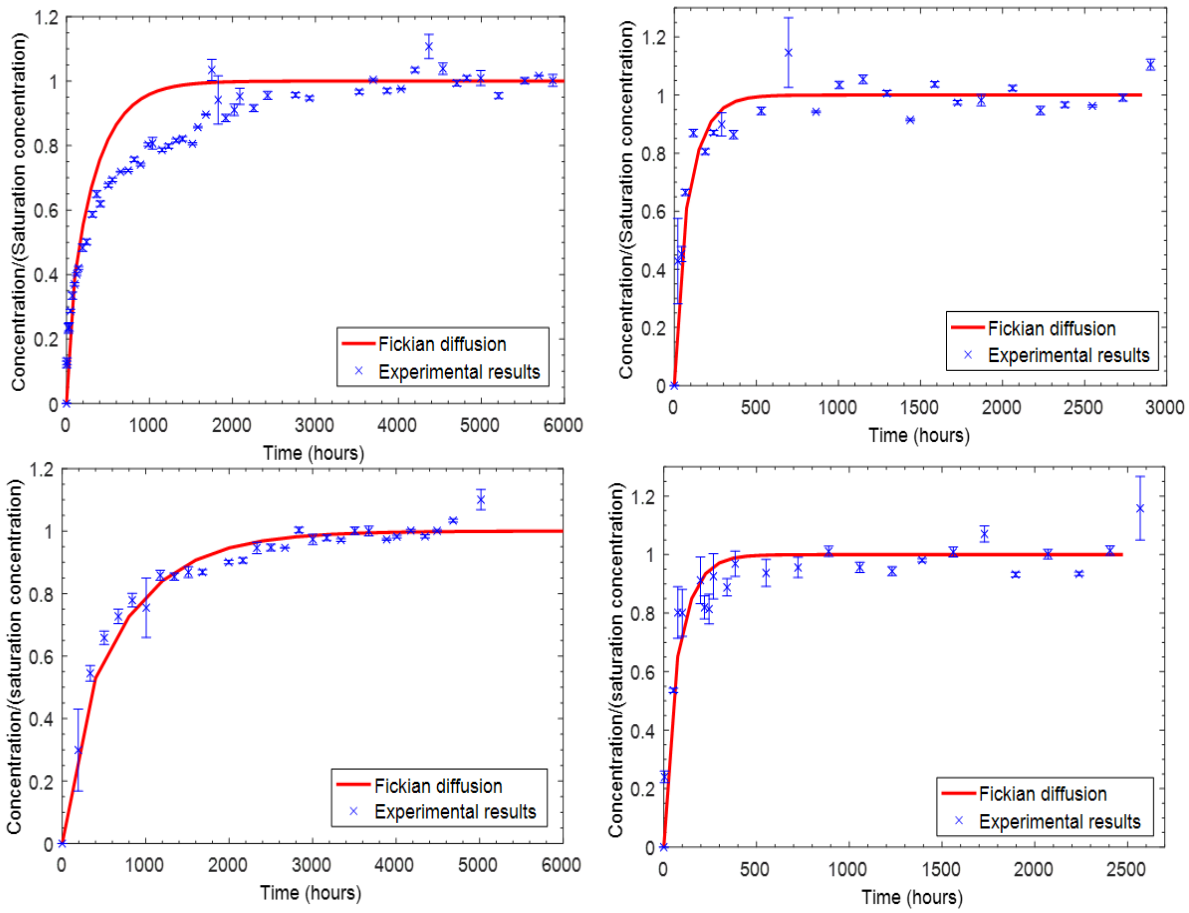

Figure 9. Simulation concentration of fluid in epoxy using a Fickian diffusion model. Top left: in deionized water at room temperature; top right in deionized water at 50 ºC; bottom left: in saline water at room temperature; bottom right: in saline water at 50 ºC.

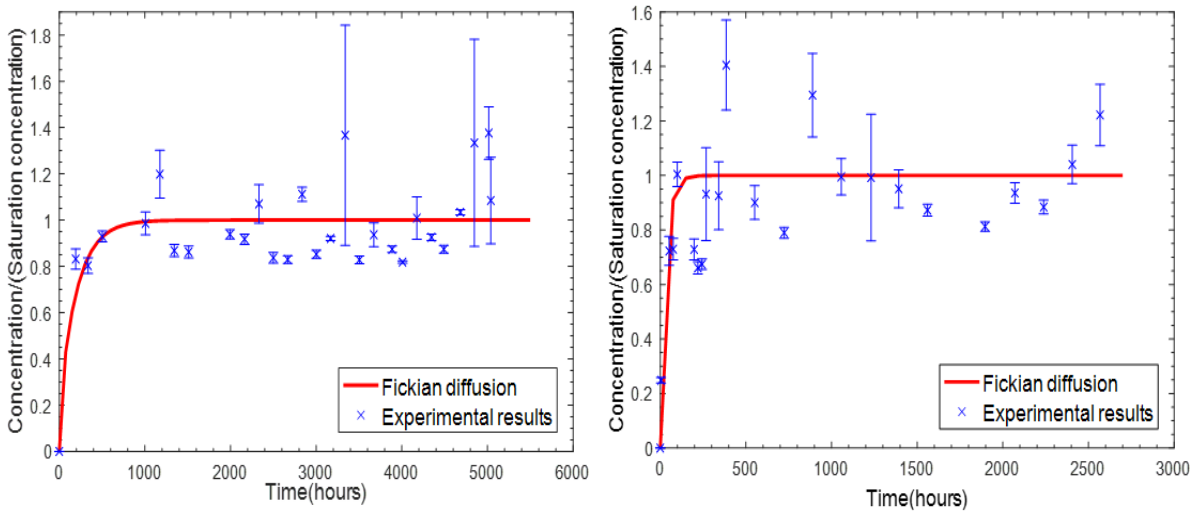

Figure 10. Simulation concentration of fluid in vinylester in saline water at room temperature (left) and 50 ℃ (right) using a Fickian diffusion model.

In the above responses at room temperature, the Fickian diffusion seems to overpredict the diffusion process. This might be due to non-negligible volume changes during the diffusion. In order to improve the simulation, the coupled deformation-diffusion model of Gurtin[40] is considered. There are four material parameters, as discussed in Section 3.1: the elastic modulus E, the diffusivity D, the coupling constants α and β. The elastic modulus E is determined from quasi-static uniaxial tensile tests performed on epoxy specimens after undergoing different environmental conditions (Figure 11). After immersion at 25 ^{o}C, the elastic modulus of the epoxy does not change significantly, as shown in Figure 11. From the parametric studies, the influence of elastic modulus is quite significant when changes in the elastic moduli are quite large (around 3 times). In this study, the value of 2.98 GPa is adopted for E and used in the deformation-diffusion model.

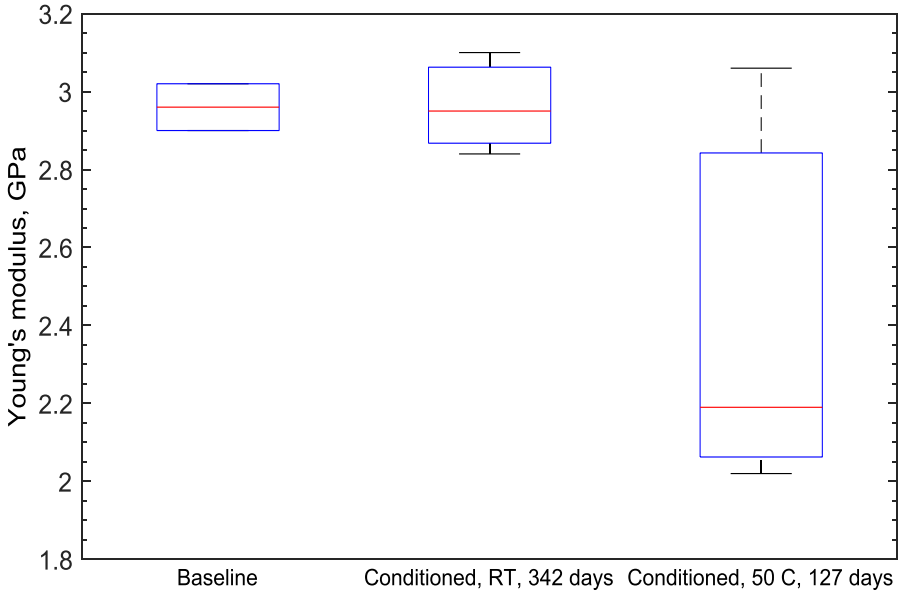

Figure 11. Elastic moduli of epoxy at room temperature for dry condition (baseline) and after immersion in deionized water at room temperature (RT) and 50 ^{o}C.

In order to determine the parameter $\beta = Eb$, where b is the coefficient of moisture expansion (i.e., a measure of through-the-thickness strain increase per unit concentration), we examine the strain and concentration curve in the linear region (less than 0.6 concentration), as shown in Figure 12. A linear regression gives b = 0.1954, and thus the parameter β is equal to 0.582 GPa. The next step is to determine the parameters D and α in order to capture the diffusion response. Figure 13 shows the response from the coupled deformation-diffusion model with D = $4\text{x}10^{-4}$ mm^2/hr =$1.11\text{x}10^{-7}$mm^2/s, and α =$5.19\text{x}10^{-4}\frac{mm^2}{hr}$. The responses are also compared to the Fickian diffusion model. Although there is still a slight mismatch between the coupled deformation-diffusion model and experimental data, an improvement in the model is observed. It

is possible that the mismatch is due to the use of linear coupled deformation-diffusion model, as at higher moisture content the responses might not necessarily be linear.

The responses from the coupled diffusion-deformation model can be improved by having diffusivity to depend on the concentration of fluid. Here, to improve the model, we assume the diffusivity to depend linearly on the concentration $D = D_0 - \kappa C$. Figure 13 also shows the response from the coupled deformation-diffusion model with concentration-dependent diffusion. In this case, the following material parameters are considered: $D_0 = 4.5\times10^{-4}\,\frac{mm^2}{hr} = 1.25\times10^{-7}\,\frac{mm^2}{s}$, $\kappa = 3\times10^{-4}\,\frac{mm^2}{hr} = 8.33\times10^{-7}\,\frac{mm^2}{s}$, $\alpha = 3\times10^{-4}\,\frac{mm^2}{hr} = 8.33\times10^{-7}\,\frac{mm^2}{s}$.

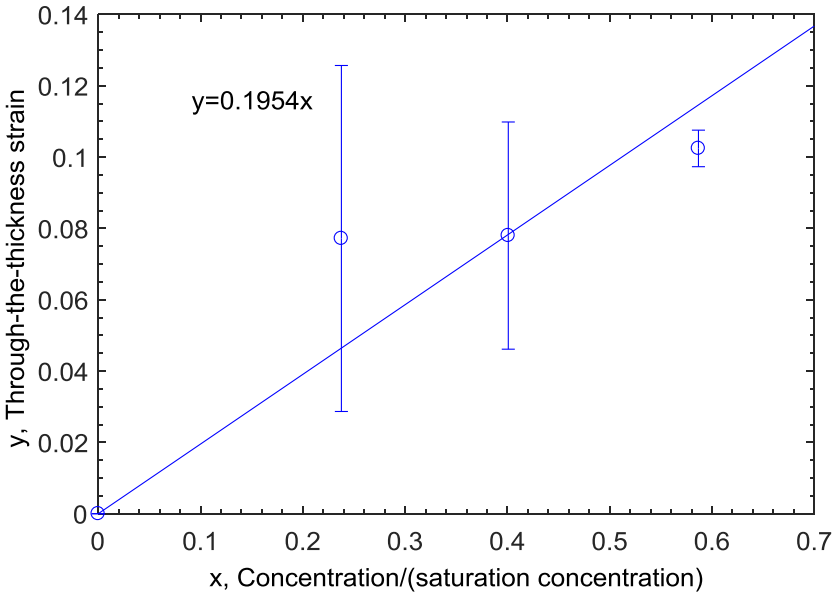

Figure 12. Strain versus concentration (room temperature).

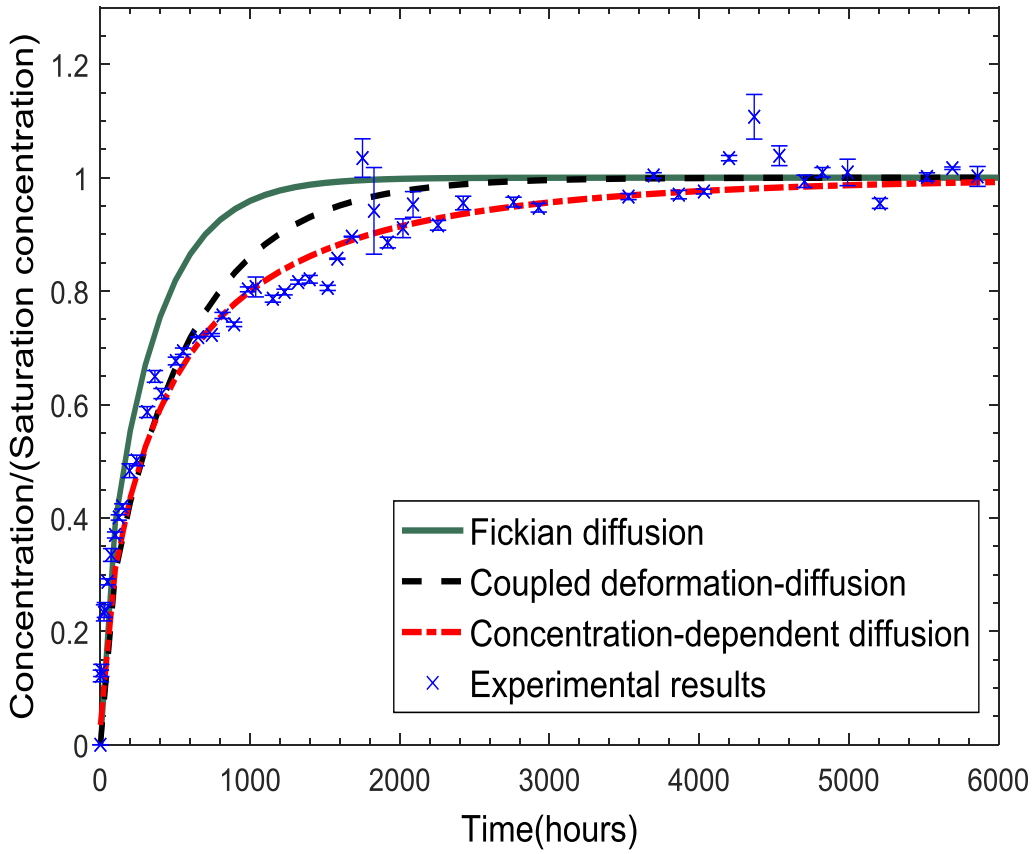

Figure 13. Responses of epoxy immersed in deionized water at room temperature (comparisons between Fickian diffusion, coupled deformation-diffusion with constant diffusivity, and coupled deformation-diffusion with concentration dependent diffusivity).

As mentioned above, the diffusion behavior of dogbone polymer specimens were also considered in order to understand how well the two models (Fickian and Gurtin) can reproduce multi-axial diffusion behaviors with the calibrated material parameters from the standard thin plate diffusion testing. Both epoxy and vinylester specimens are assumed isotropic. The material parameters related to diffusion-deformation responses have been calibrated from standard thin-plate specimens, following ASTM D5229-92(04), in which the one-dimensional diffusion process is considered. In this section, the moisture sorption in dogbone samples is simulated. Because of

the samples' dimensions, a three-dimensional diffusion process is considered. A simplified geometry corresponding to one-eighth of a dogbone specimen was modeled, see Figure 14 (right). The following boundary conditions were applied: due to the symmetric condition imposed on the dogbone sample, on the symmetric surfaces, a zero flux condition normal to the surface is considered ($f_0^m = 0$) while, for the boundaries immersed in fluids, a fully saturated condition is considered ($C = 1$).

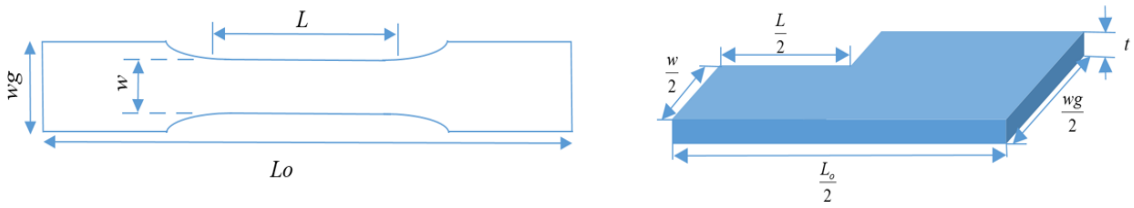

Figure 14. Left: a schematic of dog bone sample simplified; right: one eighth of dogbone sample.

Figure 15 shows results from the three-dimensional moisture sorption of epoxy dogbone specimens immersed in deionized water at 50 ℃. Fickian diffusion is first considered in all cases. The response from the multi-axial moisture sorption simulation is capable of capturing the diffusion process in dogbone specimens for epoxy immersed in deionized water at 50 ºC and vinylester sample immersed in saline water. These behaviors correspond to the results from the one-dimensional diffusion process. At room temperature, the Fickian model overpredicts the transient behavior of epoxy dogbone specimens immersed in deionized water, which is also observed in the results from the one-dimensional diffusion. The coupled diffusion-deformation

model with both constant parameters and concentration-dependent diffusivity is then considered for the epoxy samples immersed in deionized water at room temperature. Figure 16 shows the response from the coupled deformation-diffusion model. The material parameters calibrated from the one-dimensional diffusion of thin plates are used. The result shows that the coupled deformation-diffusion model gives better prediction of the moisture diffusion than the Fickian model. The slight mismatch is possibly due to the simplified geometry of the dogbone sample.

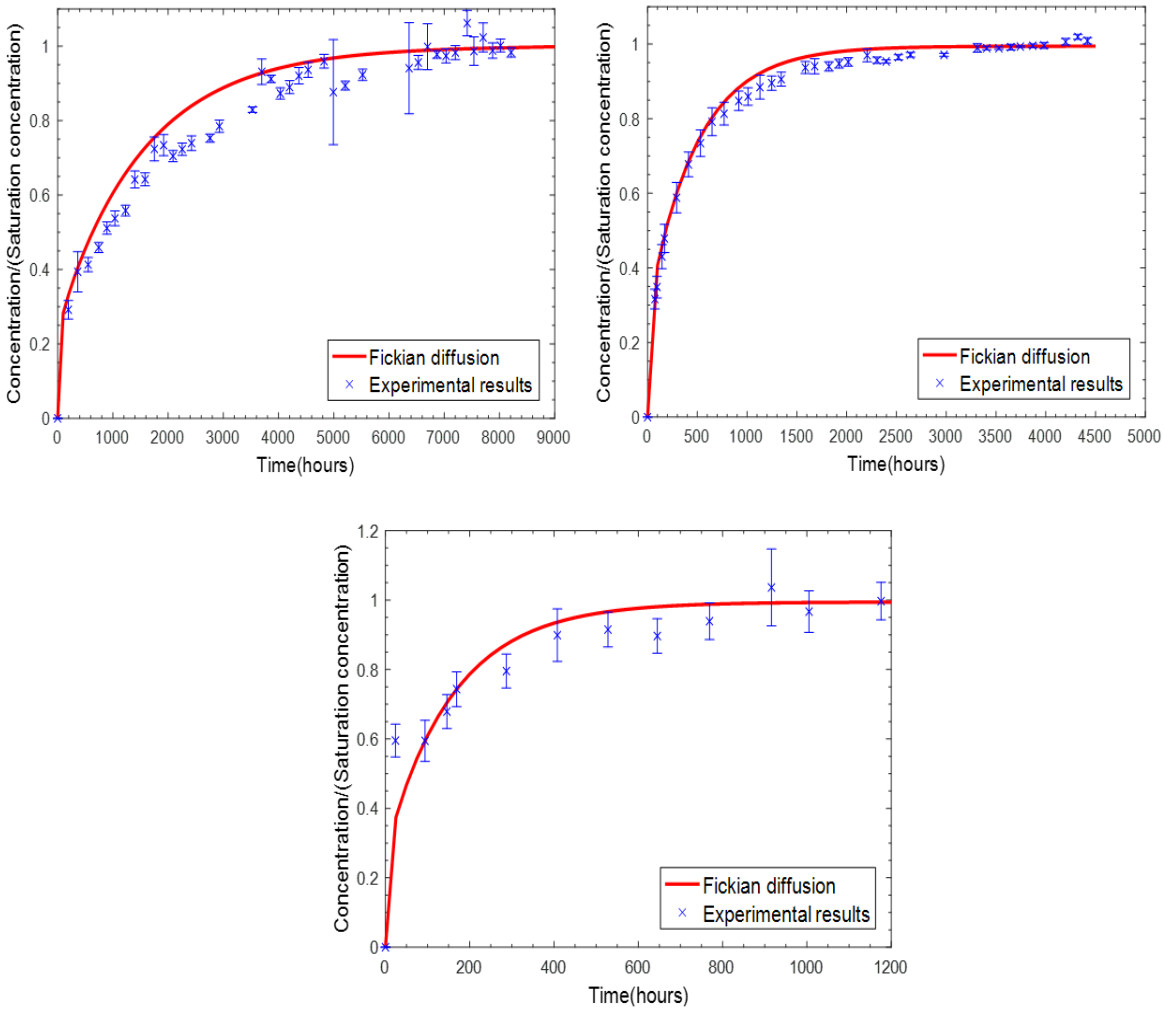

Figure 15. Moisture diffusion behaviors of dogbone specimens: (top left) epoxy immersed in deionized water at room termperature; (top right) epoxy immersed in deoinized water at 50 ºC ; (bottom) vinylester immersed in saline water at 50 ºC.

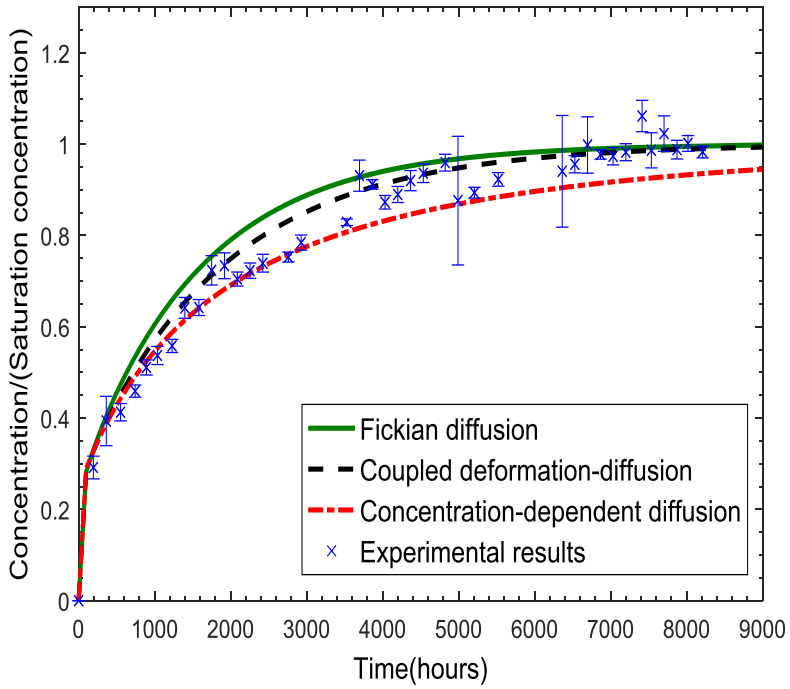

Figure 16. Response of epoxy dogbone specimens immersed in deionized water at room termperature.

In this section, experimental and numerical investigations have been conducted to understand moisture sorption behaviors of two polymers, i.e., epoxy and vinylester, immersed in different fluids at two temperatures (room temperature and 50 ^{o}C). Epoxy samples were immersed in both deionized water and saline water, while the vinylester samples were immersed in saline water. During the diffusion process, the overall mass changes and dimension changes were recorded. In order to describe the diffusion process, the Fickian diffusion and coupled deformation-diffusion model for linear elastic isotropic materials presented by Gurtin[40] are adopted. Two types of specimens, i.e., thin plate rectangular and dogbone specimens, have been considered. The thin plate specimens were considered for calibrating material parameters following the ASTM

standard. Material parameter calibrations from experimental data have also been discussed. The dogbone specimens were considered in order to validate the diffusion model and calibrated material parameters.

In all cases, elevated temperatures accelerate the diffusion process, which is expected, and is consistent with the literature. The effect of temperatures are more pronounced on epoxy samples than on the vinylester samples. This might be because the glass transition temperature of vinylester is higher than that of epoxy (see Appendix C); thus 50 ^{o}C only slightly alter the properties and microstructures of vinylester. It is also noted that volume changes in the epoxy due to moisture sorption influence the diffusion processes, even at relatively low volume changes (around 10%). The Fickian model can capture the diffusion process when the volume changes in the specimens during the diffusion process are relatively small, e.g. for epoxy and vinylester immersed in saline water. The volume changes are pronounced in the case of epoxy immersed in deionized water at room temperatures. In such case, the Fickian model overpredicts the diffusion behaviors and the coupled deformation-diffusion model can reasonably describe the effect of deformation on the diffusion process. The model prediction on the diffusion process in dogbone specimens confirms the sensible choice of the diffusion models, for different diffusion cases, and validates the calibrated material parameters. Some discrepancies between the model and experimental results are observed, which might be due to considering linear constitutive relations.

4.3 Fluid Diffusion in Polymeric Foams

This section discusses diffusion of fluid through thick-section polymer specimens, i.e. polyurethane and PVC foams. The manufacturability of the polymeric foams determines that

they cannot be cut into the low width-thickness ratio required by the standard ASTM D5229-92(04). Polyurethane and PVC specimens are tested with dimensions specified in Table 2. It is seen that the specimens are in the form of thick section and three-dimensional diffusion behavior is considered. Polyurethane foam samples and PVC foam samples were fully immersed inside two custom-made tanks, one containing deionized water, the other containing a solution of deionized water and 3.5 % wt. content of NaCl, which simulates sea water. Polyurethane foam samples were immersed only in the deionized solution while PVC foam samples were only immersed in saline solution. Experimental data is obtained by measuring the overall weight and dimension changes in the specimens. These two combinations of solid and fluid are chosen to examine whether the model considered in this study is general enough for different polymers immersed in different fluids.

Tests were conducted at room temperature and at 50 °C (in the latter case, immersion heaters were used). The 50 °C was selected to be representative of a service temperature for a fiber-reinforced polymeric structure, and it is below the published glass transition temperature of the polyurethane foam and PVC foam. Information of the type of fluid used for immersion and the temperature are also given in Table 4.

Table 4 Dimensions of polyurethane/PVC foam squares

Materials	Temperature	Thickness(mm)	Length(mm)	Width(mm)
Polyurethane/deionized water	Room	19.20	67.70	63.32
	50ºC	19.05	63.95	64.41
PVC/saline water	Room	25.66	63.83	63.86
	50ºC	25.52	62.97	63.23

It is noticed that at room temperature, the polyurethane samples are fully saturated after about 2000 hours, while under 50 °C, the samples did not reach saturation after 3000 hours. It is also seen that percent mass change at higher temperature (around 200%) is much higher than the ones at room temperature(around 90%). The volume changes of polyurethane foams immersed in deionized water at room temperature and 50 °C are also recorded. It is noticed that at room temperature, the volume changes are quite significant while at higher temperature, the volume changes are relatively small. By comparing mass changes of PVC foam samples immersed in saline water at room temperature and at 50 °C, it is also found that higher temperature accelerates the diffusion process. The difference between polyurethan foam is that the percent mass change at higher temperature is very close to the ones at room temperature. It is noticed that the volume changes of PVC foam samples immersed in saline water at room temperature and at 50 °C are very small, which can ge considered negligible.

First, the Fickian diffusion is considered in order to determine the diffusivity of polymeric foams immersed in different fluid at different temperatures. Shen and Springer[77],

Springer [89] presented the method for calibrating one-dimensional diffusivity, which is discussed in section 4.2. This method is developed from the one-dimensional solution of the diffusion equation and is based on the assumption that there is only through-thickness diffusion in polymer plates. Many investigations considered this method, even for thick polymeric plates and laminates. Shen and Springer [77] also includes the edge effects correction to the calibration. The edge effect correction is based on the assumption that there is no interaction between the diffusion process from each side of the specimen and the one-dimensional Fickian equation is applied to each side independently. Consider moisture diffusion in a foam with thickness *h* and width *a* and *b*. The edge effects correction is written as:

$$D = D_z(1+\frac{h}{a}\sqrt{\frac{D_x}{D_z}}+\frac{h}{b}\sqrt{\frac{D_y}{D_z}}) \tag{64}$$

where D_x, D_y, D_z represents the in-plane diffusivities relative to the x, y, z direction. The diffusivity calibrated by applying edge effects correction is given in Table 5.

For a better calibration, the three-dimensional Fickian model is used instead of the one-dimensional model. Whitney [97] considered three-dimensional Fickian model and gave a better calibration method for the diffusion coefficient. Consider moisture diffusion through a foam with thickness *h* and width *a* and *b*. Because of the relatively high width to thickness ratio, a three-dimensional solution to Fickian equation should be considered, which is written as:

$$\frac{\partial C}{\partial t} = D_x\frac{\partial^2 C}{\partial x^2}+D_y\frac{\partial^2 C}{\partial y^2}+D_z\frac{\partial^2 C}{\partial z^2} \tag{65}$$

where D_x, D_y, D_z represents the in-plane diffusivities relative to the x, y, z direction, but since we have isotropic material, the diffusion coefficient in each direction are equal.

Consider the following boundary conditions:

$$C = 0, \quad t \le 0$$
$$C(\pm\frac{a}{2}, y, z, t) = C(x, \pm\frac{b}{2}, z, t) = C(x, y, \pm\frac{h}{2}, t) = 1, \quad t > 0 \tag{66}$$

Whitney's discussed the analytical solution of the Fickian equation, which is written as:

$$G = \frac{M\%}{M_m} = \frac{4}{\sqrt{\pi}}\sqrt{t}(\frac{1}{a} + \frac{1}{b} + \frac{1}{h})\sqrt{D} - \frac{16}{\pi}t(\frac{1}{ab} + \frac{1}{ah} + \frac{1}{hb})D + \frac{64}{\pi\sqrt{\pi}}t\sqrt{t}\frac{1}{abh}D\sqrt{D} \tag{67}$$

This solution can be a good approximation of diffusion coefficient. Since the percent mass change varies linearly with $\sqrt{t}$ at least for a short time after exposure to the environment, we can use least squares method to approach the diffusivity in the above expression. The values of diffusivities from the three-dimensional Fickian model are given in Table 5 under the column "Diffusivity". It is seen that the diffusivities determined from three-dimensional Fickian model and one-dimensional model with edge correction factor differ significantly. The Fickian model with edge correction factor assumes that the fluid diffuses into the substrate from all edges with no interceptions. This assumption lead to under-predicted diffusivity parameters.

Table 5 Diffusion coefficient of polyurethane/PVC foam

Materials	Temperature	Edge-effects diffusivity($\frac{mm^2}{s}$)	Diffusivity($\frac{mm^2}{s}$)
Polyurethane	Room	$1.10x10^{-5}$	$1.82x10^{-5}$
PVC	Room	$2.99\ x10^{-5}$	$6.56x10^{-5}$
	50ºC	$9.15x10^{-5}$	$2.01x10^{-4}$

It should be noted that the experimental results show that polyurethane foam immersed in deionized water under 50°C did not reach saturation after 3000 hours. In order to get the diffusivity from experimental data, the least square method is used and gives diffusivity D=3.83x10$^{-6}\frac{mm^2}{s}$ for the maximum percent mass change of 195%. The simulation results are discussed in this section.

The Fickian diffusion model is used to predict the fluid diffusion in polyurethane and PVC foams. Based on symmetry, the one-eighth model is used. Figure 17 shows the schematic of three-dimensional finite difference nodes used for the one-eighth model. The geometrical center of the foam square is at the origin of the coordinate. At the boundaries, the following conditions are satisfied at all time *(m = 0, 1, ...)* : the concentration at the outer surface (3 surfaces) remains fully saturated, which is described as $C^m_{np,kl} = 1,\ for\ \ k = 1, \dots, kp, l = 1, \dots, lp$, $C^m_{n,kp,l} = 1,$ $for\ \ n = 1, \dots, np, l = 1, \dots, lp$, $C^m_{nk,lp} = 1,\ for\ \ n = 1, \dots, np, k = 1, \dots, kp$. At any time, all the surfaces of the foam are stress-free, i.e. $\sigma^m_{np,kl} = 0,\ for\ \ k = 1, \dots, kp, l = 1, \dots, lp$, $\sigma^m_{n,kp,l} =$ $0\ for\ \ n = 1, \dots, np, l = 1, \dots, lp$, $\sigma^m_{nk,lp} = 0,$ for $\ n = 1, \dots, np, k = 1, \dots, kp$. Due to the symmetric condition imposed on the foam, the displacement at the inner surfaces are fixed, i.e. $U^m_{1,kl} = 0$, *for* $k = 1, \dots, kp, l = 1, \dots, lp$, $V^m_{n,1,l} = 0$, for $n = 1, \dots, np, l = 11, \dots, lp$, $W^m_{nk,1} = 0$, for $n = 11, \dots, np, k = 11, \dots, kp$. On the inner surfaces, a zero flux condition is considered: $f^m_{1,kl} = 0$ *for* $k = 11, \dots, kp, l = 11, \dots, lp$, $f^m_{n,1,l} = 0$, *for* $n = 1, \dots, np, l = 1, \dots, lp$, $f^m_{nk,1} = 0$, for $n =$ $1, \dots, np, k = 1, \dots, kp$.

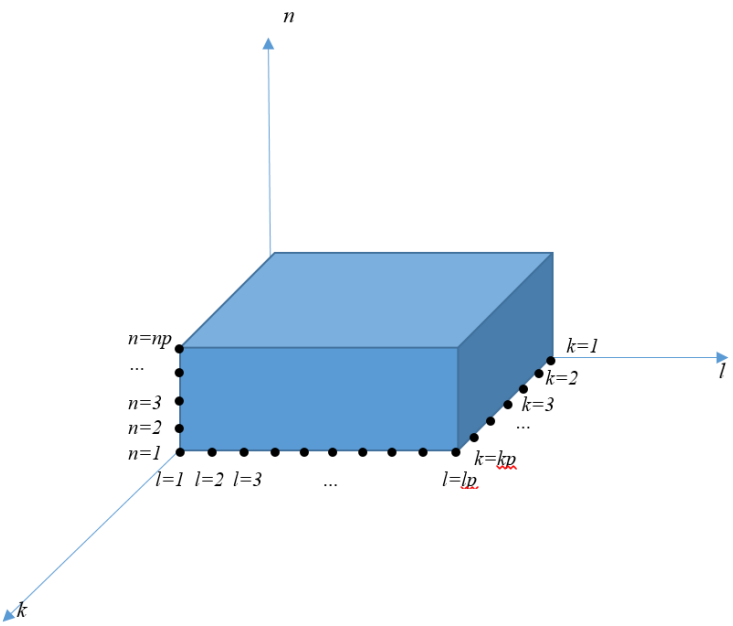

Figure 17. A schematic of three-dimensional finite difference nodes.

In order to impose the conditions on the inner surfaces, a forward difference method is used for nodes on or near the inner surfaces. Thus, the derivatives of the displacement and concentration near the boundaries are:

$$\frac{\partial^2 U}{\partial x^2} \approx \frac{U^m_{3,kl} - 2U^m_{2,kl} + U^m_{1,kl}}{\Delta x^2}, n = 1, k = 1, 2, ...kp, l = 1, 2, ..., lp$$
$$\frac{\partial^2 V}{\partial y^2} \approx \frac{V^m_{n,3,l} - 2V^m_{n,2,l} + V^m_{n,1,l}}{\Delta y^2}, n = 1, 2, ...np, \mathrm{k} = 1, l = 1, 2, ..., lp \quad (68)$$
$$\frac{\partial^2 W}{\partial z^2} \approx \frac{W^m_{nk,3} - 2W^m_{nk,2} + W^m_{nk,1}}{\Delta z^2}, n = 1, 2, ...np, k = 1, 2, ...kp, \mathrm{l} = 1$$

$$\frac{\partial^3 U}{\partial x^3} \approx \frac{-3U^m_{\mathrm{n}-1,kl} + 9U^m_{\mathrm{n},kl} - 9U^m_{\mathrm{n}+1,kl} + 3U^m_{\mathrm{n}+2,kl}}{2\Delta x^3}$$

$$\frac{\partial^3 V}{\partial y^3} \approx \frac{-3V^m_{\mathrm{n},\mathrm{k}-1,l} + 9V^m_{\mathrm{n},\mathrm{k},l} - 9V^m_{\mathrm{n},\mathrm{k}+1,l} + 3V^m_{\mathrm{n},\mathrm{k}+2,l}}{2\Delta y^3}, n = 2,3,\ldots,\mathrm{np}-2, k = 2,3,\ldots,kp-2, l = 2,3,\ldots,lp-2 \quad (69)$$

$$\frac{\partial^3 W}{\partial z^3} \approx \frac{-3W^m_{\mathrm{n},k,l-1} + 9W^m_{\mathrm{n},k,l} - 9W^m_{\mathrm{n},k,l+1} + 3W^m_{\mathrm{n},k,l+2}}{2\Delta z^3}$$

$$\frac{\partial^3 U}{\partial x^3} \approx \frac{-U^m_{\mathrm{n}-2,k,l} + 3U^m_{\mathrm{n}-1,k,l} - 3U^m_{\mathrm{n},k,l} + U^m_{\mathrm{n}+1,k,l}}{\Delta x^3}$$

$$\frac{\partial^3 V}{\partial y^3} \approx \frac{-V^m_{\mathrm{n},k-2,l} + 3V^m_{\mathrm{n},k-1,l} - 3V^m_{\mathrm{n},k,l} + V^m_{\mathrm{n},k+1,l}}{\Delta y^3}, n = 3,4,\ldots,,np-1, k = 3,4,\ldots,kp-1, l = 3,4,\ldots,lp-1 \quad (70)$$

$$\frac{\partial^3 W}{\partial z^3} \approx \frac{-W^m_{\mathrm{n},k,l-2} + 3W^m_{\mathrm{n},k,l-1} - 3W^m_{\mathrm{n},k,l} + W^m_{\mathrm{n},k,l+1}}{\Delta z^3}$$

The initial conditions are taken as normalized concentrations $C^0_{nkl} = 0,\ for\ n = 1,\ldots,np-1, k = 1,\ldots,kp-1, l = 1,\ldots,lp-1$ and $U^0_{nkl} = 0,\ for\ n = 1,\ldots,np, k = 1,\ldots,kp, l = 1,\ldots,lp, V^0_{nkl} = 0,$ for $n = 1,\ldots,np, k = 1,\ldots,kp, l = 1,\ldots,lp, W^0_{nkl} = 0,$ for $n = 1,\ldots,np, k = 1,\ldots,kp, l = 1,\ldots,lp.$

Examples are shown below in Figure 18 for the polyurethane and PVC foam samples immersed in deionized and saline water. At room temperature, the Fickian model overpredicts the transient behavior of moisture diffusion for polyurethane specimens immersed in deionized water under room temperature. For the polyurethane foam samples immersed in deionized water under 50^{o}C, the volume changes are small and the Fickian model provides a good match with the experimental results. For the PVC foam samples immersed in saline water, relatively small volume changes are observed(<0.6%) , and the Fickian model predicts the diffusion process well at both room temperatures and 50 ^{o}C.

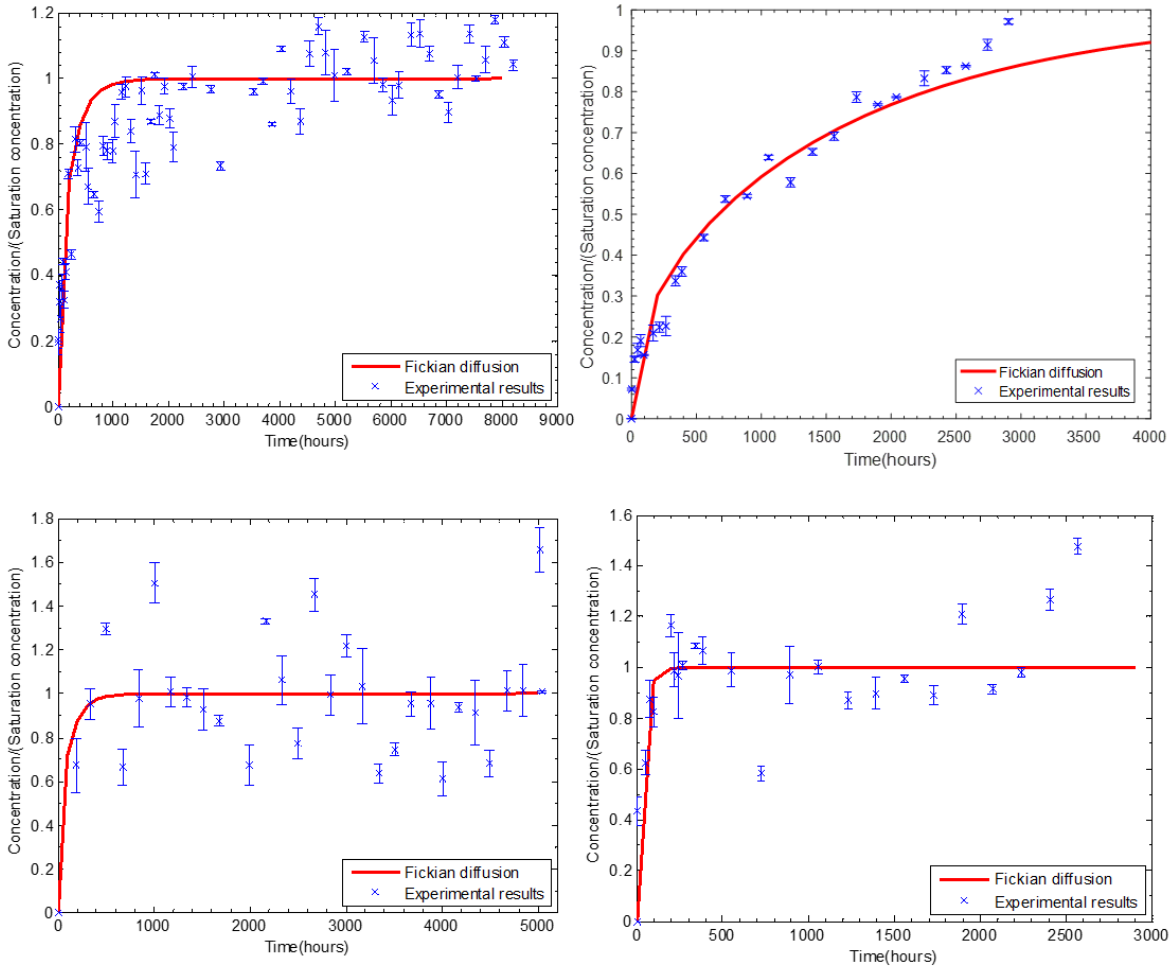

Figure 18. Simulation concentration of fluid in polymer foams using a Fickian diffusion model. Top: polyurethane foams in deionized water at room temperature; middle: PVC foams in saline water at room temperature; bottom: PVC foams in saline water at 50^{o}C.

The Fickian model seems to have a good agreement with the experimental data when volume changes are insignifican. However, in the above responses at room temperature, the Fickian diffusion seems to slightly over-predict the diffusion process for polyurethane, which has a percent volume change for about *2%*. In order to improve the simulation, the coupled deformation-diffusion model of Gurtin (1977) is considered. There are four material parameters:

the shear modulus *G*, Lame's constant λ , coupling constants α and β. The machanical properties are given by the polyurethane foam and PVC foam manufacturer. In this study, material properties provided by the polymer manufacturer General Plastics is used: the value of 5.62 MPa is adopted for *G* and the value of 8.4 MPa is adopted for λ .

In order to determine the parameter β the following constitutive relation is considered:

$$\underline{S} = l\,(tr\underline{E})\,\underline{1} + 2G\underline{E} - b\underline{C}\,\underline{1} \tag{71}$$

$$S_{ij} = \lambda\delta_{ij}E_{kk} + 2GE_{ij} - \beta C\delta_{ij} \tag{72}$$

where δ_{ij} is the Kronecker delta. Since the concentration is considered to be constant, equation (71) and (72) can be written as:

$$S_{kk} = (3\lambda + 2G)E_{kk} - 3\beta C \tag{73}$$

Under purely immersion, in absent of stresses, then Eq. (73) reduces to

$$\beta = \frac{E_{kk}}{3C}(3\lambda + 2G) = \frac{1}{3}b(3\lambda + 2G) \tag{74}$$

where *b* is the coefficient of moisture expansion, which is a measurement of percent volume change increase per unit concentration, we examine the percent volume change and concentration curve, as shown in Figure 19. A linear regression gives *b* = 0.0229, and thus the parameter β is equal to 0.278 MPa. The next step is to determine the parameters *D* and α in order to capture the diffusion response. Fig. 15 shows the response from the coupled deformation-diffusion model with *D* = 0.04 $\frac{\text{mm}^2}{\text{hr}}$ and α =0.15 $\frac{\text{mm}^2}{\text{hr}}$. The responses are also compared to experimental results and the Fickian diffusion model in Figure 20 and the linear coupled diffusion-deformation model shows a better agreement with experimental results.

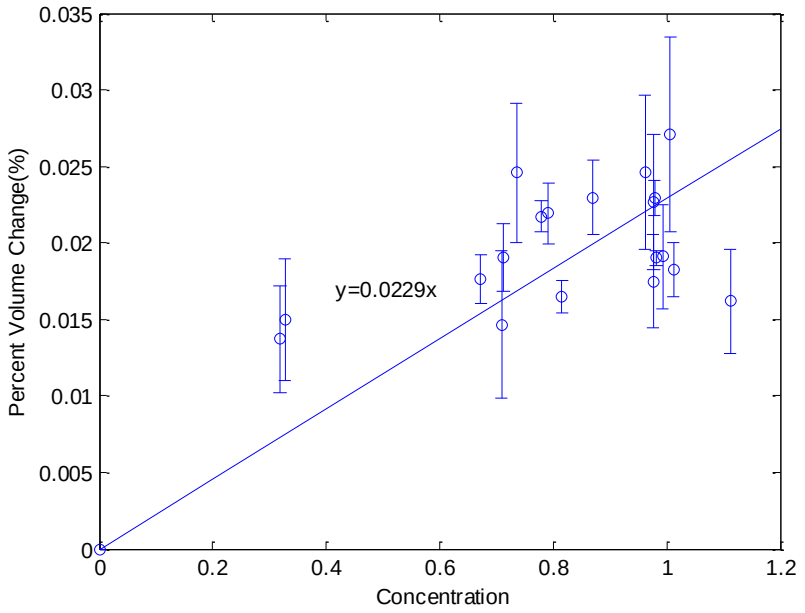

Figure 19. Correlation between Percent volume change and concentration.

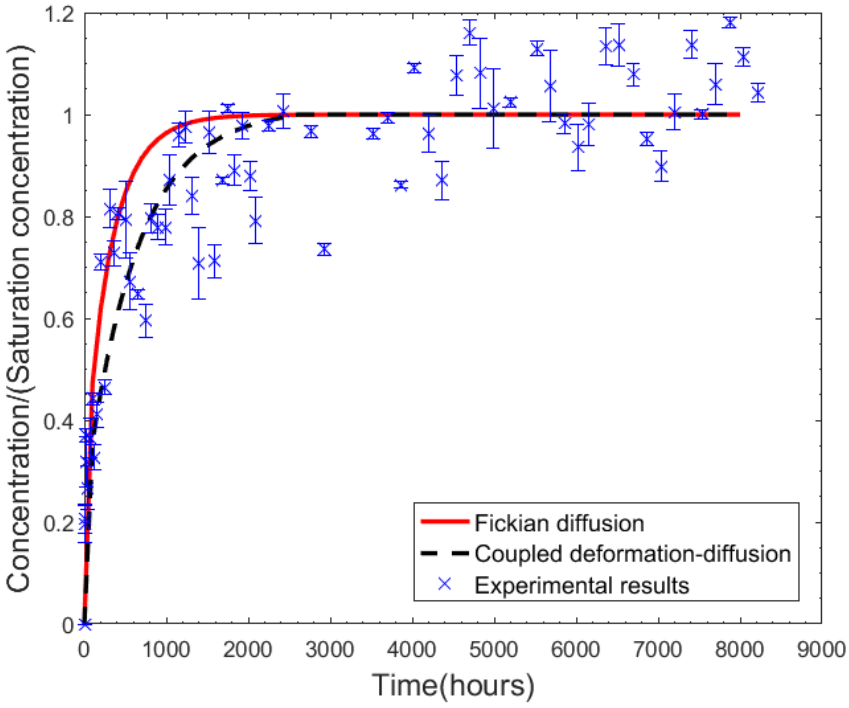

Figure 20. Responses of polyurethane foam immersed in deionized water at room temperature.

It can be seen that the maximum percent mass change for polymeric foams is much higher compared to that in the polymeric resin. And the polymeric foams reached fully saturated very fast.

4.5 Fluid Diffusion in Fiber-reinforced Polymeric Composites

Fluid diffusion in FRP composites is different from that of pure resins and polymeric foams. The diffusion process is usually anisotropic because of the presence of the fibers. And the diffusivity in the fiber direction is faster than that in the transverse direction. The goal of this part is to understand the fluid diffusion in GFRP skins and how it affects the fluid diffusion in sandwich composites. The widely accepted Fickian model and the Springer model are used to predict the fluid diffusion in GFRP. Except the traditional models, the volumetric expansion in GFRP is studied and the couple deformation-diffusion model is considered. The micromechanical model is implemented and the fiber bundles and its diffusion property is studied.

The first part of this section is modeling of diffusion behavior in GFRP specimens based on the testing data of from Professor La Saponara's lab. The diffusion properties of GFRP is characterized and the different models are implemented and compared. The second part of this section is based on the experimental results from Professor Andreas Echtermeyer's group. This study considered two different fiber arrangements for testing samples and the effects of fiber bundles is considered.

This part is based on the testing data from Professor La Saponara's group. The GFRP samples is the same material as the skins of the sandwich composites. GFRP square samples with

layup $[0]_4$ were prepared with nominal dimensions of 1.5 mm thickness and 150 mm width, according to the requirements for one-dimensional diffusion from ASTM D5229-92(04). The specimens are made into nominally square plates with dimension that satisfy the maximum width-to-thickness ratio: 100. The GFRP samples (six per condition) were fully immersed inside deionized water and held in place with waterproof fishing lines. A stainless steel immersion heater held a temperature of (25.9 ± 1.52) °C (herein indicated as room temperature) for 342 days and (49.7± 0.168) °C (herein indicated as 50 °C) for 127 days. The different duration of the tests was due to the goal of achieving saturation or conduct immersion up to 6 months. GFRP square samples are immersed in deionized water under room temperature and 50 °C. The dimensions of the final samples prior to immersion are reported in Table 6.

Table 6 Average ± standard deviations of the square GFRP plates prior to immersion

Materials	Temperature	Thickness (mm)	Length (mm)	Width (mm)
GFRP plates	Room	1.566 ± 0.01910	151.1 ± 0.2226	150.9 ± 0.2076
	50 °C	1.635 ± 0.01580	151.1 ± 0.1973	151.3 ±0.1533

Since the samples have a very large width to thickness ratio, it can be assumed that the diffusion through the thickness direction is dominant. The one-dimensional Fickian and Springer models are first used to determine the diffusivity of the GFRP in the through-the-thickness direction (transverse fiber direction). Table 7 presents the diffusivity for the GFRP samples at different temperatures. It is noted that the calibrated diffusivity is significantly larger than the

transverse diffusivity. It is also seen that the diffusivity increases significantly with increasing temperatures, which leads to faster fluid sorption. With respect to results in the literature, the author is not aware of similar studies on exactly these materials in these particular conditions. For the Springer transverse diffusivity, the matrix diffusivity was obtained from immersion of the epoxy samples, as discussed in Section 4.1.

Table 7 Average moisture diffusivities calibrated from Fickian diffusion model

Materials	Temperature	Fickian Calibrated diffusivity ($\frac{mm^2}{s}$)	Fiber volume fraction	Springer Transverse diffusivity($\frac{mm^2}{s}$)
GFRP/deionized water	Room	$1.38x10^{-7} \pm 1.31\ x10^{-8}$	0.33	$4.96x10^{-8} \pm 5.50\ x10^{-9}$
	50℃	$7.31x10^{-7} \pm 7.15\ x10^{-8}$		$1.61x10^{-7} \pm 9.06\ x10^{-9}$

The Fickian diffusion can predict the diffusion process very well when the moisture-induced deformation is quite small, which has been widely used in simulation of moisture diffusion in solid polymers. The Springer model has been considered for fiber-reinforced polymers to include the effects of fibers on moisture diffusion. Both models assume that the solid body has no deformation when the moisture absorption took place. In Figure 21, it is seen that at room temperature, the Fickian model tends to over-predict the moisture absorption while the Springer model can better capture the response. It is also seen that, at 50^{o}C, the Fickian model can better predict the evolution of the concentration as compared to the prediction using the Springer model. For the GFRP specimens immersed in deionized water at room temperature

where the deformation is quite significant, the Fickian model over-predicts the moisture diffusion process. In order to include the effects of moisture-induced deformation on diffusion, the coupled deformation-diffusion model developed by Gurtin[40] is considered. The simulation results using Springer model indicate that the moisture diffusion in fiber-reinforced polymers cannot be simply captured by incorporating only resin diffusivity and fiber volume content. In order to include the effects of fibers on moisture diffusion, the micromechanical model of Muliana and Kim[65] is considered.

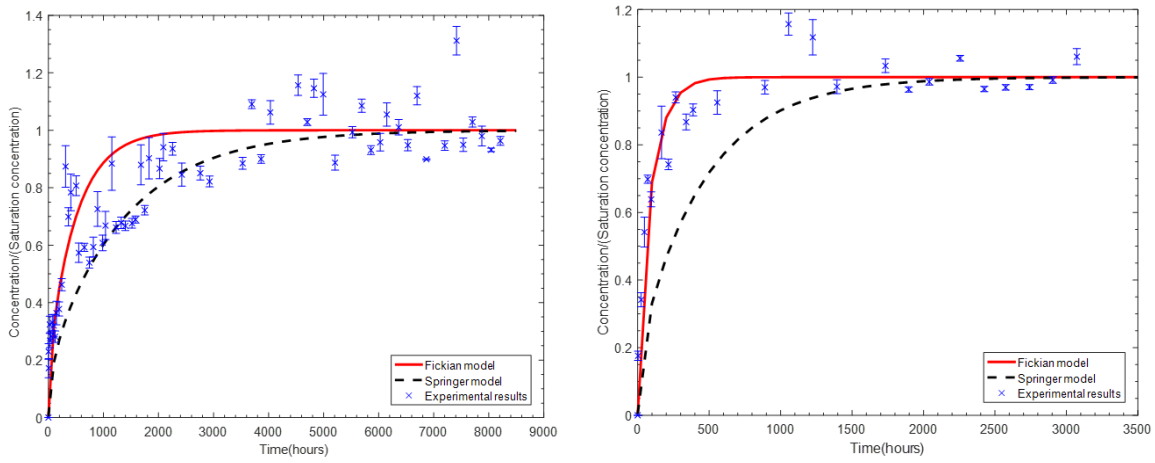

Figure 21. Simulation concentration of fluid in GFRP in deionized water at room temperature (top) and at 50℃ (bottom) using Fickian model.

In the above responses at room temperature, the Fickian model seems to over-predict the diffusion process. The reason might be due to the volumeric changes during the diffusion process. In order to improve the simulation results, the coupled deformation-diffusion model with a concentration dependent diffusivity ($D = D_0 - \kappa C$) is considered (i.e. Fan et al.[30]).

There are five material parameters, that need to be obtained: the elastic modulus *E*, diffusivity *D*, α, β and κ.

The elastic modulus *E* is determined from mechanical tests applied to rectangular GFRP samples located in the immersion tanks of this study, following ASTM D3039. The average of the elastic modulus perpendicular to the fiber direction, labeled as *E*, is used in our case (the experimental values being E_{22} = (5.51 ± 0.19) GPa). Moreover, we need to determine the parameter $\beta = Eb$, where *b* is considered as a coefficient of moisture expansion, which is a measure of axial strain increase per unit concentration. For this assessment, we examine the strain and concentration curve in the linear region (less than 0.6 concentration), as shown in Figure 22. It is seen that a linear regression gives *b*=0.16, and thus the parameter β= 0.88 GPa. The next step is to determine the parameters *D,* α and κ in order to capture the diffusion response. In this case since the lateral diffusion is governed by the matrix diffusion, the diffusivity of resin discussed in Fan et al. [30] is considered. The following material parameters are considered: $D_0 = 4.5\times10^{-4}\,\frac{mm^2}{hr} = 1.25\times10^{-7}\,\frac{mm^2}{s}$, $\kappa = 3\times10^{-4}\,\frac{mm^2}{hr} = 8.33\times10^{-7}\,\frac{mm^2}{s}$, $\alpha = 3\times10^{-4}\,\frac{mm^2}{hr} = 8.33\times10^{-7}\,\frac{mm^2}{s}$. Figure 23 shows the response from the coupled deformation-diffusion model with concentration dependent diffusivity. The responses are also compared to the Fickian and Springer diffusion models.

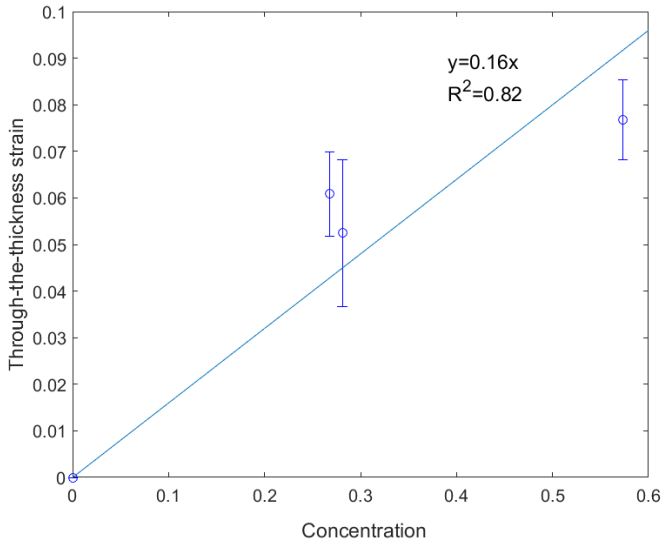

Figure 22. Strain versus concentration (room temperature) with least squares fit.

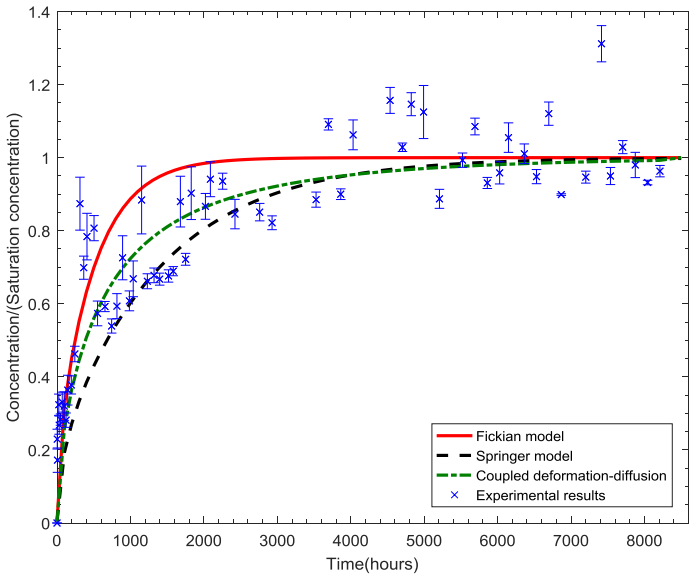

Figure 23. Responses of GFRP immersed in deionized water at room temperature.

Finally the micromechanics model is used to describe the diffusion behavior of GFRP. Figure 28 shows the simulation results of moisture diffusion in GFRP in deionized water at room temperature and at 50°C. For room temperature, the following diffusivities are considered: $D_{matrix} = 5.08\times10^{-4}\,\frac{mm^2}{hr} = 1.41\times10^{-7}\,\frac{mm^2}{s}$, $D_{fiber} = 5.08\times10^{-6}\,\frac{mm^2}{hr} = 1.41\times10^{-9}\,\frac{mm^2}{s}$. The diffusivity of the epoxy matrix is calibrated by Fan et al.[30]. Moreover, the diffusivity of the fibers is almost negligible compared to the diffusivity of the matrix, so it is set as 1/100 of the diffusivity of the matrix in this model. The concentration field at several instants of time during the diffusion process along the axial fiber direction in the GFRP composites are shown in Figure 25. Figure 24 shows the cross-section selected for the contour plot. The cross-section is perpendicular to the fiber direction (x axis) and based on symmetry, only half of the cross-section is needed. A good agreement between the simulation results using micromechanical model and the experimental data is achieved (Figure 28). The results are also compared with Fickian model, Springer model and the coupled deformation-diffusion model. It can be seen that both coupled deformation-diffusion model and micromechanical model can describe the moisture diffusion behavior in FRP composites. For 50°C, the following matrix diffusivity calibrated by Fan et al.[30] are considered: $D_{matrix} = 1.65\times10^{-3}\,\frac{mm^2}{hr} = 4.57\times10^{-7}\,\frac{mm^2}{s}$ and the diffusivities of fibers in the longitudinal and transverse directions are achieved based on a parametric study discussed in the Appendix. The diffusivity of fiber in the longitudinal direction is $D_{11} = 8.25\times10^{-3}\,\frac{mm^2}{hr} = 2.29\times10^{-6}\,\frac{mm^2}{s}$, while the one in the transverse direction is $D_{22} = 8.25\times10^{-4}\,\frac{mm^2}{hr} = 2.29\times10^{-7}\,\frac{mm^2}{s}$. Here, the diffusivity in the longitudinal direction is higher

than that in the transverse direction and the diffusivity of the resin. The high diffusivity along the fibers can be supported by experimental observation of softer resin at fiber/matrix interface and was discussed by Rocha et al.[72]. Figure 26 and Figure 27 show an example of the concentration of fluid at the middle planes in the thickness and width direction of GFRP plate in deionized water at 50^{o}C. The normalized concentration in the GFRP plate is calculated by using Equation (20) and (21). A Matlab code is generated for reading the nodal concentration and numerically integrating them to obtain the overall fluid concentration (Figure 28). The results show that micromechanical model has good agreement with the experimental results of GFRP immersed in deionized water at 50^{o}C.

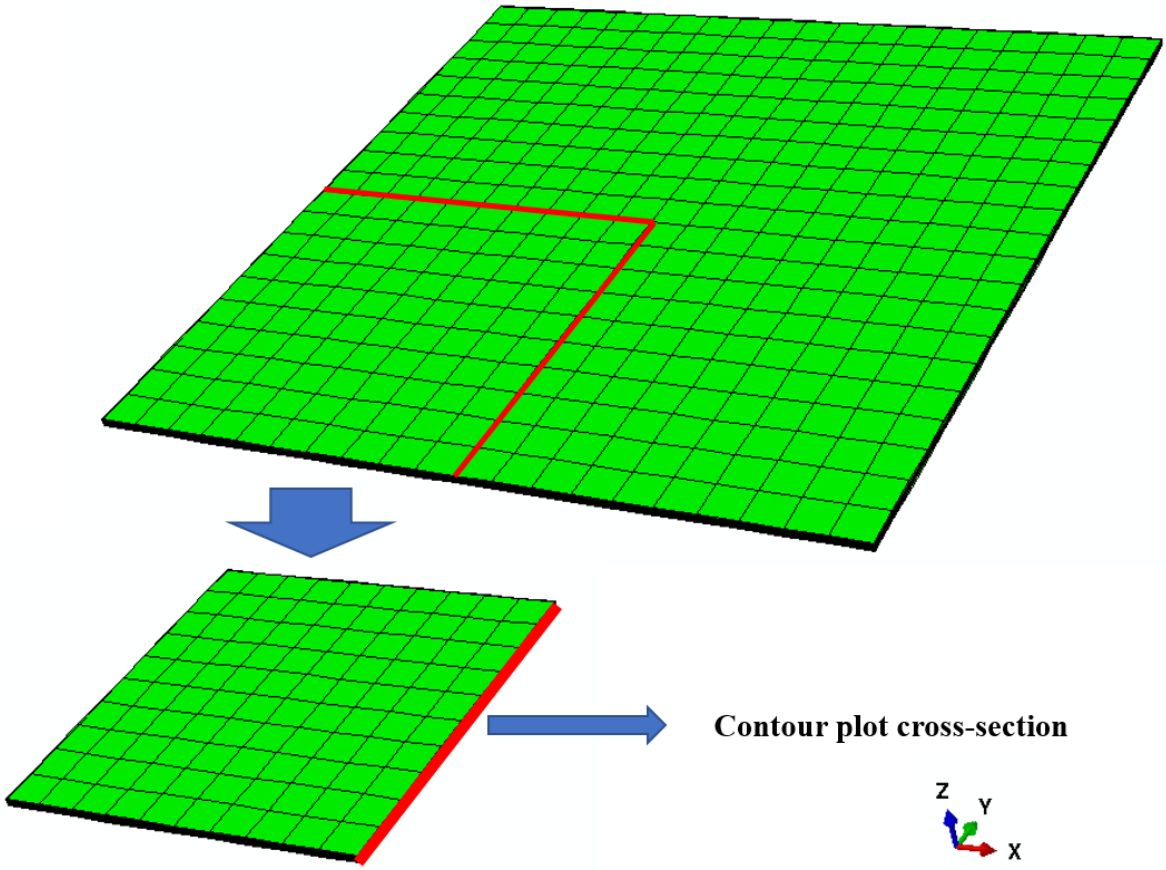

Figure 24. Schematic of GFRP sample and the selected cross-section for contour plot.

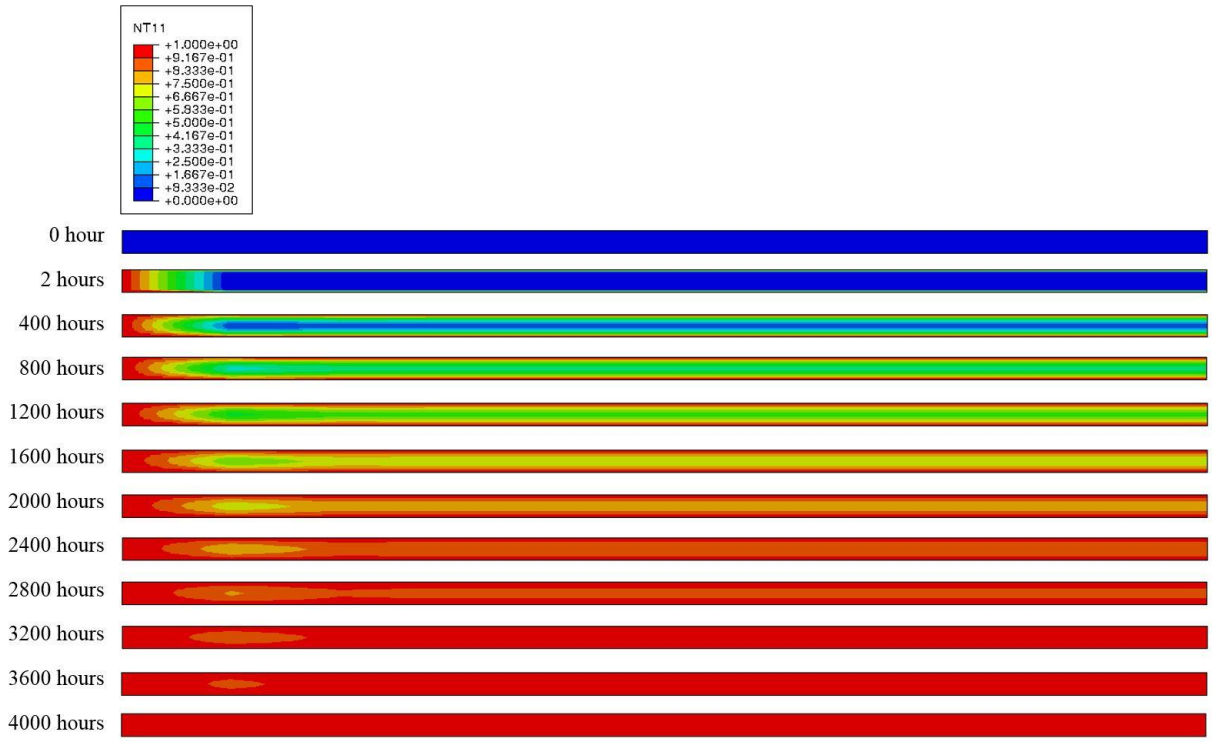

Figure 25. Concentration contours for fluid diffusion.

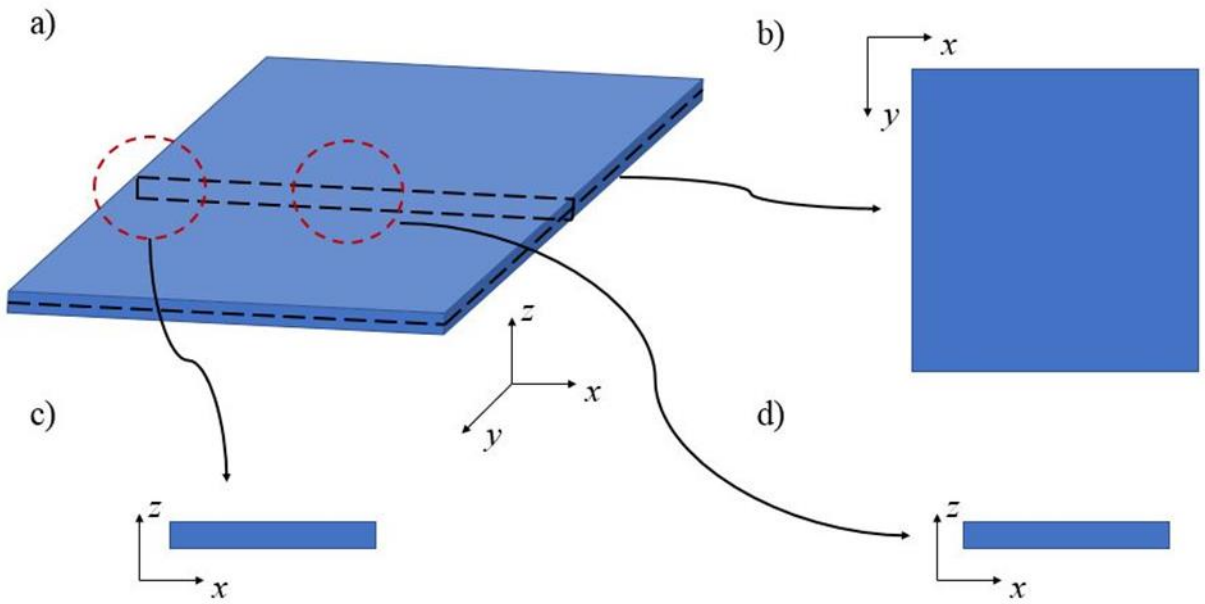

Figure 26. Schematic of the selected cross-sections in the GFRP plate: a) GFRP plate, b) middle plane in the thickness direction, c) Left end of the middle plane in the width direction d) middle part of the middle plane in the width direction.

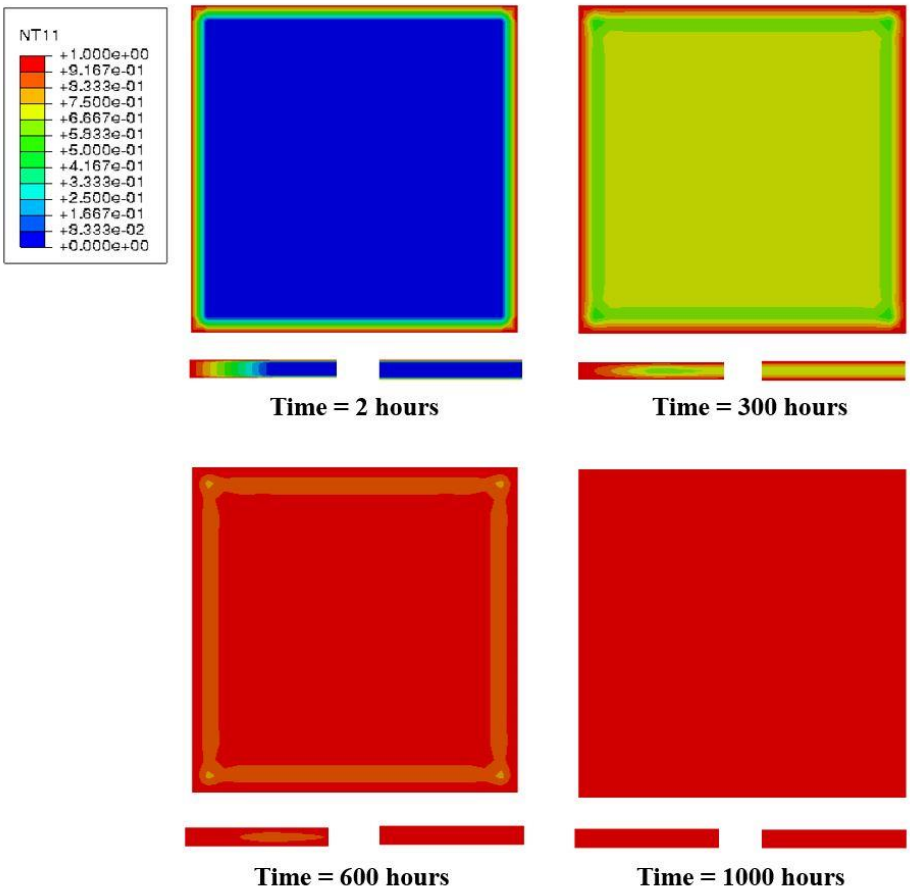

Figure 27. Simulation concentration of fluid at the cross-sections in GFRP plate in deionized water at 50^{o}C.

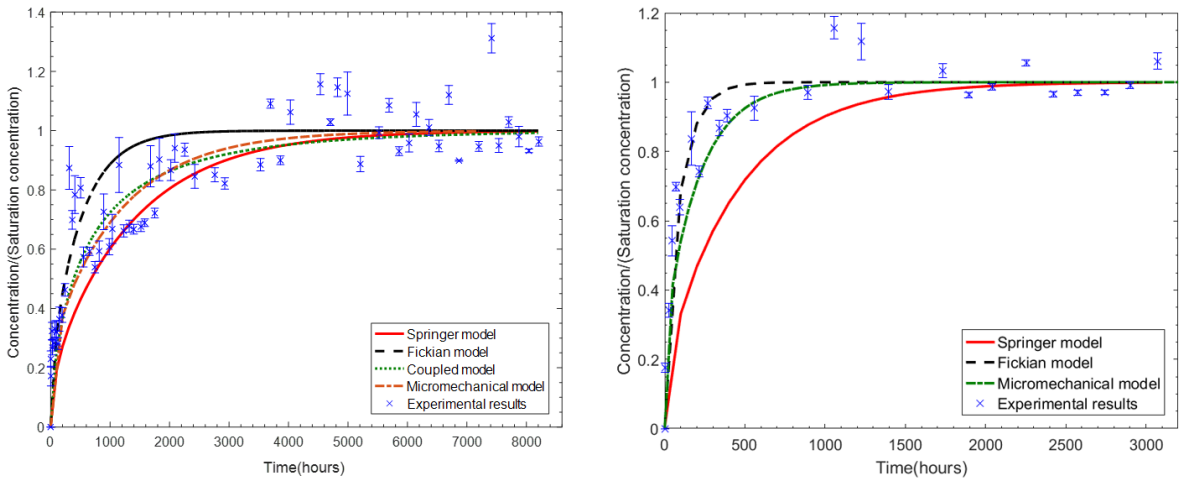

Figure 28. Simulation concentration of fluid in GFRP in deionized water at room temperature (left) and at 50°C (right).

The effective diffusivities of micromechanical model are calculated from equations (54) and (55), which is summarized in Table 8. It is showed that the simplified Springer model, neglecting the fiber diffusivity, under-predicts the fluid diffusion behavior. However, the Springer model is reduced from the general expression based on the assumption that the diffusivity of the fiber (D_f) is small compared to the diffusivity of the matrix (D_r). Equation (29) - (31) are the general expression of the Springer model and it contain the diffusivity of fiber compared to the reduced model. The diffusivities of the general Springer model are calculated by considering the same fiber diffusivities used in the FE analysis. For room temperature, the diffusivity of fiber is assumed to be very small in the FE analysis ($D^f_{11} = D^f_{22} = 0.01D_m$). D_{11} is calculated based on the general equations of Springer model. In the equation of D_{22}, the square root term in the equation gives imaginary number. As a result, D_{22} in the table is based on the reduced equations. For 50℃, micromechanical model uses $D^f_{11} = 0.01D_m$, $D^f_{22} = 0.5D_m$. In the

calculation, it is assumed that $D_f = 0.01D_m$ for D_{11}, and $D_f = 0.5D_m$ for D_{22}. The calculated diffusivity is still smaller compared to micromechanical model's effective diffusivity. If assuming $D^f{}_{11} = D^f{}_{22} = 0.01D_m$, we will get $D_{11} = 3.06\text{x}10^{-7}\ \frac{mm^2}{s}$, $D_{22} = 1.61\text{x}10^{-7}\ \frac{mm^2}{s}$ by using the reduced equations. However, Eq. (30) is not applicable when $D^f{}_{22} = 0.01D_m$. The results are included in Table 8 and it shows that compared to micromechanical model, the general Springer model leads to the same diffusivity along the fiber direction and smaller diffusivity transverse to the fiber direction. The general Springer model is implemented in finite difference approach by using Fortran. Figure 29 and Figure 30 show the simulation concentration of fluid by using the general Springer model. The results show that the general Springer model has relatively good agreement with the experimental data.

Table 8 Diffusivities determined by Springer model and micromechanical model

Materials	Temperature	*Diffusivity*	*Springer diffusivity* ($\frac{mm^2}{s}$)	*Micromechanical effective diffusivity* ($\frac{mm^2}{s}$)
GFRP/deionized water	Room	D_{11}	$9.49\text{x}10^{-8}$	$9.49\text{x}10^{-8}$
		D_{22}	$4.96\text{x}10^{-8}$	$6.14\text{x}10^{-8}$
	50℃	D_{11}	$3.08\text{x}10^{-7}$	$3.08\text{x}10^{-7}$
		D_{22}	$2.87\text{x}10^{-7}$	$3.61\text{x}10^{-7}$

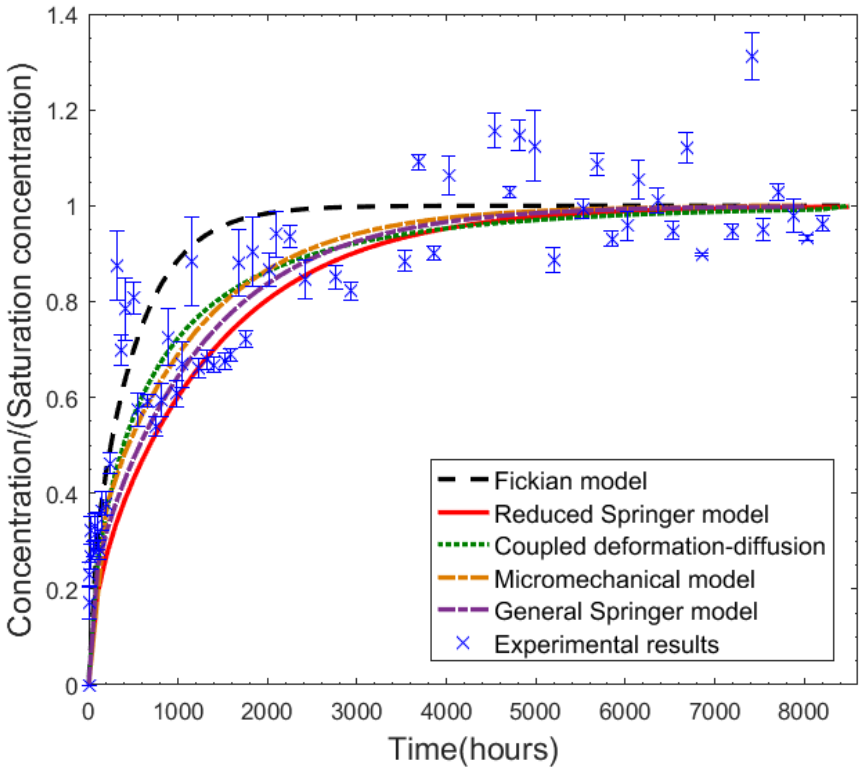

Figure 29. Simulation concentration of fluid in GFRP in deionized water at room temperature.

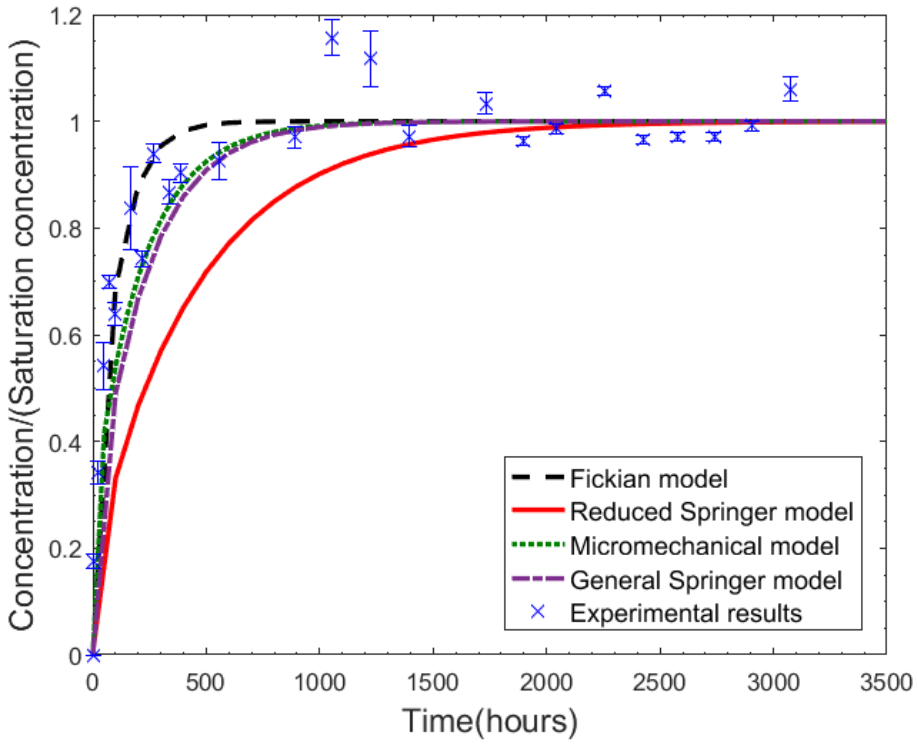

Figure 30. Simulation concentration of fluid in GFRP in deionized water at 50°C.

The general Springer model has good agreement with the experimental data of GFRP. However, the constraints of the general Springer model should be considered before applying it to predict fluid diffusion behavior. The maximum fiber volume fraction allowed by Springer model is 0.785. It is noted that Eqs. (30) and (31) also impose a constraint to the ratio of the matrix and fiber diffusivity, $\frac{D_r}{D_f} < 1 + 0.5\sqrt{\frac{\pi}{v_f}}$. Figure 31 illustrates the relation between $\frac{D_r}{D_f}$ and v_f. Based on the constraints, the ratio of matrix and fiber diffusivity should be under the curve to ensure a valid solution for the equations. These constraints of the general Springer model limit its usage for the material system with certain combinations of matrix and fiber diffusivity ratio

and fiber volume fraction. In comparison, the micromechanical model does not have any of those constraints. Thus, the micromechanical model has wider applications in fluid diffusion prediction for fiber-reinforced composites.

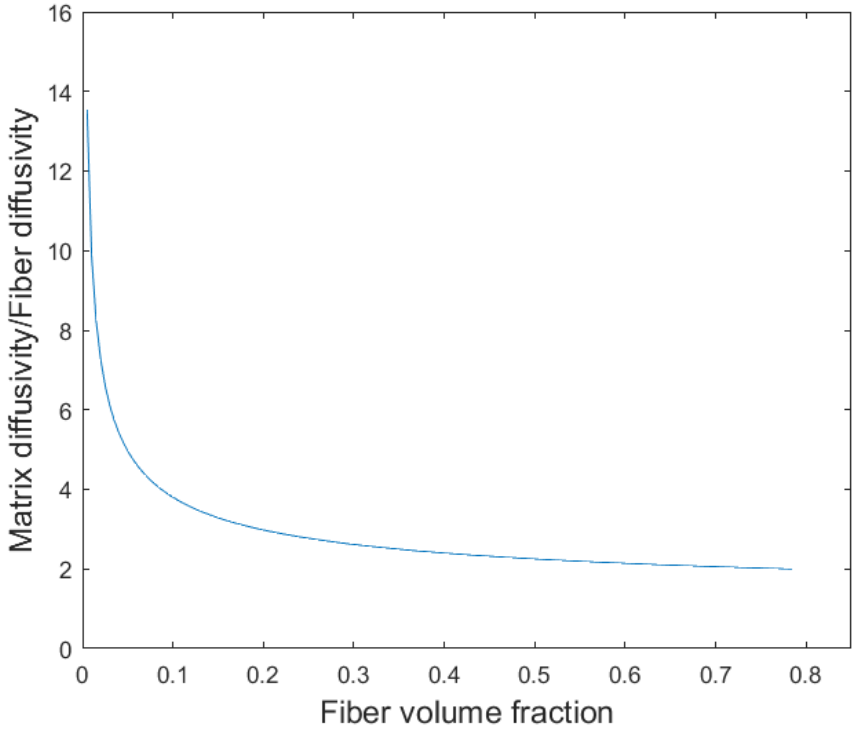

Figure 31. Ratio of matrix and fiber diffusivity versus fiber volume fraction

Through the experimental and numerical investigations, it is found that the higher temperature accelerates the fluid absorption. In order to describe the diffusion behavior, the Fickian and Springer models were applied. However, the Fickian model over-predicts the moisture absorption behavior, while the Springer model under-predicts it. The general Springer model provides better prediction compared to the reduced Springer model. For the general

Springer model, limitations exist for small fiber diffusivity and high fiber volume content. The effects of fibers on fluid diffusion are considered and the micromechanical model is used to model the anisotropy FRP composites. In this case, the micromechanical model can better predict the fluid absorption in the FRP composites. The swelling (shrinking) of the GFRP under fluid diffusion could be the reason that the Fickian and Springer models cannot capture the concentration curve. Considering the volumetric changes of the GFRP, the coupled deformation-diffusion model is applied, and the results shows that it can effectively describe the moisture diffusion process when the volume change are ineligible.

Measuring the diffusivity of composites in fiber direction is inherently difficult. Typical composite laminates are thin plates and the fibers are only exposed on the thin surface. Transverse diffusion dominates such samples. If applying the calibration method in ASTM D5229-92(04), the fluid diffuses through the thin surface will be neglected. Making thick laminates can compensate the problem of a small exposed surface, but then the diffusion takes a long time. Making thick laminates and cutting thin slices creating thin specimens with a large exposed surface for fiber ends solved the problem and good measurements could be taken. In order to capture the diffusion bahavior of fluid in fiber-reinforced composites, two configurations of samples are used: parallel and transverse samples (Figure 32).

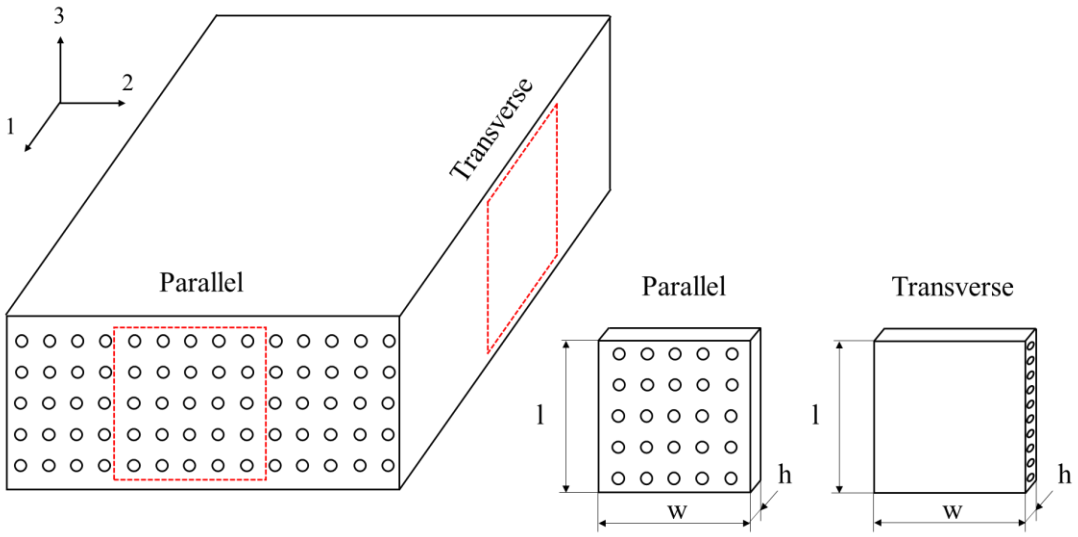

Figure 32. Composite samples configurations. Dimensions are 50mm × 50mm × 1.5mm.

The specimens are glass fiber-reinforced composites with epoxy matrix. And the details of the specimens are discussed in Abedin et al. [33]. Except for the FRP composites samples, epoxy samples are also tested in order to get the matrix properties of the FRP composites. All specimens had open edges. In order to enforce 1-D flow conditions in a diffusion experiment it is good practice to maximize the width to thickness ratio of the samples or to seal the edges with stainless steel. The sealant is often glued to the small surface of the samples' edges. This glue may absorb water, influencing the measurement, or, even worst, fall off from the sample during the experiment. It was therefore decided to keep open the edges of all samples, as the width to thickness ratio was quite big: 33. Saturation was measured up to 506 hours, when the weight gain curve had flattened out.

The weight increase in the epoxy specimens at saturation is about 3.18 %. By applying the calibration method given in ASTM D5229 which is valid for 1-D diffusion in an infinitely

wide plate, the matrix diffusivity obtained is 0.0067 mm^2/h ($1.86\ 10^{-6}$ mm^2/s). By applying the general calibration method discussed in Section 4.1 which is valid for 3-D diffusion in plates of finite width, the diffusivity obtained is 0.0062 mm^2/h ($1.71\ 10^{-6}$ mm^2/s). The 1-D diffusion equation, yields a higher diffusivity prediction than the 3-D diffusion equation, as it does not consider the edge effects as a cause for steeper weight gain curve. The difference is quite small, 7.4 %. One of the reasons for this difference is the finite width of the sample that is taken into account by the 3-D diffusion equation.

As discussed in Section 3, a micromechanical model, which is implemented in FE analysis, is presented for determining the homogenized diffusion behavior in FRP composites. The main advantages of using the homogenization approach are it can be used to easily determine anisotropic diffusivities of FRP with different fiber volume contents while incorporating different diffusivities of fiber bundle and matrix, making it easy for material selections with desired diffusion performance, it permits predictions of the diffusion behavior in laminated composites with different fiber orientations, and it allows performing diffusion of FRP structures with more complex geometries and boundary conditions. The concentration of water during the diffusion process is shown in Figure 33.

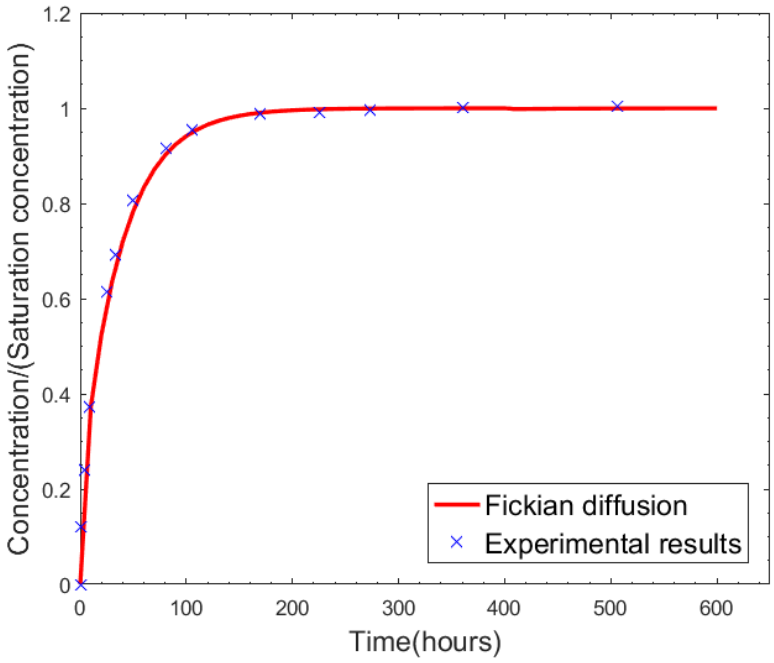

Figure 33. Simulation concentration of fluid in epoxy in deionized water at 60℃ using Fickian model.

The micromechanics model is now used to determine the anisotropic diffusivity of fiber bundles in the FRP composites. Prior to determining the diffusivities of fiber bundles in the longitudinal and lateral directions using the micromechanics model, parametric studies were considered, see Appendix. From the analyses, the diffusivity of the fiber bundle in the lateral direction is $D_{22}^{(f)}$= 0.0031 mm^2/h (0.86 10^{-6} mm^2/s), while the one in the longitudinal direction is $D_{11}^{(f)}$= 0.0308 mm^2/h (8.55 10^{-6} mm^2/s). The diffusivity of the fiber bundle along the longitudinal direction is much higher than the diffusivity of fiber bundle in the lateral direction, and also higher than the diffusivity of matrix. Figure 34 shows the diffusion behavior in FRP composites, tested transverse and parallel to the longitudinal fiber direction. From the micromechanics

analyses, the effective diffusivities can be easily determined from Eq. (54) and Eq. (55). The overall diffusivities of the FRP with 59.5 fiber volume content are: $\bar{D}_{11}$= 0.021 mm^2/h (5.80 10^{-6} mm^2/s) and $\bar{D}_{22}$= 0.0042 mm^2/h (1.16 10^{-6} mm^2/s).

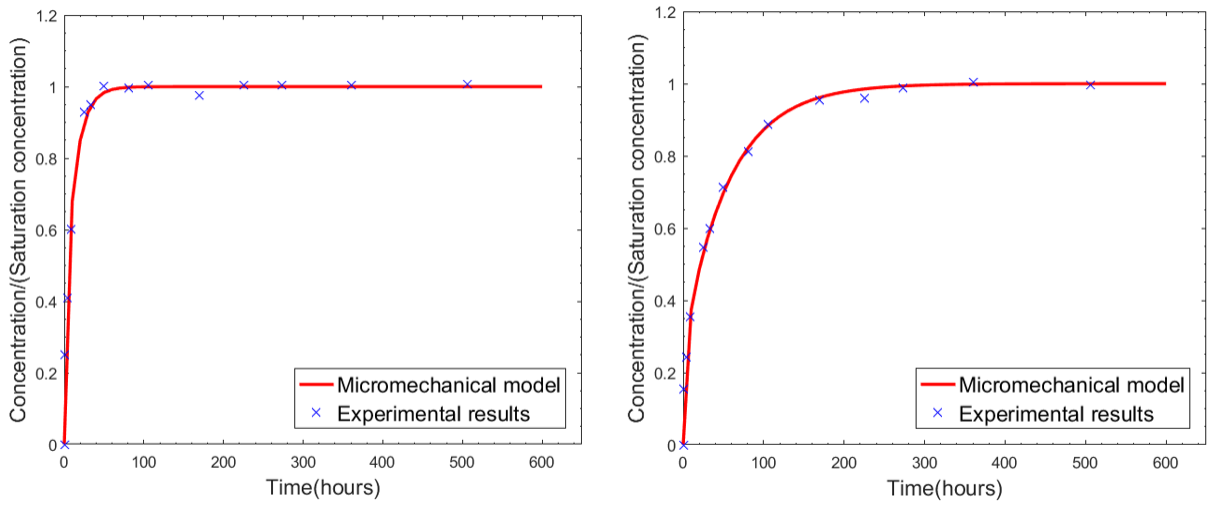

Figure 34. Simulation concentration of fluid in GFRP parallel specimens (left) and transverse specimens (right) in deionized water at 60℃ using Micromechanical model.

For the water uptake of neat resin and using thin plates the effect of the edges was small and using the 1-D or 3-D equation gave roughly the same results. It is recommended though to use the 3-D equation as it is more accurate and can also be used for thicker specimen geometries with more pronounced edge effects. The same can be said for measuring the water uptake of composite laminates.

For the glass fiber epoxy system investigated here, the diffusivity in the fiber direction was found to be about four times the diffusivity transverse to the fibers, see Table 1. This is a

significant difference and anisotropic diffusion should be considered when calculating the fluid concentration profiles of structures and components. It is also noted that the diffusivity in the fiber direction is higher than the diffusivity of pure resin. These results show that when considering only fiber bundle and matrix as constituents, the diffusivities of the fiber bundle cannot be assumed as zero, especially for the longitudinal fiber direction. However, assuming that individual glass fibers have 0 or very low diffusivity is often considered to predict diffusivity of the composite by knowing the diffusivity of the resin and geometric arrangement of the fibers. Using the assumption that fibers have zero or nearly zero diffusivity, e.g. the model developed by Shen and Springer [80] or the finite element based modes developed in [73], could not model the observed anisotropy. Several possible explanations to the above issue are as follows. This discrepancy is most likely because within fiber filaments in a single fiber bundle, resin and air pockets are present, which allow water to seep into fiber bundles. As a result, the net diffusivity of fiber bundle cannot be taken as zero. The glass fiber filaments themselves can be considered as zero or nearly zero permeability. However, considering that the fibers are arranged in bundles and the fibers are surrounded by a sizing (interface layer), diffusion channels may open up between fiber filaments and in the sizing. It is convenient to model this as diffusion within the fibers, but on a physical level another phase must be present that allows different diffusion than observed in the resin.

The presented micromechanics model could predict the observed global anisotropy by giving the fiber constituent (fiber bundle) an anisotropic diffusivity. The diffusivity across the fibers was less than that of the matrix and the diffusivity along the fibers was higher than the homogenized diffusivity of the materials. While the presented micromechanics approach seems to capture the anisotropy diffusivity in FRP composites with some rationale behind it, the detail

mechanisms of the diffusion in FRP composites are very complex and still not fully understood. From an engineering point of view, it is sufficient to accurately measure the anisotropic diffusion characteristics. From a materials point of view another phase allowing higher diffusivity must be present in the composite.

4.6 Fluid Diffusion in Sandwich Composites

Sandwich composites consist of different constitutes with various geometries. Thus, the diffusion behaviors of sandwich composites depend on the diffusivities of the different constitutes and also the concentration field in the entire composites. It is showed that the proposed constitutive model can well capture the fluid diffusion in pure resins, GFRP skins and polymeric foams. This chapter presents time-dependent analyses of polymeric composites immersed in fluid.

Figure 35 shows a schematic of sandwich composite specimen discussed in this chapter. The sandwich specimens were prepared and tested by Professor La Saponara's group. The sandwich composites consists of a closed-cell polyurethane PU foam core and two thin GFRP sheets covering the top and bottom of the core. The GFRP skin has unidirectional glass fibers and epoxy matrix and $[90]_4$ skins are used for the sandwich composites. The thickness per skin is 2 *mm* and the total thickness of the sandwich composites is 22.10 *mm*.The immersion condition was at 50 °C in deionized water and the immersion range is up to 184 days for the sandwich composites. A total of 12 samples are tested and the average dimensions of the sandwich specimens is in Table 9. The mass changes during the diffusion process of the GFRP/PU sandwich specimens are recorded. Because of the corrosion issue of the heater in the testing

system, the experiment had to be stopped unexpectedly at 184 days. And the sandwich composites did not reach fully saturation after 4500 hours of experiment.

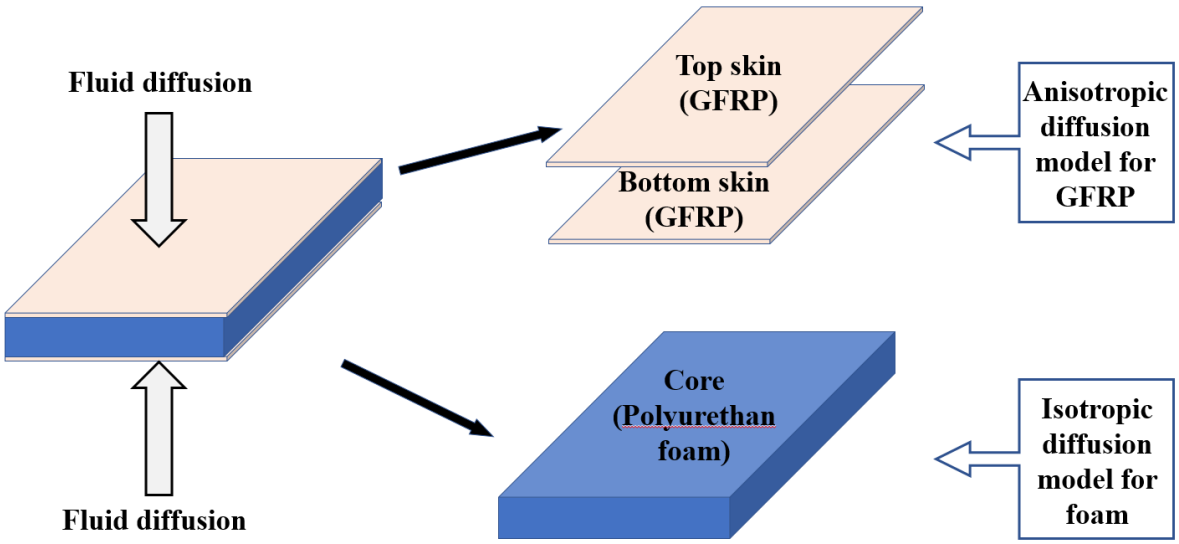

Figure 35. A schematic of the sandwich specimen with two GFRP skins and a polyurethane foam core.

Table 9 Average dimensions of sandwich composites specimens

Materials	Temperature	Skin Thickness(mm)	Thickness(mm)	Length(mm)	Width(mm)
GFRP/PU sandwich	50°C	2.00	22.10	178.08	51.11

The general Fickian diffusion model is considered for the polyurethane foam core of the sandwich composites. And the diffusivity used for the Fickian model is D=3.83x10$^{-6}\frac{mm^2}{s}$. It is

seen in the previous section that the polyurethane foam core only has limited swelling when immersed in deionized water at 50 °C. And the Fickian model has a good agreement with the testing data. In order to include the anisotropic diffusion in the GFRP skins, the micromechanical model is applied to the skins in the sandwich composites. The GFRP skin is discussed in the previous section and it showed that the micromechanical model can better describe the moisture diffusion compared to Fickian model. The following diffusion properties are used for the micromechanical model: diffusivity of fiber in the longitudinal direction is $D_{11} = 8.25 \times 10^{-3} \frac{mm^2}{hr} = 2.29 \times 10^{-6} \frac{mm^2}{s}$, while the one in the transverse direction is $D_{22} = 8.25 \times 10^{-4} \frac{mm^2}{hr} = 2.29 \times 10^{-7} \frac{mm^2}{s}$.

In this study the user material subroutine within ABAQUS commercial FE, written in Fortran, is used to integrate the micromechanics model to FE analyses. While for the polyurethane foam core, the general Fickian model is used. For the post-processing, the total amount of fluid in the composites is determined by integrating the field variables at the nodes obtained from the FE analyses. For this purpose, a Matlab code was generated for reading the nodal field variables and numerically integrating them to obtain the overall fluid concentration. Finite element meshes with 8 node hexahedral elements were generated for the sandwich composites with dimension 178.08 × 51.11 × 22.10 *mm*. The skin thickness is 2 *mm* for both sides of the skins and a perfectly bonded condition is assumed between the GFRP skin and the polyurethane core. A convergence study was first conducted in order to determine sufficient numbers of elements by comparing the overall fluid concentration to the analytical solution of isotropic diffusion in resin. In this study, a total of 48000 elements was sufficient in capturing the fluid sorption response. Figure 36 shows the FE meshes of the sandwich and the details of the

GFRP skin and the interface between skin and core. The fibers in the GFRP skins are along the x-axis.

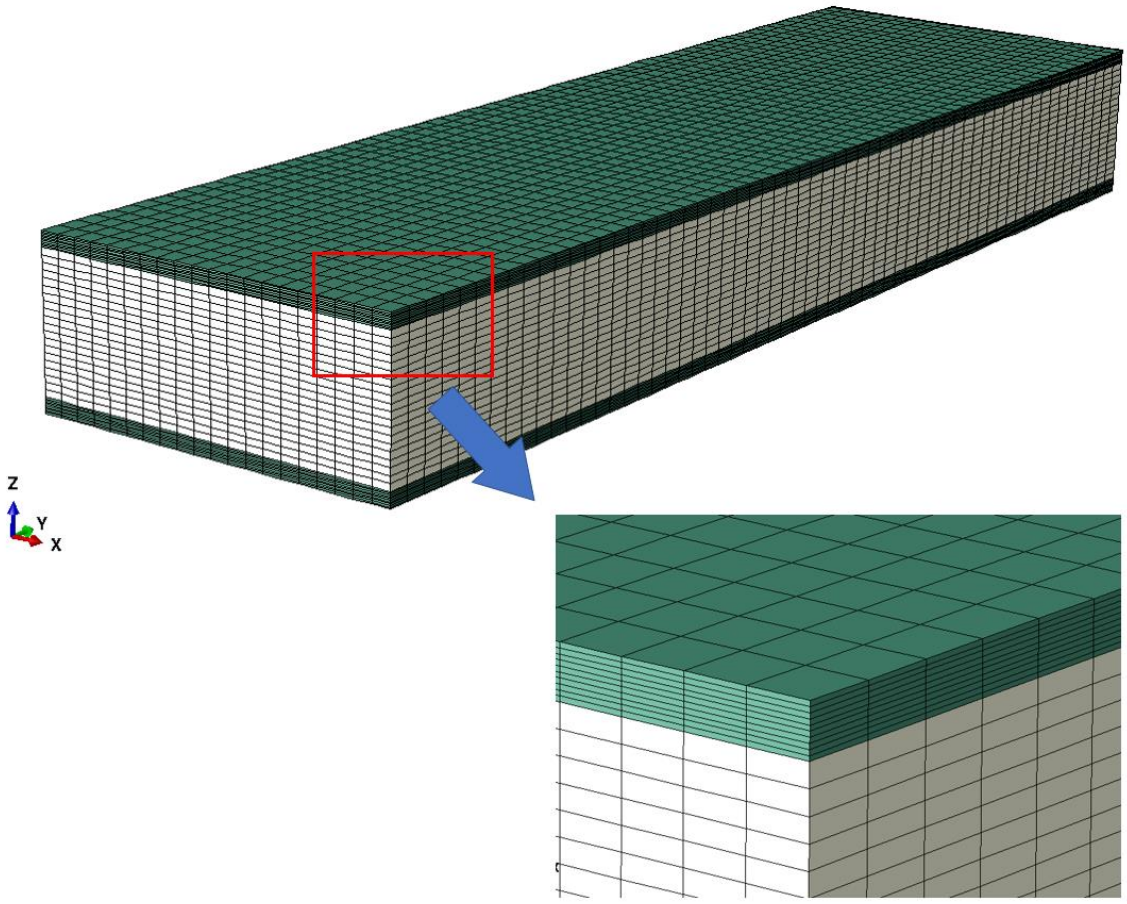

Figure 36. Mesh used for the FE analysis. FE: finite element.

For the FE analysis of the sandwich composite, initially the sandwich composite is under dry conditions, which means a zero concentration for the entire sandwich. Upon immersion, the surfaces of the sandwich are in contact with a fully saturated fluid, corresponding to a

normalized concentration C = 1. The analysis conducted is up to 4000 hours in order to compare with the testing data. Figure 37 shows the middle plane of the sandwich composite in the longitudinal direction. The concentration profiles of the middle plane during the moisture diffusion analysis are shown in Figure 38. And it shows that the presence of the GFRP sheets delays the fluid sorption of the polyurethane foam core. One-eighth of the sandwich composite is selected to show the three-dimensional concentration profile inside the sandwich composites (Figure 39). Figure 40 shows the three-dimensional concentration profile and it can be seen that the fluid diffuses through the open edges of the polyurethane foam and this diffusion process is much faster without the GFRP skins.

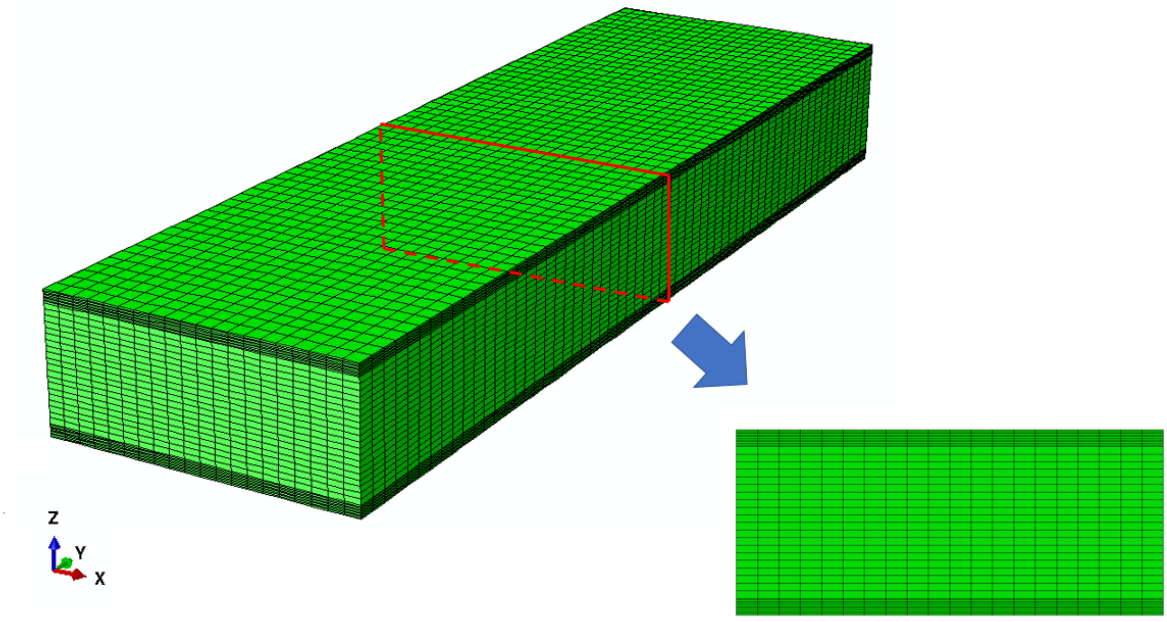

Figure 37. A schematic of the sandwich composite and the cross-section selected for contour plot.

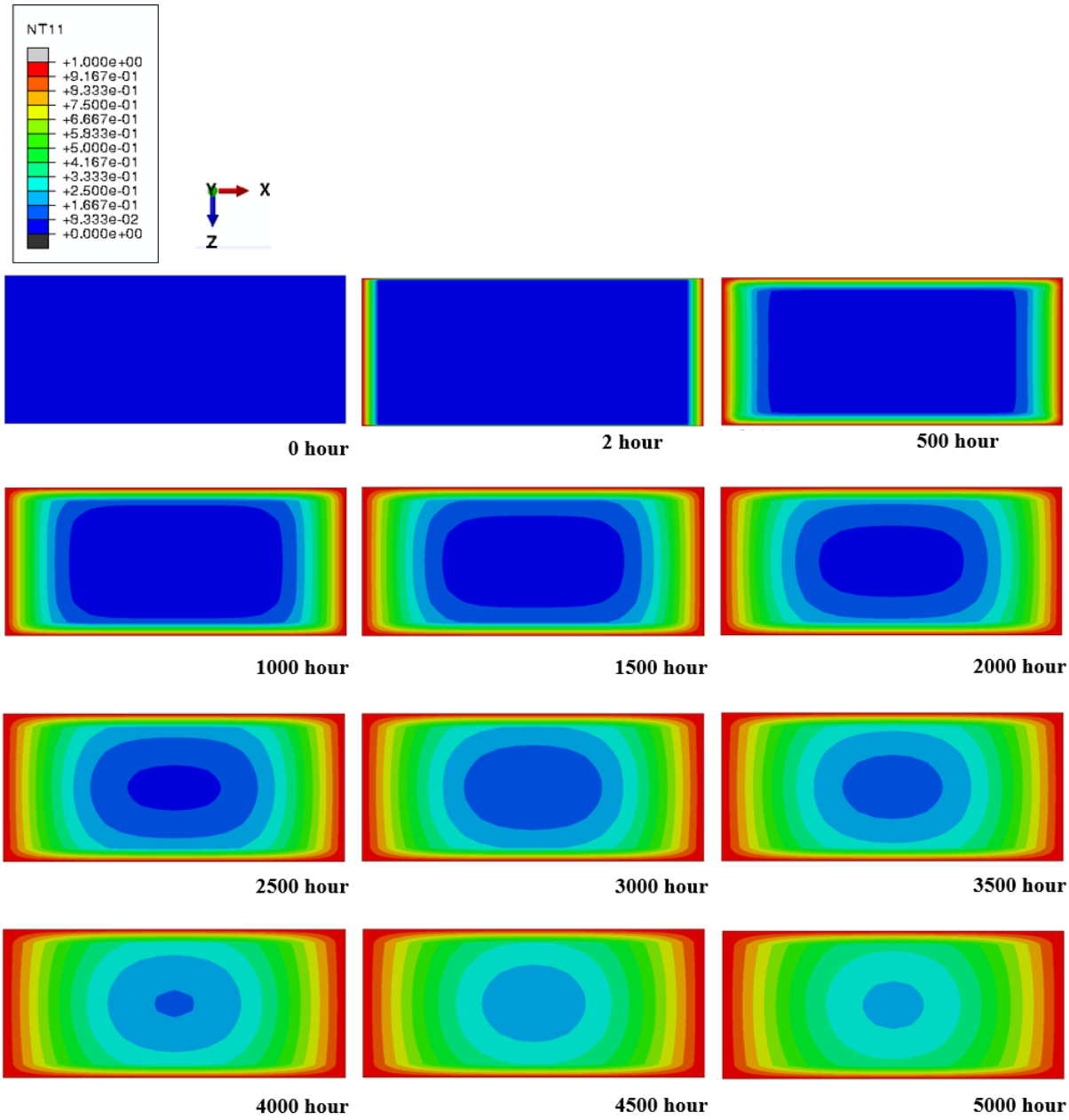

Figure 38. Concentration contours of the middle plane of the sandwich composite.

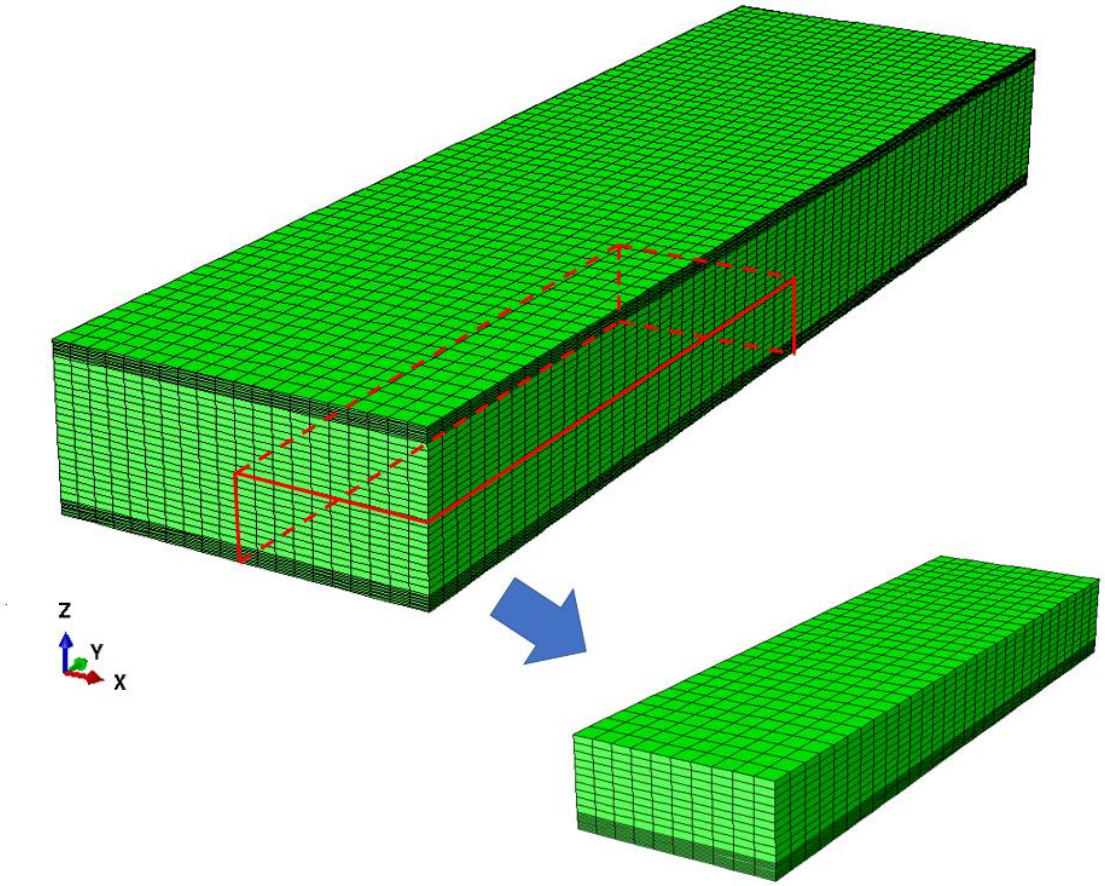

Figure 39. A schematic of the sandwich composite and the part selected for contour plot based on symmetry.

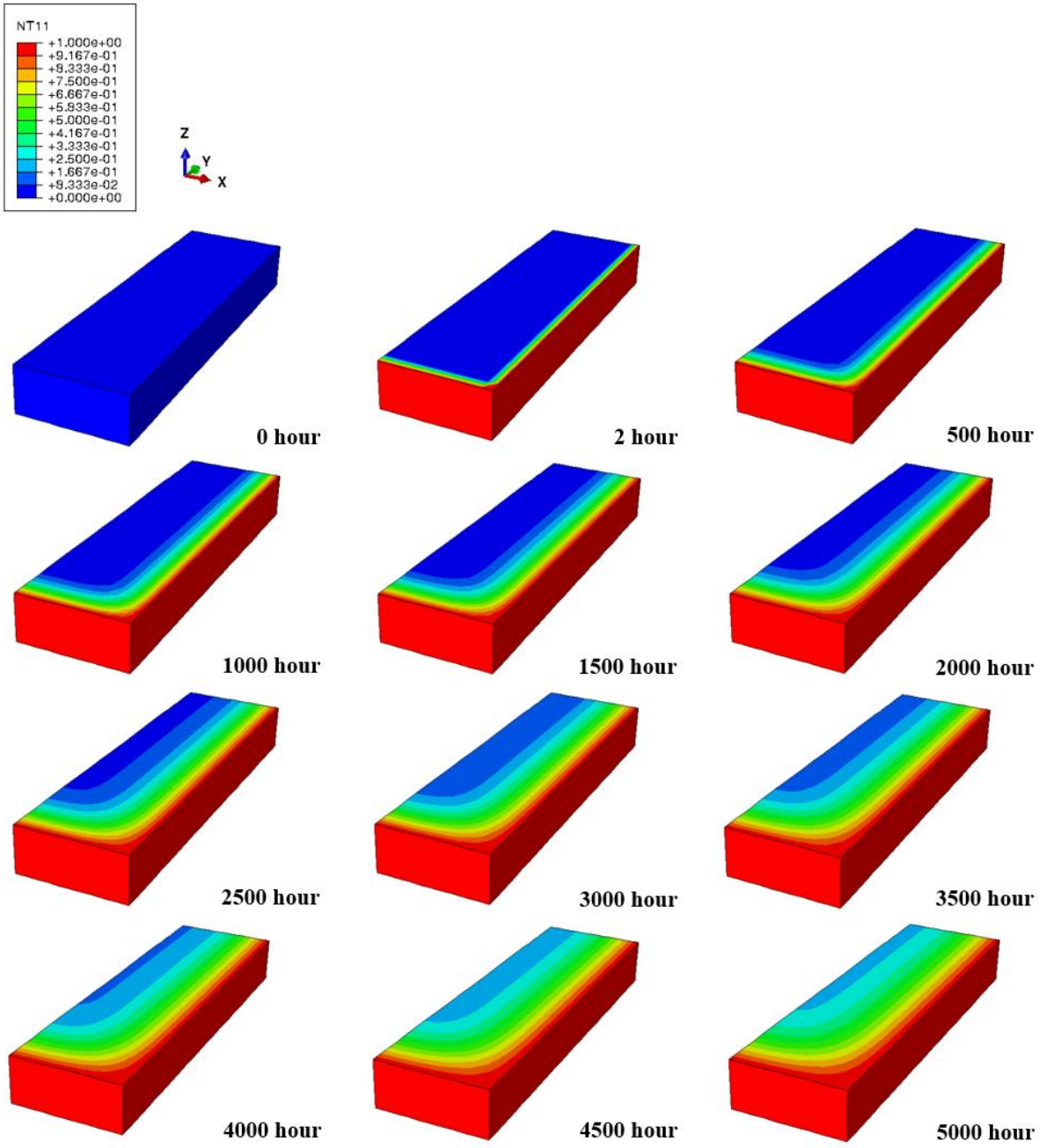

Figure 40. Concentration contours of the one-eighth sample of the sandwich composite.

Figure 41 shows the simulation results of the sandwich composite. It is seen that the multi-scale framework has a good agreement with the sandwich composite immersed in deionized water at 50 °C.

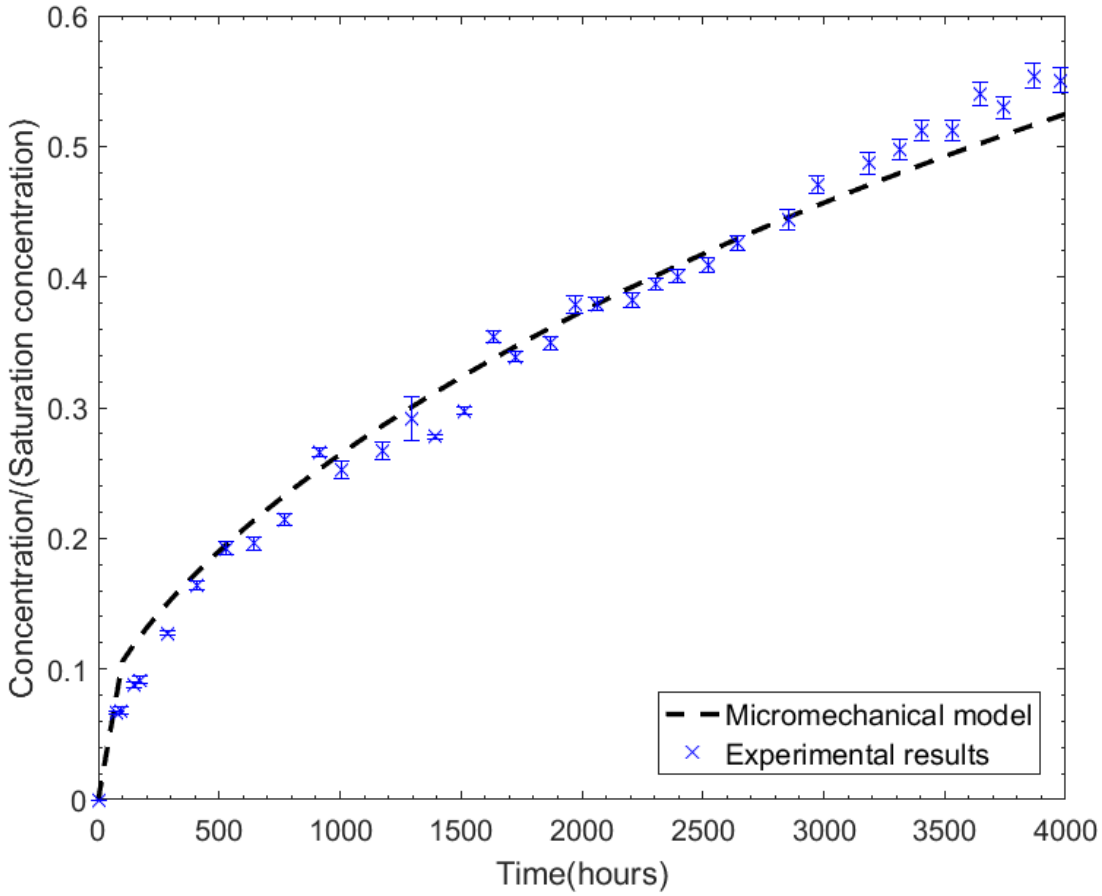

Figure 41. Simulation concentration of fluid in sandwich composite in deionized water at 50 °C.

Polymeric sandwich composites have been widely used in marine vessel applications, see for example: Vallbo [93], Neser [66], Kolat et al. [53] and Makinen et al. [60]. The following section presents a qualitative study of fluid diffusion into ship hull structure which is built with

polymeric sandwich composites. Part of the curved ship hull is selected for the study as shown in Figure 42. The selected ship hull has inner and outer radius of 100 *mm* and 121.1 *mm* respectively, and the length of the ship hull is 50 *mm*. The material and the thickness of the core and skins are the same with the GFRP/PU sandwich composites discussed above. Unidirectional fiber arrangement is assumed for the GFRP skins and the fibers are parallel to the x-axis. The outer surface of the ship hull is assumed to be completely immersed in fluid. We examine the fluid diffusion through the outer surface into the ship hull and predict the concentration of fluid in the sandwich structure. The multi-scale analysis is performed and Abaqus commercial FE is used to incorporate the micromechanical model for the GFRP skins and the Fickian model for the polyurethane foam core. Continuum three-dimensional element is considered for the sandwich composites and Figure 42 shows the FE mesh of the ship hull. Initially the ship hull is assumed to be completely dry, which corresponds to a normalized concentration $C=0$. Upon immersion, the outer surface of the ship hull is in contact with a fully saturated fluid corresponding to a normalized concentration $C = 1$. The analysis conducted is up to 8000 hours which is about a year of immersion duration. Figure 43 illustrates the concentration profiles of the ship hull during the fluid diffusion analysis. This qualitative study shows an example how this research can support the design of engineering structures using polymers and polymeric composites.

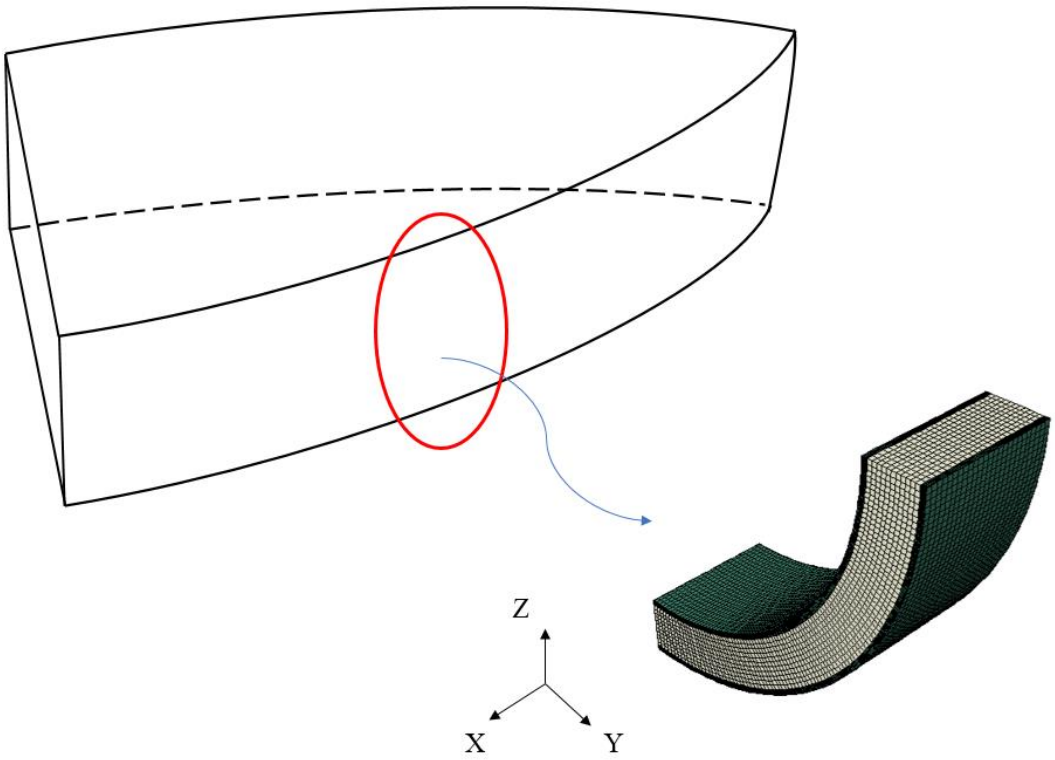

Figure 42. Schematic of ship hull and mesh used for FE analysis. FE: finite element.

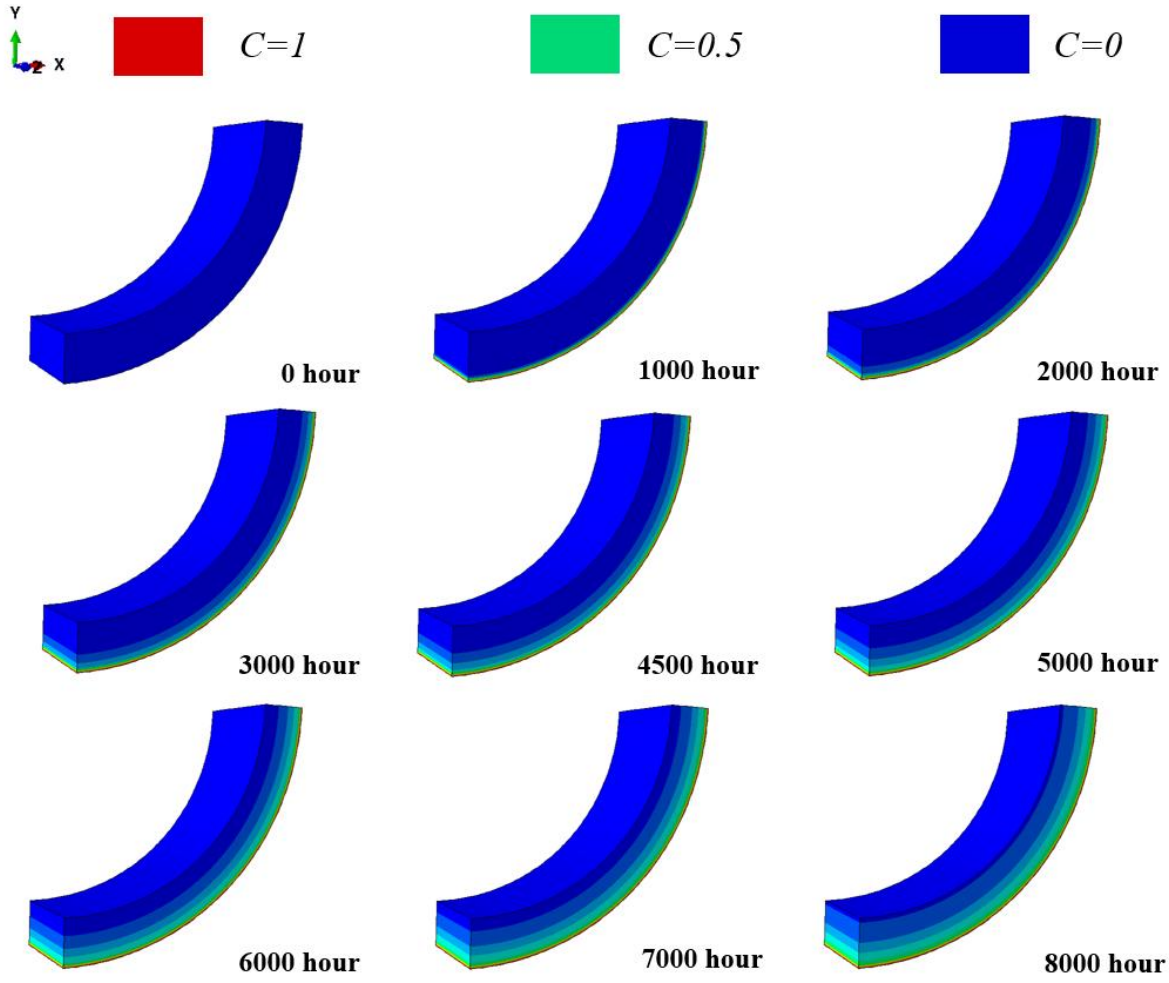

Figure 43. Concentration contours of the ship hull structure.

5. CONCLUSION

This research focuses on modeling the fluid diffusion behavior in polymers and polymer composites. The Fickian model is considered for materials with neglegible volumetric changes during the diffusion process. The assumption of Fickian model is that the diffusion of fluid through a rigid body and the rate of diffusion is much faster than that of polymer relaxation. For many polymers, the diffusion process deviates from the Fickian model. In order to include the interaction between diffusion and polymer deformation, a coupled deformation-diffusion model is adopted. The coupled model introduces a linear deformation-diffusion relation analogous to linear thermo-elasticity for solids. This study also examines an anisotropic diffusion in fiber-reinfoced composites. A micromechanical model is presented, and the matrix and the fiber bundles can have different diffusion behaviors. The Fickian model and the coupled deformation-diffusion model are implemented in finite different method in FORTRAN. The micromechanical model is implemented in user material subroutine (UMATHT) in commercial FE software, ABAQUS. The studied materials includes pure resins, fiber-reinforced polymer (FRP) composites, polymeric foams and sandwich composites. For analyzing diffusion behaviors in polymeric sandwich composites, a multi-scale finite element analysis is considered. The micromechanics model is used to determine the overall diffusion behaviors in the FRP skins of the sandwich composites, and 3D Fickian diffusion is considered for the foam. The research findings are discussed below:

Numerical investigations have been conducted to understand the fluid sorption behaviors of the structural materials of sandwich composites, namely epoxy, vinylester, polyurethane foam and PVC foam immersed in different fluids (deionized water and saline water) at two

temperatures (room temperature and 50 ^{o}C). In order to describe the diffusion process, the Fickian diffusion and coupled deformation-diffusion model for linear elastic isotropic materials presented by Gurtin[40] are adopted. For epoxy and vinylester, two types of specimens, i.e., thin plate rectangular and dogbone specimens, have been considered. The thin plate specimens were considered for calibrating material parameters following the ASTM standard. The material parameter calibrations from the experimental data have also been discussed. The dogbone specimens were considered in order to validate the diffusion model and calibrated material parameters. In all cases, elevated temperatures accelerate the diffusion process, which is expected, and is consistent with the literature. It is also noted that volume changes in the epoxy due to moisture sorption influence the diffusion processes, even at relatively low volume changes (around 10%). The Fickian model can capture the diffusion process when the volume changes in the specimens during the diffusion process are relatively small, e.g. for epoxy and vinylester immersed in saline water. The volume changes are pronounced in the case of epoxy immersed in deionized water at room temperatures. In such case, the Fickian model overpredicts the diffusion behaviors and the coupled deformation-diffusion model can reasonably describe the effect of deformation on the diffusion process. The model prediction on the diffusion process in dogbone specimens confirms the sensible choice of the diffusion models, for different diffusion cases, and validates the calibrated material parameters. The polyurethane foam and PVC foam samples are thick blocks and cannot meet the low width-thickness ratio required by the standard ASTM D5229-92. ASTM standard adopts a one-dimensional Fickian model and only provides an accurate calibration for thin-plate samples. Instead, a three-dimensional calibration method is considered. It is found that testing at 50^{o}C significantly increased the diffusivity of PVC foam, while decreased the diffusivity of polyurethane foam. The volume changes in polyurethane foam

immersed in deionized water at room temperature are quite significant. The Fickian model is used to predict the diffusion process and shows good agreements with the samples that have very small volumetric changes. The coupled deformation-diffusion model is considered for the polyurethane foam, and it is showed that the model can capture the diffusion process when the volume change is not negligible.

Numerical analyses have been conducted in order to understand the fluid diffusion in FRP composites. GFRP samples are tested in deionized water and under two different temperatures (room temperature and 50 ^{o}C). It is found that the higher temperature accelerates the fluid absorption, which is expected. In order to describe the overall diffusion behavior, the Fickian model was first considered. However, the Fickian model over-predicts the fluid absorption behavior. It is also seen that the Fickian model can better capture the diffusion response in a solid body when the volumetric changes during the diffusion process is insignificant, as in the case of immersion at 50˚C. Immersion at room temperature shows more pronounced volume changes, which can be better captured when using coupled deformation-diffusion model.

An anisotropic fluid diffusion behavior in glass/epoxy composites is studied. In order to examine the effect of fiber diffusivity and fiber volume content, the Springer and micromechanics models were considered. The Springer model incorporates the fiber volume content and assumes that the fiber diffusivity is negligible. The response computed by the Springer model under-predicts the diffusion of fluid in the GFRP composites. The general Springer model has a better agreement with experimental data compared to the reduced Springer model. However, the general Springer model has several constraints that limit its application. The second approach is using a simplified micromechanics model to capture the anisotropic

diffusivity in the GFRP composites. Fiber bundle and matrix are taken as two constituents within the micromechanics model. The anisotropic diffusion behavior is captured by considering nonzero anisotropic diffusion coefficients for the fiber bundle and isotropic diffusion for the matrix. The rationale behind choosing nonzero diffusivity for the fiber bundle is due to occurrence of water seeping within fiber filament in the bundles during the diffusion process. The micromechanical model allows to model the anisotropy diffusivity in the GFRP composites, and it can predict the fluid absorption in the GFRP composites.

Finally, the research examines the fluid diffusion behavior in sandwich composites using the integrated micromechanical model and FE framework. The sandwich composite consists of two thin GFRP skins and a thick polyurethane foam core. The micromechanical model is considered to describe the anisotropic diffusion in GFRP skins while the Fickian model is used for the isotropic polyurethane foam core. The sandwich composite was immersed in deionized water at 50 °C. The multi-scale analysis shows a good agreement with the testing data. A qualitative study of a fluid diffusion in a portion of a sandwich composite ship hull is performed by using the multi-scale analysis. This qualitative study provides an example of how this research can contribute to engineering structural designs using polymers and polymeric composites.

REFERENCES

[1] Standard Test Method for Moisture Absorption Properties and Equilibrium Conditioning of Polymer Matrix Composite Materials, ASTM International, 2014.

[2] J.L. Abot, A. Yasmin, I.M. Daniel, Hygroscopic Behavior of Woven Fabric Carbon-Epoxy Composites, J. Reinf. Plast. Compos. 24(2) (2005) 195-207.

[3] J. Aboudi, Mechanics of Composite Materials: A Unified Micromechanical Approach, Elsevier, Amsterdam, 1991.

[4] E.C. Aifantis, On the problem of diffusion in solids, Acta Mechanica 37(3) (1980) 265-296.

[5] T. Alfrey, E.F. Gurnee, W.G. Lloyd, Diffusion in glassy polymers, Journal of Polymer Science Part C: Polymer Symposia 12(1) (1966) 249-261.

[6] V.A. Alvarez, A.N. Fraga, A. Vazquez, Effects of the moisture and fiber content on the mechanical properties of biodegradable polymer-sisal fiber biocomposites, J. Appl. Polym. Sci. 91(6) (2004) 4007-4016.

[7] J.C. Arnold, S.M. Alston, F. Korkees, An assessment of methods to determine the directional moisture diffusion coefficients of composite materials, Composites Part A: Applied Science and Manufacturing 55(Supplement C) (2013) 120-128.

[8] ASTM International, Standard Test Method for Moisture Absorption Properties and Equilibrium, Conditioning of Polymer Matrix Composite Materials, ASTM D5229/D5229M-92(04), West Conshohocken (PA), USA.

[9] F. Avilés, M. Aguilar-Montero, Mechanical degradation of foam-cored sandwich materials exposed to high moisture, Compos. Struct. 92(1) (2010) 122-129.

[10] F. Avilés, M. Aguilar-Montero, Moisture absorption in foam-cored composite sandwich structures, Polym. Compos. 31(4) (2010) 714-722.

[11] F. Avilés, M. Aguilar-Montero, Moisture absorption in foam-cored composite sandwich structures, Polym. Compos. 31(4) (2010) 714-722.

[12] S. Baek, A.R. Srinivasa, Diffusion of a fluid through an elastic solid undergoing large deformation, International Journal of Non-Linear Mechanics 39(2) (2004) 201-218.

[13] L.-R. Bao, A.F. Yee, Moisture diffusion and hygrothermal aging in bismaleimide matrix carbon fiber composites—part I: uni-weave composites, Compos. Sci. Technol. 62(16) (2002) 2099-2110.

[14] L.-R. Bao, A.F. Yee, Moisture diffusion and hygrothermal aging in bismaleimide matrix carbon fiber composites: part II—woven and hybrid composites, Composites Science and Technology 62(16) (2002) 2111-2119.

[15] L.-R. Bao, A.F. Yee, C.Y.C. Lee, Moisture absorption and hygrothermal aging in a bismaleimide resin, Polymer 42(17) (2001) 7327-7333.

[16] M. Beringhier, A. Simar, M. Gigliotti, J.C. Grandidier, I. Ammar-Khodja, Identification of the orthotropic diffusion properties of RTM textile composites for aircraft applications, Compos. Struct. 137(Supplement C) (2016) 33-43.

[17] M. Blikstad, Three-Dimensional Moisture Diffusion in Graphite/Epoxy Laminates, J. Reinf. Plast. Compos. 5(1) (1986) 9-18.

[18] M. Blikstad, P.O.W. Sjöblom, T.R. Johannesson, Long-Term Moisture Absorption in Graphite/Epoxy Angle-Ply Laminates, J. Compos. Mater. 18(1) (1984) 32.

[19] D.A. Bond, Moisture Diffusion in a Fiber-reinforced Composite: Part I - Non-Fickian Transport and the Effect of Fiber Spatial Distribution, J. Compos. Mater. 39(23) (2005) 2113-2141.

[20] P. Bonniau, A.R. Bunsell, A Comparative Study of Water Absorption Theories Applied to Glass Epoxy Composites, J. Compos. Mater. 15(3) (1981) 272-293.

[21] P. Bonniau, A.R. Bunsell, Water Absorption by Glass Fibre Reinforced Epoxy Resin, in: I.H. Marshall (Ed.), Compos. Struct., Springer Netherlands, Dordrecht, 1981, pp. 92-105.

[22] H. Bouadi, C.T. Sun, Hygrothermal Effects on the Stress Field of Laminated Composites, J. Reinf. Plast. Compos. 8(1) (1989) 40-54.

[23] C.E. Browning, G.E. Husman, J.M. Whitney, Moisture Effects in Epoxy Matrix Composites, Composite Materials: Testing and Design(Fourth Conference) ASTM STP617 (1977) 481-496.

[24] L.W. Cai, Y. Weitsman, Non-Fickian moisture diffusion in polymeric composites, J. Compos. Mater. 28(2) (1994) 130-154.

[25] D.S. Cairns, D.F. Adams, Moisture and Thermal Expansion Properties of Unidirectional Composite Materials and the Epoxy Matrix, J. Reinf. Plast. Compos. 2(4) (1983) 239-255.

[26] H.G. Carter, K.G. Kibler, LANGMUIR-TYPE MODEL FOR ANOMALOUS MOISTURE DIFFUSION IN COMPOSITE RESINS, J. Compos. Mater. 12 (1978) 118-131.

[27] C. Chen, R. Lakes, Analysis of the structure-property relations of foam materials, Cell. Polym. 14(3) (1995) 186-202.

[28] H.S. Choi, K.J. Ahn, J.D. Nam, H.J. Chun, Hygroscopic aspects of epoxy/carbon fiber composite laminates in aircraft environments, Composites Part A: Applied Science and Manufacturing 32(5) (2001) 709-720.

[29] J. Crank, The mathematics of diffusion, 2nd ed., Oxford University Press, New York, 1975.

[30] Y. Fan, A. Gomez, S. Ferraro, B. Pinto, A. Muliana, V. La Saponara, The effects of temperatures and volumetric expansion on the diffusion of fluids through solid polymers, J. Appl. Polym. Sci. (2017).

[31] G. Fernandez, H. Usabiaga, D. Vandepitte, Subcomponent development for sandwich composite wind turbine blade bonded joints analysis, Compos. Struct. 180 (2017) 41-62.

[32] M. Fichera, L.A. Carlsson, Moisture transport in unidirectional carbon/vinylester panels with imperfect fiber/matrix interface, J. Compos. Mater. 50(6) (2016) 751-760.

[33] A. Gagani, Y. Fan, A. Muliana, A. Echtermeyer, Micromechanical modeling of anisotropic water diffusion in glass fiber epoxy reinforced composites, 2017.

[34] A. Gagani, A. Krauklis, A.T. Echtermeyer, Anisotropic fluid diffusion in carbon fiber reinforced composite rods: Experimental, analytical and numerical study, Marine Structures 59 (2018) 47-59.

[35] A. Gagani, Krauklis, A., Echtermeyer, A. T., Anisotropic fluid diffusion in carbon fiber reinforced composite rods: Experimental, analytical and numerical study, Manuscript submitted for publication (2017).

[36] A. Göpferich, Mechanisms of polymer degradation and erosion, Biomaterials 17(2) (1996) 103-114.

[37] L.R. Grace, M.C. Altan, Non-fickian three-dimensional hindered moisture absorption in polymeric composites: Model development and validation, Polym. Compos. 34(7) (2013) 1144-1157.

[38] D.M. Granville, Moisture Effects and Peel Testing of Polymethacrylimide and Honeycomb Core in Sandwich/Skin Structures, International Joint Military/Government-Industry Symposium on Structural Adhesive Bonding (5th), Armament Research Development and Engineering Center, Picatinny Arsenal, Dover, NJ, pp. p224-230.

[39] O. Gullberg, K.A. Olsson, Design and construction of GRP sandwich ship hulls, Marine Structures 3(2) (1990) 93-109.

[40] M.E. Gurtin, Virginia Polytechnic Institute, Blacksburg,VA, 1977.

[41] C.S. Helbling, V.M. Karbhari, Investigation of the sorption and tensile response of pultruded E-glass/vinylester composites subjected to hygrothermal exposure and sustained strain, J. Reinf. Plast. Compos. 27(6) (2008) 613-638.

[42] R. Hill, Elastic properties of reinforced solids: some theoretical aspects, J. Mech. Phys. Solids 11 (1963) 357 to 372.

[43] W. Hong, X. Zhao, J. Zhou, Z. Suo, A theory of coupled diffusion and large deformation in polymeric gels, Journal of the Mechanics and Physics of Solids 56(5) (2008) 1779-1793.

[44] C. Humeau, P. Davies, F. Jacquemin, Moisture diffusion under hydrostatic pressure in composites, Materials & Design 96 (2016) 90-98.

[45] Z. Huo, M. Mohamed, J. Nicholas, X. Wang, K. Chandrashekhara, Experimentation and simulation of moisture diffusion in foam-cored polyurethane sandwich structure, Journal of Sandwich Structures and Materials (2015) 1099636215582218.

[46] Z. Huo, M. Mohamed, J.R. Nicholas, X. Wang, K. Chandrashekhara, Experimentation and simulation of moisture diffusion in foam-cored polyurethane sandwich structure, Journal of Sandwich Structures & Materials 18(1) (2016) 30-49.

[47] U.S. Ishiaku, H. Hamada, M. Mizoguchi, W.S. Chow, Z.A. Mohd Ishak, The effect of ambient moisture and temperature conditions on the mechanical properties of glass fiber/carbon fiber/nylon 6 sandwich hybrid composites consisting of skin-core morphologies, Polym. Compos. 26(1) (2005) 52-59.

[48] S.R. J., C.W. J., The effect of moisture and loading rate on the interfacial fracture properties of sandwich structures, Polym. Compos. 23(3) (2002) 406-417.

[49] F. Jacquemin, S. Fréour, R. Guillén, Prediction of local hygroscopic stresses for composite structures – Analytical and numerical micro-mechanical approaches, Composites Science and Technology 69(1) (2009) 17-21.

[50] O.K. Joshi, THE EFFECT OF MOISTURE ON THE SHEAR PROPERTIES OF CARBON-FIBER COMPOSITES, Composites 14(3) (1983) 196-200.

[51] S. Joshi, G. Astarita, Diffusion-relaxation coupling in polymers which show two-stage sorption phenomena, Polymer 20(4) (1979) 455-458.

[52] H.A. Katzman, R.M. Castaneda, H.S. Lee, Moisture diffusion in composite sandwich structures, Composites Part A: Applied Science and Manufacturing 39(5) (2008) 887-892.

[53] K. Kolat, G. Neşer, Ç. Özes, The effect of sea water exposure on the interfacial fracture of some sandwich systems in marine use, Compos. Struct. 78(1) (2007) 11-17.

[54] L. Kumosa, B. Benedikt, D. Armentrout, M. Kumosa, Moisture absorption properties of unidirectional glass/polymer composites used in composite (non-ceramic) insulators, Composites Part A: Applied Science and Manufacturing 35(9) (2004) 1049-1063.

[55] V. La Saponara, Environmental and chemical degradation of carbon/epoxy and structural adhesive for aerospace applications: Fickian and anomalous diffusion, Arrhenius kinetics, Compos. Struct. 93(9) (2011) 2180-2195.

[56] G. LaPlante, A.V. Ouriadov, P. Lee-Sullivan, B.J. Balcom, Anomalous moisture diffusion in an epoxy adhesive detected by magnetic resonance imaging, J. Appl. Polym. Sci. 109(2) (2008) 1350-1359.

[57] M.C. Lee, N.A. Peppas, Water transport in graphite/epoxy composites, J. Appl. Polym. Sci. 47(8) (1993) 1349-1359.

[58] A.C. Loos, Springer G. S., MOISTURE ABSORPTION OF GRAPHITE-EPOXY COMPOSITES IMMERSED IN LIQUIDS AND IN HUMID AIR, J Compos Mater 13(2) (1979) 131-147.

[59] A.C. Loos, G.S. Springer, Moisture Absorption of Graphite-Epoxy Composites Immersed in Liquids and in Humid Air, J. Compos. Mater. 13(2) (1979) 131-147.

[60] K.-E. Mäkinen, S.-E. Hellbratt, K.-A. Olsson, The Development of Sandwich Structures for Naval Vessels During 25 Years, Springer Netherlands, Dordrecht, 1998, pp. 13-28.

[61] B. Manujesh, V. Rao, M.S. Aan, Moisture absorption and mechanical degradation studies of polyurethane foam cored E-glass-reinforced vinyl-ester sandwich composites, J. Reinf. Plast. Compos. 33(5) (2014) 479-492.

[62] R.J. Morgan, J.E. O'neal, D.L. Fanter, The effect of moisture on the physical and mechanical integrity of epoxies, Journal of Materials Science 15(3) (1980) 751-764.

[63] F. Morganti, M. Marchetti, G. Reibaldi, Effects of moisture and thermal ageing on structural stability of sandwich panels, Acta Astronautica 11(7) (1984) 489-508.

[64] A.H. Muliana, A micromechanical formulation for piezoelectric fiber composites with nonlinear and viscoelastic constituents, Acta Materialia 58(9) (2010) 3332-3344.

[65] A.H. Muliana, J.S. Kim, A two-scale homogenization framework for nonlinear effective thermal conductivity of laminated composites, Acta Mechanica 212(3) (2010) 319-347.

[66] G. Neşer, Polymer Based Composites in Marine Use: History and Future Trends, Procedia Engineering 194 (2017) 19-24.

[67] S.S. Parthasarathy, A. Muliana, K. Rajagopal, A fully coupled model for diffusion-induced deformation in polymers, Acta Mechanica 227(3) (2016) 837-856.

[68] M. Patel, P. Morrell, J. Cunningham, N. Khan, R.S. Maxwell, S.C. Chinn, Complexities associated with moisture in foamed polysiloxane composites, Polym. Degrad. Stab. 93(2) (2008) 513-519.

[69] E. Pérez-Pacheco, J.I. Cauich-Cupul, A. Valadez-González, P.J. Herrera-Franco, Effect of moisture absorption on the mechanical behavior of carbon fiber/epoxy matrix composites, Journal of Materials Science 48(5) (2012) 1873-1882.

[70] D. Perreux, C. Suri, A study of the coupling between the phenomena of water absorption and damage in glass/epoxy composite pipes, Compos. Sci. Technol. 57(9–10) (1997) 1403-1413.

[71] S. Popineau, C. Rondeau-Mouro, C. Sulpice-Gaillet, M.E.R. Shanahan, Free/bound water absorption in an epoxy adhesive, Polymer 46(24) (2005) 10733-10740.

[72] I.B.C.M. Rocha, S. Raijmaekers, F.P. van der Meer, R.P.L. Nijssen, H.R. Fischer, L.J. Sluys, Combined experimental/numerical investigation of directional moisture diffusion in glass/epoxy composites, Compos. Sci. Technol. 151(Supplement C) (2017) 16-24.

[73] I.C.B.M. Rocha, Raijmaekers, Nijssen R. P. L., van der Meer F. P., Sluys, L. J., Experimental/numerical study of anisotropic water diffusion in glass/epoxy composites, 37th Risø International Symposium on Materials Science, IOP Publishing Ltd, Risø, Denmark, 2016.

[74] P. Scott, J.M. Lees, Water, salt water, and alkaline solution uptake in epoxy thin films, J. Appl. Polym. Sci. 130(3) (2013) 1898-1908.

[75] R.J. Scudamore, W.J. Cantwell, The effect of moisture and loading rate on the interfacial fracture properties of sandwich structures, Polym. Compos. 23(3) (2002) 406-417.

[76] R. Selzer, K. Friedrich, Mechanical properties and failure behaviour of carbon fibre-reinforced polymer composites under the influence of moisture, Composites Part a-Applied Science and Manufacturing 28(6) (1997) 595-604.

[77] C.-H. Shen, G.S. Springer, Moisture Absorption and Desorption of Composite Materials, J. Compos. Mater. 10(1) (1976) 2-20.

[78] C.-H. Shen, G.S. Springer, Effects of Moisture and Temperature on the Tensile Strength of Composite Materials, J. Compos. Mater. 11(1) (1977) 2-16.

[79] C.-H. Shen, G.S. Springer, Environmental Effects on the Elastic Moduli of Composite Materials, J. Compos. Mater. 11(3) (1977) 250-264.

[80] C.H. Shen, G. Springer, C.H. Shen, Moisture absorption and desorption of composite materials, Journal of Composite Materials 10 (1976) 2-20.

[81] G.C. Sih, Michopoulos, J.G. ,Chou, S.C. , Hygrothermoelasticity, Martinus Nijhoff Publishers, Dordrecht, 1986.

[82] G.C. Sih, A. Ogawa, S.C. Chou, TWO-DIMENSIONAL TRANSIENT HYGROTHERMAL STRESSES IN BODIES WITH CIRCULAR CAVITIES: MOISTURE AND TEMPERATURE COUPLING EFFECTS, Journal of Thermal Stresses 4(2) (1981) 193-222.

[83] G.C. Sih, M.T. Shih, Hygrothermal stress in a plate subjected to antisymmetric time-dependent moisture and temperature boundary conditions, Journal of Thermal Stresses 3(3) (1980) 321-340.

[84] G.C. Sih, M.T. Shih, S.C. Chou, Transient hygrothermal stresses in composites: Coupling of moisture and heat with temperature varying diffusivity, International Journal of Engineering Science 18(1) (1980) 19-42.

[85] A. Siriruk, D. Penumadu, A. Sharma, Effects of Seawater and Low Temperatures on Polymeric Foam Core Material, Experimental Mechanics 52(1) (2012) 25-36.

[86] A. Siriruk, D. Penumadu, Y.J. Weitsman, Effect of sea environment on interfacial delamination behavior of polymeric sandwich structures, Compos. Sci. Technol. 69(6) (2009) 821-828.

[87] A. Siriruk, Y.J. Weitsman, D. Penumadu, Polymeric foams and sandwich composites: Material properties, environmental effects, and shear-lag modeling, Compos. Sci. Technol. 69(6) (2009) 814-820.

[88] G. Springer, S. Tsai, G. Springer, Thermal conductivities of unidirectional materials (Thermal conductivities of unidirectional composite materials parallel and normal to filaments, using analogy to shear loading response), JOURNAL OF COMPOSITE MATERIALS 1 (1967) 166-173.

[89] G.S. Springer, Environmental Effects on Epoxy Matrix Composites, Composite Materials: Testing and Design (Fifth Conference) ASTM STP674 (1979) 291-312.

[90] G.S. Springer, S.W. Tsai, Thermal Conductivities of Unidirectional Materials, J. Compos. Mater. 1(2) (1967) 166-173.

[91] O.T. Thomsen, Sandwich Materials for Wind Turbine Blades — Present and Future, Journal of Sandwich Structures & Materials 11(1) (2009) 7-26.

[92] L. Treloar, The Physics of Rubber Elasticity, 2nd ed., Oxford University Press, ,London, 1958.

[93] S. Vallbo, Material Selection Considerations for Polymer Composite Structures in Naval Ship Applications, Journal of Sandwich Structures & Materials 7(5) (2005) 413-429.

[94] Y. Weitsman, Stress Assisted Diffusion in Elastic and Viscoelastic Materials, Journal of the Mechanics and Physics of Solids 35(1) (1987) 73-93.

[95] Y.J. Weitsman, M. Elahi, Effects of fluids on the deformation, strength and durability of polymeric composites - An overview, Mechanics of Time-Dependent Materials 4(2) (2000) 107-126.

[96] Y.J. Weitsman, X. Li, A. Ionita, Sea water effects on polymeric foams and their sandwich layups, Springer, Dordrecht, 2005.

[97] J.M. Whitney, Three-Dimensional Moisture Diffusion in Laminated Composites, AIAA Journal 15(9) (1977) 1356-1358.

[98] J.M. Whitney, C.E. Browning, Some Anomalies Associated with Moisture Diffusion in Epoxy Matrix Composite Materials, Advanced Composite Materials—Environmental effects ASTM STP658 (1978) 43-60.

[99] Y.T. Yu, K. Pochiraju, Three-Dimensional Simulation of Moisture Diffusion in Polymer Composite Materials, Polymer-Plastics Technology and Engineering 42(5) (2003) 737-756.

[100] S. Zhang, Z. Huang, Y. Zhang, H. Zhou, Experimental investigation of moisture diffusion in short-glass-fiber-reinforced polyamide 6,6, J. Appl. Polym. Sci. 132(37) (2015).